# Analysis of Peristaltic Nanofluid Flow in a Microchannel

by

RONNY MAUSHI MOKGWADI

DISSERTATION

Submitted in (partial) fulfilment of the
requirements for the degree of

Master of Science
in
Applied Mathematics
in the
FACULTY OF SCIENCE AND AGRICULTURE
(School of Mathematical and Computer Sciences)
at the
UNIVERSITY OF LIMPOPO

Supervisor: Dr Lazarus Rundora

2022

# Declaration

I declare that the dissertation hereby submitted to the university of Limpopo, for the degree of master of science in applied mathematics has not previously submitted by me for a deree at this or any other university; that is my work in design and in execution, and that all material contained herein has been duly acknowledged.

Signature:........*Mokgwadi RM*......Date: 15 March 2022.....

# Abstract

Nanofluids are a class of heat transfer fluids created by suspending nanoparticles in base fluids. Due to their enhanced thermal conductivity, nanofluids are fast replacing conventional heat transfer fluids like water, mineral oil, ethylene glycol and others. They contribute to advancement of technology and modernity through pertinent applications in fields such as biomedical, automotive industry, cooling technologies and many others.

This study documents a survey of nanofluids and their applications and an investigation of peristaltic nanofluid flow through a two dimensional microchannel with and without slip effects. Peristaltic fluid transport plays an important role in engineering, technology, science and physiology. The Buongiorno model formulation is employed and the governing equations for peristaltic nanofluid flow in a two dimensional microchannel are non-dimensionalised and solved semi-analytically using the Adomian decomposition method. Series solutions for axial velocity, temperature and nanoparticle concentration profiles are coded into symbolic package MATHEMATICA for easy computation of the numerical solutions. The effects of the various parameters embedded in the model are simulated graphically and discussed quantitatively and qualitatively. The results are compared with those in literature that were obtained using other approximate analytical methods and the homotopy analysis method. The study revealed that the Brownian motion, thermophoresis, buoyance and the slip parameters have significant influence on the peristaltic flow axial velocity, temperature and nanoparticle concetration profiles. In the flow without slip, both the Brownian motion and thermophoresis parameters caused a cooling effect around the channel walls and a marginal temperature enhancement in the channel

core region and significant flow reversal was noticed in the channel half-space with maximum axial velocity recording in the channel core region. In the slip flow, both Brownian motion and thermophoresis had a retardation effect on the nanoparticle concentration profile.

# Acknowledgements

First of all, I would like to thank the Almighty God for his grace that I have managed to complete this study successfully. I would like to express my deepest gratitude to my supervisor Dr Lazarus Rundora for his guidance, support and encouragement throughout my research project. I would like to thank Ms Hazel Sekgothe and Mr Conference Nkosi for their guidance on software skills. Finally, I would like to thank my family and friends for their encouragement and support, without them this dissertation and research would not have been possible.

# Dedication

To my late parents (Manaso Ben Mokgwadi and Mmasago Martha Mokgwadi) and family.

# Contents

# List of Figures

# List of Tables

# Chapter 1

# Introduction and Basic Concepts

## 1.1 General Introduction

Fluid mechanics is a field of science which deals with moving and stationary fluids. Given that most of the observable mass in space exists in a fluid state, and as we know, life is impossible without fluids, and the atmosphere and ocean that surround this planet are fluids, fluid mechanics has indisputable scientific and practical importance (White, 1979). A fluid is a substance that deforms continuously under the application of a shear (tangential) stress no matter how small the shear stress may be (Fox *et al.,* 2020). Fluids are divided into gases and liquids. Fluid mechanics has a wide range of applications in mechanical and chemical engineering, in biological systems, and in astrophysics (White, 1979).

Heat transfer fluids such as water, mineral oil and ethylene glycol play an important role in many industrial sectors, including power generation, chemical engineering, air conditioning, transportation and microelectronics. Although different methods have been applied to enhance their heat transfer, their performance is often limited due to their low thermal conductivities. The advent of nanofluids, whose heat transfer capabilities are far superior than these traditional heat transfer fluids, has led to improved performance of machines and processes that are powered by heat transfer. In this way, nanofluids have made advancement of technology possible, and with it, achievement of better life for humankind. The contribution of nanofluids to the $4^{th}$ industrial revolution cannot be over-emphasised.

The term "nanofluid" was coined by Choi (1995), who was working a with group at Argonne National Laboratory, USA, in 1995. Nanofluids are defined as colloidal solutions made out of nanoparticles, particles between 1 and 100 nanometres in size with a surrounding interfacial layer, in some base fluid. These contemporary innovative dilute suspensions of nanoparticles possess improved synergistic heat transfer enhancement characteristics as compared to the traditional base fluids. Since the size of nanoparticles are very small, nanoparticles fluidise effectively inside the base fluid and as an outcome, clogging of channels and erosion in channel walls cannot be a problem. It is even conceivable to utilize nanofluids in microchannels (Özerinç, 2010; Chein and Chuang, 2007; Lee and Mudawar, 2007). Some experimental investigations have revealed that nanofluids have remarkably higher thermal conductivities than those of ordinary pure fluids and have great potential for heat transfer improvement (Saini and Agarwal, 2016). The types of nanoparticles determine the types of nanofluids and the distinction between them. Various types of nanoparticles are used in preparation of nanofluids. CuO, $Al_2O_3$, $TiO_2$, SiC, TiC, Ag, Au, Cu and Fe are examples of nanoprticles that are commonly used. Carbon nanotubes are also used because of their extremely high thermal conductivity. The base fluids mostly used in preparation of nanofluids are usually conductive fluids such as engine oil, ethylene glycol, bio fluids, lubricants and refrigerants.

Studies have shown that nanofluids possess enhanced thermophysical properties such as thermal conductivity, viscosity, thermal diffusivity and convective heat transfer coefficients as compared to those of base fluids such as water or oil (Bairwa *et al.,* 2015; Mutuku, 2014). Nanofluid value increases with particles concentration, temperature, particle size, dispersion and stability do play an important role in determining thermal conductivity of nanofluids. Table 1.1 shows the comparison of the thermal conductivities of some selected nanopaticles and base fluids.

Table 1.1: Thermal conductivities of some selected materials (Iborra, 2012; Prasad *el al.*, 2017).

| **Materials** | **Thermal Conductivity (W/mk)** |
|---|---|
| Engine oil (EO) | 0.145 |
| Ethylene glycol | 0.253 |
| Water | 0.613 |
| Sodium | 72.3 |
| Alumina($Al_2O_3$) | 40 |
| Silicon | 148 |
| Aluminum | 237 |
| Copper | 401 |
| Fullerenes films | 0.4 |
| Graphite | 110 - 190 |
| Diamond | 2300 |
| Nanotubes | 1800 - 6600 |

It can be concluded from Table 1.1 that metals have higher thermal conductivity as compared to conventional fluids. When metallic nanoparticles are suspended into conventional fluids it could lead to an increase in the overall heat transfer coefficient.

Nanofluids are a class of heat transfer fluids that have many advantages. They possess the following advantages which make them suitable for various applications (Bairwa *et al.*, 2015; Mishra, 2014; Saidur *et al.,* 2011).

(i) High specific surface area and therefore more heat transfer surface between particles and fluids.

(ii) Reduced pumping power as compared to pure liquids to achieve equivalent heat transfer intensification.

(iii) Reduced particle clogging as compared to conventional slurries, thus promoting system miniaturization.

(iv) Adjustable properties, including thermal conductivity and surface wettability, by varying particle concentrations to suit different applications.

Table 1.2 shows the thermophysical properties such as density, specific heat capacity, thermal conductivity, volumetric thermal expansion coefficient and electrical conductivity of some base fluids and nanoparticles.

Table 1.2: Thermophysical properties of some base fluids and nanoparticles (Mutuku, 2014; Monaledi, 2020; Ahmed *et al.*, 2018)

| Material | $\rho(kg/m^3)$ | $c_p(J/KgK)$ | $k(W/mK)$ | $\beta$x$10^{-5}(K^{-1})$ | $\sigma(s/m)$ |
|---|---|---|---|---|---|
| Pure Water | 997.1 | 4179 | 0.613 | 21 | 5.5x$10^{-6}$ |
| Ethylene glycol | 1114 | 2415 | 0.252 | 57 | 1.07x$10^{-6}$ |
| Engine oil | 884 | 1909 | 0.145 | 70 | 1.00x$10^{-7}$ |
| Mineral oil | 920 | 1670 | 0.138 | 64 | 1.00x$10^{-7}$ |
| Blood | 1063 | 3594 | 0.492 | 0.18 | 6.67x$10^{-1}$ |
| Silver(Ag) | 10500 | 235 | 429 | 1.89 | 6.3x$10^{-1}$ |
| Copper(Cu) | 8933 | 385 | 401 | 1.67 | 5.96x$10^{7}$ |
| Iron(Fe) | 7870 | 460 | 80 | 58 | 1.00x$10^{7}$ |
| Aluminium(Al) | 2701 | 902 | 237 | 2.31 | 3.5x$10^{7}$ |
| Copper Oxide(CuO) | 6510 | 540 | 18 | 0.85 | 5.96x$10^{7}$ |
| Alumina($Al_2O_3$) | 3970 | 765 | 40 | 085 | 3.5x$10^{7}$ |
| Titanium Oxide(Ti$O_2$) | 4250 | 686.2 | 8.9538 | 0.9 | 2.38x$10^{6}$ |
| Iron Oxide($Fe_3O_4$) | 5180 | 670 | 80.4 | 20.6 | 1.12x$10^{5}$ |

Nanofluids can be used in various engineering applications. In industrial cooling application, the use of nanofluids will lead to great energy saving and emission reduction (Bairwa *et al.*, 2015). For example, in tyre plants, the productivity of many industrial processes are limited by the lack of facility to cool the rubber efficiently as it is being processed, and as a result lots of heat transfer fluids are therefore required. The use of water-based nanofluids can reduce the cost of production of the tyres leading to increased profit margin. When extracting energy from the earth's crust that varies in length between 5 to 10 km and temperature between 5000°C and 10000°C, nanofluids can be employed to cool the pipes exposed to such high temperatures

(Bairwa *et al.,* 2015).

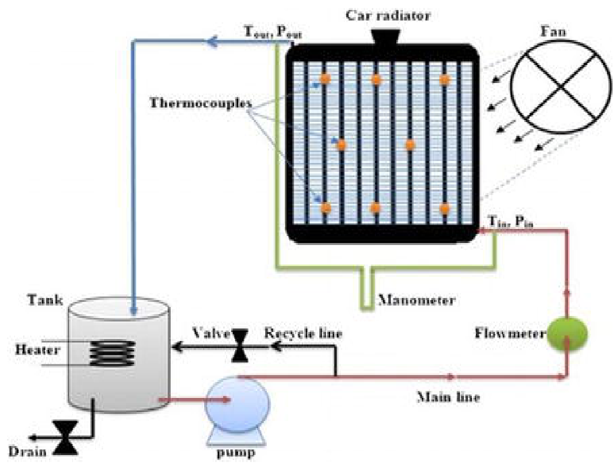


Figure 1.1: Flow diagram showing flow of nanofluid through radiator[ Source: Ali *et.al.*, 2017]

In automobiles, nanofluids are used as the cooling liquid in radiators (Fig 1.4), fuel additives, lubricants and in shock absorbers. The current engine oils, automatic transmission fluids, coolants, lubricants, and other synthetic high-temperature heat transfer fluids found in conventional truck thermal systems radiators, engines, heating, ventilation and air-conditioning (HVAC)—have inherently poor heat transfer properties (Mutuku, 2014). These could benefit from the high thermal conductivity offered by nanofluids. Nanofluids are also used in power electronics for hybrid electric vehicles. Figure 1.5 shows the the cooling of radiator using nanofluid.

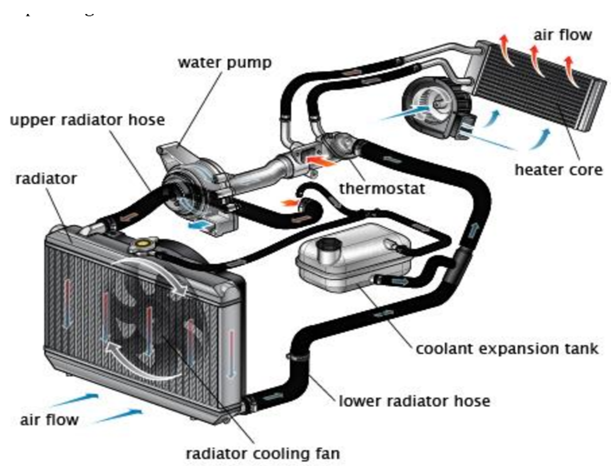


Figure 1.2: Automotive cooling system components [ Source: Molana, 2017]

Nanofluids were also developed for medical applications, including cancer therapy. Iron-based nanofluids could be used to produce higher temperatures around the tumor cells, for killing cancerous cells without affecting the nearby healthy tissues (Jordan *et. al.*, 1999). Nanofluids could also be used for safer surgery by cooling around the surgical region, thereby enhancing a patient's chance of survival and reducing the risk of organ damage (Saidur *et. al.*, 2010). Figure 1.6 is a schematic representation of the carbon-nanotubes as a drug delivery system under the influence of external magnetic field.

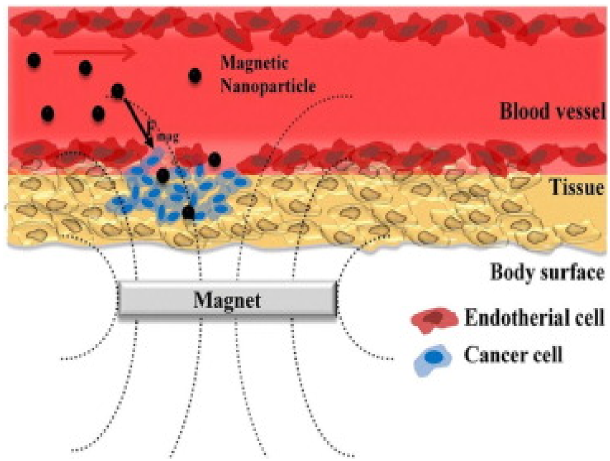


Figure 1.3: Schematic representation of the carbon-nanotubes as a drug delivery system under the influence of external magnetic field[ Source: Saleh *et.al.*, 2017]

A principal limitation on developing smaller microchips is the rapid heat dissipation (Wong and Leon, 2009). However, nanofluids can be used for liquid cooling of computer processors due to their high thermal conductivity. The manipulation of small volumes of liquid is necessary in fluidic digital display devices, optical devices, and microelectromechanical systems (MEMS) such as lab-on-chip analysis systems (Wong and Leon, 2009). This can be done by electrowetting, or reducing the contact angle by an applied voltage, the small volumes of liquid. Electrowetting on dielectric (EWOD) actuation is one very useful method of microscale liquid manipulation. Nanofluids are effective in engineering the wettability of the surface and possibly of surface tension (Wong and Leon, 2009).

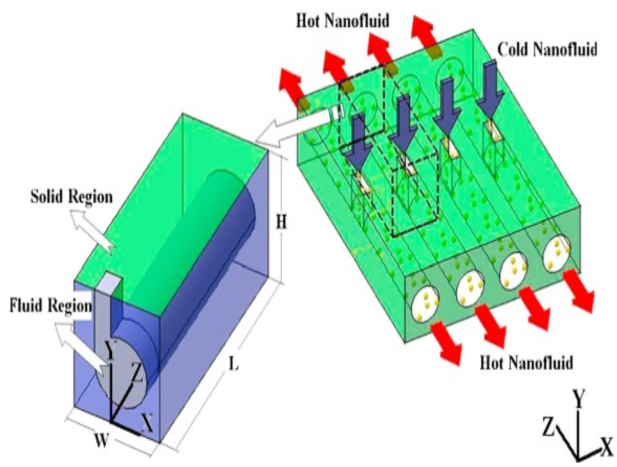


Figure 1.4: Electronics cooling with nanofluid [ Source: Bahiraei and Heshmatian, 2018]

## 1.2 Channel Flow

A channel flow is an internal flow in which the boundary wall changes the hydrodynamic structure of the flow from any state at the channel inlet to a specific state at the exit (Ibragimov, 2011). It is a very important class of flows in fluid dynamics because of its numerous applications in biological, industrial and engineering systems. Consequently, it is important to study the properties of this flow. The property of interest is how the fluid viscosity effects change the structure of the flow.

### 1.2.1 Types of Channel Flow

There are two types of channel flow, namely open channel flow and closed channel flow.

#### 1.2.1.1 Open Channel Flow

An open channel flow is defined as a flow of fluid with a free surface open to the atmosphere (Nakayama, 2018). Streams and rivers are of examples of open channel flow. Open channel flow requires constant surface pressure.

#### 1.2.1.2 Closed Channel Flow

A closed channel flow is defined as the flow of fluid through rigid boundaries such as pipes or air ducts (Nakayama, 2018). Many closed channel flows in engineering applications are either circular or rectangular in cross section.

### 1.2.2 Poiseuille and Couette flow

#### 1.2.2.1 Poiseuille Flow

Poiseuille flow is the flow between two parallel fixed plates due to an imposed constant pressure gradient (El-Mistikawy, 2018). A typical characteristic is a parabolic axial velocity profile.

#### 1.2.2.2 Couette Flow

Couette flow is flow that occurs between two moving plates or between a stationary and moving plate with the effect of viscosity due to temperature changes (El-Mistikawy, 2018). Figures 1.1 and 1.2 show examples of couette and poiseuelle flow respectively.

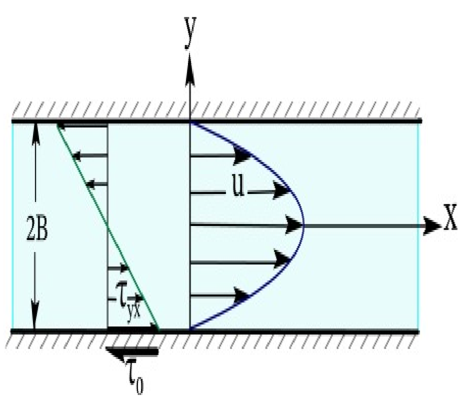


Figure 1.5: Couette flow [Source: Lai *et al.*, (2009)]

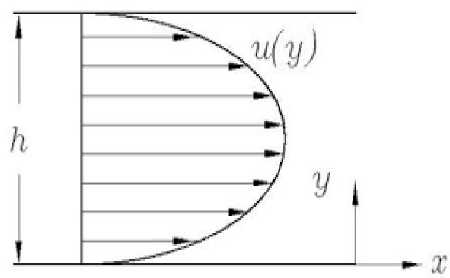


Figure 1.6: Poiseuille flow [Source: Study.com/academy/answer]

## 1.3 Microchannel

A microchannel in microtechnology is a channel with a hydraulic diameter of less than 1 millimeter (Monaledi, 2020).

## 1.4 Peristalsis

Peristalsis is an important mechanism of fluid transportation that involves area contraction or expansion of a progressive wave propagating along the flexible walls of a channel or tube.

## 1.5 Heat Transfer

Heat transfer is the transmission of heat energy through temperature gradient. Heat transfer can occur through conduction, convection and radiation mechanisms. In engineering, the term convective heat transfer is used to describe the combined effects of heat conduction. The different modes of heat transfer are illustrated in Fig 1.3.

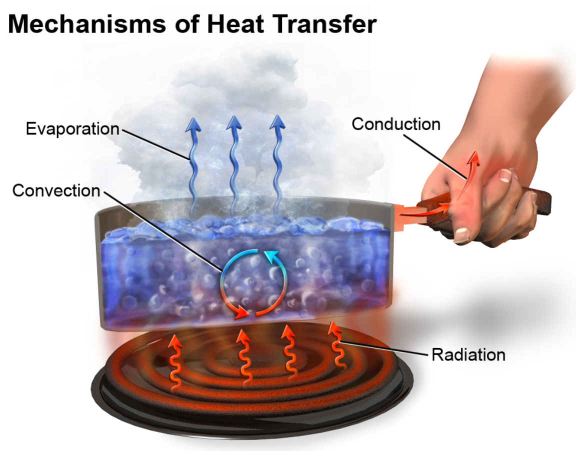


Figure 1.7: Illustration of conduction, convection and radiation heat transfer [Source: en.wikiversity.org/wiki]

### 1.5.1 Conduction

Conduction is the process by which thermal energy is transferred by collisions between adjacent atoms or molecules. Conduction occurs more readily in solids and liquids where particles are closer together than in gases where the particles are more distant.

### 1.5.2 Convection

Convective heat transfer is heat transfer between two objects through fluid flow. There are three types of convection, namely natural, forced and mixed convection.

#### 1.5.2.1 Natural Convection

Natural (free) convection is a mechanism or pattern of mass and heat transfer in which the motion of a fluid is caused only by the density differences in the fluid due to temperature gradients (Sheikholeslami and Ganji, 2017).

#### 1.5.2.2 Forced Convection

Forced convection is a mechanism of heat transfer in which the motion of the fluid is under the influence of an external force and pressure difference (Sheikholeslami and Ganji, 2017).

#### 1.5.2.3 Mixed convection

Mixed convection is the combination of forced and natural convection, which is the case for common convection when the flow is determined simultaneously by an external system.

### 1.5.3 Radiation

Radiation describes the phenomenon of heat transfer from one object to another by spreading independently of the medium. All bodies constantly emit energy by electromagnetic radiation. The strength of this energy flow depends not only on the temperature of the body, but also on the properties of the surface (Monaledi, 2020). The rate of radiant heat exchange between a small surface and a large environment is given by the specified equation

$$Q = \epsilon\sigma^* A(T_s^4 - T_{sur}^4),$$

where $\epsilon$ is the surface emissivity, $A$ is the surface area, $\sigma^*$ is the Stefan-Boltzmann constant, $T_s$ is the absolute temperature of the surface and $T_{sur}$ is the absolute temperature of the surroundings.

## 1.6 Definition of Terms

### 1.6.1 Density

The density of a fluid is defined as the ratio of the mass of fluid to the volume of the fluid. Its units are $kg/m^3$ (Nakayama, 2018). Mathematically, density, $\rho$, is represented as

$$\rho = \frac{m}{V}, \tag{1.1}$$

where $m$ is the mass of the fluid and $V$ is the volume of the fluid.

### 1.6.2 Thermal Conductivity

Thermal conductivity is a measure of an object's ability to resist heat transfer. Its units are $W/mK$ (Nave, 2000). Mathematically, thermal conductivity, $k$, is represented as

$$k = \frac{QL}{A\Delta T}, \tag{1.2}$$

where $Q$ is the heat flow,$L$ is the length of the channel, $A$ is the surface area of the material and $\Delta T$ is the temperature gradient.

### 1.6.3 Specific Heat Capacity

Specific heat capacity is defined as the ratio of the amount of energy that has to be transferred to or from one unit of mass or amount of substance to change the system temperature by one degree (Li and Yu, 2022). It is usually in $J/kgK$ and represented as

$$c_p = \frac{Q}{m\Delta T}, \tag{1.3}$$

where $c_p$ is the specific heat capacity, $Q$ is the heat flow, $m$ is the mass and $\Delta T$ is the temperature gradient.

### 1.6.4 Pressure

The pressure of a fluid is the force applied by it per unit area (Alonso and Finn, 1967). It is measured in $N/m^2$. Mathematically, the pressure $p$ at a point is defined as

$$p = \frac{F}{A}, \tag{1.4}$$

where $F$ is the force and $A$ is the area.

### 1.6.5 Temperature

Temperature is one of the thermodynamic properties of fluids that determines the state of hotness or coldness of the fluid. Temperature is measured in Kelvin (K), degrees Celsius (°C) or degrees Fahrenheit (°F) (Alonso and Finn, 1967).

### 1.6.6 Viscosity

Viscosity is a measure of a fluid's resistance to flow (Fanchi and Christiansen, 2016). Mathematically, viscosity, $\mu$, is given by

$$\mu = \rho\nu, \tag{1.5}$$

where $\rho$ is the fluid density and $\nu$ is the kinematic viscosity.

## 1.7 Fluid Parameters

### 1.7.1 Boltzmann's Constant

Boltzmann's constant is physical constant that relates the average kinetic energy of a fluid's particles and its temperature (Feynman *el al.,* 1965). Mathematically, Boltzmann's constant, $k_B$, is given by

$$k_B = \frac{pV}{NT}, \tag{1.6}$$

where $p$ is the pressure, $V$ is the volume, $T$ is the temperature and $N$ is the number of molecules of the fluid.

### 1.7.2 Reynolds Number

The Reynolds number is the ratio of the inertial forces to viscous forces (Rehm *et al.,* (2008). Mathematically, it can be defined as

$$Re = \frac{\rho v d}{\mu}, \tag{1.7}$$

where $\rho$ is the density, $v$ is the velocity, $d$ is the diameter of the channel and $\mu$ is the viscosity.

### 1.7.3 Brownian Diffusion Coefficient

The Brownian diffusion coefficient is defined as a measure of the random motion of nanoparticles within the base fluid (Buongiorno, 2006). Mathematically, the Brownian diffusion constant, $D_B$, is given by

$$D_B = \frac{k_B T}{3\pi\mu d_p}, \tag{1.8}$$

where $k_B$ is the Boltzmann's constant, $T$ is the temperature, $\mu$ is the viscosity and $d_p$ is the particle diameter.

### 1.7.4 Grashof Number

The Grashof number is a dimensionless parameter which is defined as the ratio of the buoyant to viscous forces acting on a fluid in the velocity boundary layer (Smith *et al.,* 2013). Mathematically, the Grashof number, $Gr$, is expressed as

$$Gr = \frac{g\beta(T_w - T_0)L^3}{\nu^2}, \tag{1.9}$$

where $g$ is acceleration due to gravity, $\beta$ is the coefficient of thermal expansion, $T_w$ is the wall temperature, $T_0$ is the reference temperature, $L$ is the length of the channel and $\nu$ is the kinematic viscosity.

### 1.7.5 Prandtl Number

The Prandtl number is a dimensionless number that approximates the ratio of momentum diffusivity (kinematic viscosity) to thermal diffusivity (Smith *et al.,* 2013). It is denoted as Pr, and the mathematical expression is written as

$$Pr = \frac{\nu}{\alpha}, \tag{1.10}$$

where $\nu$ is the momentum diffusivity and $\alpha$ is the thermal diffusivity.

### 1.7.6 Brinkmann Number

The Brinkmann number is a non-dimensional number that is defined as the the ratio between heat generated by viscous dissipation and heat carried by molecular conduction (Incropera *et al.*, 1996). The mathematical expression for the Brinkmann number, Br, is

$$Br = \frac{\mu v^2}{k(T_w - T_0)}, \tag{1.11}$$

where $\mu$ is the dynamic viscosity, $v$ is velocity of the fluid, $T_w$ is the temperature at the wall, $T_0$ is the reference temperature and $k$ is the thermal conductivity.

### 1.7.7 Eckert Number

The Eckert number is a dimensionless number defining the ratio between the kinetic energy of flow and the enthalpy (Monaledi, 2020). Mathematically, the Eckert number, $Ec$, is given by

$$E_c = \frac{u_w^2}{C_p(\Delta T)}, \tag{1.12}$$

where $u_w$ is the characteristic flow velocity, $C_p$ is the specific heat and $\Delta T$ is the temperature gradient.

### 1.7.8 Biot Number

The Biot number is a dimensionless number that represents the ratio of the resistance to heat transfer from the inside of the body to the surface of the body (Incropera *et al.*, 1996). Mathematically, the Biot number, $Bi$, is represented as

$$Bi = \frac{hL}{k}, \tag{1.13}$$

where $h$ is the convective heat transfer coefficient, $L$ is the charactaristic length and $k$ is the thermal conductivity.

### 1.7.9 Thermophoresis

Thermophoresis is a phenomenon where the particles of a fluid diffuse under the effect of the temperature gradient (Buongiorno, 2006). This phenomenon tend to move light molecules to elevated temperature regions and heavy molecules to depressed temperature regions. This is the so-called soret effect. Dufour effect is the energy flux caused by concentration differences (Srinivasacharya *et al.,* 2015).

## 1.8 Properties of Nanofluids

### 1.8.1 Density

Density ($\rho$) is a factor that affects heat transfer properties. It is an important thermophysical property such that it plays an important role in evaluating heat transfer performances of nanofluids. It directly affects the Reynolds number, friction factor, pressure loss, and Nusselt number. However, reports on the effect of density are found to be scarce (Deshmukh *et al.,* 2019). Since the nanoparticle's density is higher than that of liquids, an increase in the volume concentration of the nanoparticles would lead to increased density values of the nanofluid. Most researchers obtain the theoretical density values from the mixing equation

$$\rho_{nf} = \rho_f(1-\sigma) + \rho_p\sigma, \tag{1.14}$$

as reported by Pak and Choi (Deshmukh *et al.,* 2019). Here, $\rho$ is the density, $\sigma$ is the volume concentration, and nf, f and p subscripts refer to nanofluid, base fluid and nanoparticle respectively.

### 1.8.2 Specific Heat Capacity

Specific heat capacity ($C_p$) measures the quantity of heat absorbed per unit mass of the material when its temperature increases. It is important to acquire accurate values of the specific heat capacity as it is used to calculate important properties, which include thermal conductivity, thermal diffusivity and the flow's spatial temperature. Researchers mostly use deferential scanning calorimeter (DSC) and double hot wire to measure the specific heat capacity of nanofluids. Several models are used to predict the $C_p$ values of nanofluids at different conditions. One model is based on a mixture of liquid and nanoparticle and is stated as (Deshmukh *et al.,* 2019),

$$C_{nf} = C_f(1 - \sigma) + C_p\sigma. \tag{1.15}$$

### 1.8.3 Thermal Conductivity

Thermal conductivity ($k$) is the rate at which a material passes heat. It is a major factor in determining nanofluid efficiency in heat transfer. The rate of heat transfer by conductivity through solids is much higher than that through liquids and gases. It is for this reason that nanofluids have higher $k$ values compared to their base fluids. From the experimental results of many researchers, it was found that the thermal conductivity of nanofluids depends on parameters including, the thermal conductivity of base fluids and the particles, volume fraction, the surface area, the shape of the nanoparticles and the temperature (Wang and Mujumdar, 2008). There are several methods used to measure the thermal conductivity of a material. Transient hot wire method, thermal constants analyzer, steady state parallel plate and $3\omega$ are some of the methods. Among all these techniques the most commonly used method is transient hot wire method (Deshmukh *et al.,* 2019).

### 1.8.4 Viscosity

Viscosity ($\mu$) is the most important parameter in determining the convective heat transfer coefficient. However, this property is difficult due to lack of understanding of viscosity mechanism and lack of a general mathematical model that predicts the behavior of viscosity of nanofluids (Deshmukh *et al.,* 2019). Several mathematical models were developed to predict the viscosity of nanofluids. The first model is Einstein's model of effective viscosity for suspended rigid spherical solids in liquids as a function of volume. The model was developed in 1906 and it was derived from linear hydrodynamic equations. This model only predicts the viscosity for spherical rigid particles and for a low particle concentration. Nowadays viscometers are mostly used to measure the viscosity of nanofluids. The viscosity of nanofluids depends on various factors such as volume concentration, particle size, shear rate, temperature and morphology (Deshmukh *et al.,* 2019).

## 1.9 Preparation Methods for Nanofluids

Preparation of nanofluids is the intial key step in experimental studies with nanofluids. Nanofluids are not just scattering of solid particles in a fluid. The basic requirements that a nanofluid must satisfy are even and stable suspension, durable suspension, negligible agglomeration of particles, no chemical change of the fluid (Bairwa *et al.,* 2015). In the synthesis of nanofluids, agglomeration is a major problem. There are mainly two methods used to synthesize nanofluids, namely the single-step method and the two-step method (Deshmukh *et al.,* 2019).

### 1.9.1 Single-Step Method

The single-step method consists of simultaneously producing and dispersing the nanoparticles directly into a base fluid. The method is good for metallic nanofluids. The single-step processes prepares consistently dispersed nanoparticles and the particles can be stably suspended in the base fluid. This method avoids processes such as drying, storage, transportation and dispersion of nanoparticles, so that the agglomeration of nanoparticles is minimized and stability of fluids is increased (Mutuku, 2014; Iborra, 2012).

The vacuum submerged arc nanoparticle synthesis system is another useful method to prepare nanofluids using dielectric liquids. This method was developed by (Lo *et al.*, 2005) to prepare Cu-based nanofluids. The different morphologies are mainly influenced and determined by various thermal conductivity properties of the dielectric liquids. The nanoparticles prepared exhibit neddle-like, polygonal, square and circular morphological shapes. The method avoids undesired nanoparticles agglomeration fairly well.

### 1.9.2 Two-Step Method

The two step method is the most commonly used method for preparing nanofluids (Bairwa *et al.,* 2015). In this method, nanoparticles, nanofibres, nanotubes or any other nanomaterials are initially produced as dry powders by using chemical or physical methods (Mutuku, 2014). Thereafter the nanosized powder will be dispersed into a fluid in the second processing step with the help of intensive magnetic force agitation, ultrasonic agitation, high shear mixing, homogenizing and ball willing. The two-step method is the most economic method to produce nanofluids in large scale, since nanopowders synthesis techniques have already been scaled up to industrial production levels (Mutuku, 2014). The main disadvantage of the two-step technique is that the nanoparticles form clusters during the preparation of the nanofluid which prevents the proper dispersion of nanoparticles inside the base fluid (Özerinç, 2010) .

## 1.10 Basic Equations Governing Nanofluid Flow

By following (Sheikholeslami and Ganji, 2017; Mutuku, 2014; Monaledi, 2020), the governing equations for nanofluid flow are described in the following section.

### 1.10.1 Continuity Equation

The continuity equation is derived from the law of conservation of mass, which states that "mass cannot be created or destroyed". This implies that the rate of change of particle mass is zero. The equation of continuity is

$$\frac{\partial \rho}{\partial t} + \nabla . \rho V = 0, \tag{1.16}$$

where $\rho$ is the density, $V$ is the velocity vector and $t$ is the time. For an incompressible fluid, $\rho$ is constant so that equation (1.16) reduces to

$$\nabla . V = 0. \tag{1.17}$$

### 1.10.2 Navier-Stoke's (Momentum) Equation

The equation of momentum is derived based on Newton's second law of motion

$$\sum F = ma,$$

where $F$ is the net force, $m$ is the mass and $a$ is the acceleration . The Navier-Stokes equation for a nanofluid is given as

$$\rho_f \left[ \frac{\partial V}{\partial t} + (V.\nabla)V \right] = -\nabla P + \mu \nabla^2 V + \mathbf{f}, \tag{1.18}$$

where $V$ is the velocity vector, $P$ is the pressure, $\rho_f$ is the nanofluid density, $\mu$ is the dynamic viscosity of the nanofluid, $t$ is the time and $\mathbf{f}$ is the body forces.

### 1.10.3 Thermal Energy Equation

The thermal energy equation is derived from the first law of thermodynamics, which states that the amount of heat added to a system $dQ$ equals to the change in internal energy $dE$ plus the work done $dW$ , that is

$$dQ = dE + dW.$$

In other words, if net energy transfer to a system occurs, the energy stored in the system must increase by an amount equal to the energy transferred. The First Law of Thermodynamics requires that

$$(\rho c)_f \left[ \frac{\partial T}{\partial t} + (V.\nabla)T \right] = k \nabla^2 T + \mu_f \Theta + q''', \tag{1.19}$$

where $(\rho c)_f$ is the nanofluid specific heat capacity, $\Theta$ is the viscous dissipation term, $T$ is the nanofluid temperature, $k$ is nanofluid thermal conductivity and $q'''$ is heat source term.

### 1.10.4 Nanoparticle Volume Fraction Equation

The equation is derived based on the Ficks law of mass transfer of nanoparticles and the dispersion rate of nanoparticles in the base fluid coupled with the thermophoresis and Brownian motion effects and is stated as,

$$\frac{\partial C}{\partial t} + (V.\nabla)C = D_B \nabla^2 C + \left(\frac{D_T}{T_0}\right)\nabla^2 T, \tag{1.20}$$

where $C$ is the nanoparticles concentration, $D_B$ is the Brownian diffusion coefficient, $D_T$ is the thermophoresis diffusion coefficient, $T$ is the temperature and $T_0$ is the reference temperature.

## 1.11 Wave Equation

The wave equation is one of the most important second-order linear partial differential equations (Rapp, 2016). It usually describes sound waves, light waves, water waves, the vibrating string, or a membrane or the transmission of electric signals in a cable. Such waves are described by a wave equation which sets out how the disturbance proceeds over time. Depending on the type of a wave, the mathematical form of this equation varies. It is a good description for a wide range phenomena because it is typically used to model small oscillations about an equilibrium, for which system can often be approximated by Hook's law. The wave equation arises in fields like acoustics, electromagnetics and fluid dynamics. The solutions to the wave equation are important in fluid dynamics and also play an important role in magnetism, optics, gravitational physics and heat transfer. The wave equation has many dimensions depending on the field of interest. The one-dimensional wave equation was discovered by d'Alembert in 1746, and within ten years, Euler discovered the three-dimensional wave equation (Speiser, 2008). The one dimensional wave equation is represented as

$$\frac{\partial^2 u}{\partial t^2} = c^2 \frac{\partial^2 u}{\partial x^2}, \tag{1.21}$$

where $u$ is the velocity of the string, $t$ is the time, $T$ is the tension of the string, $\rho$ is the density of the string and

$$c^2 = \frac{T}{\rho}.$$

## 1.12 Problem Statement

Nanofluids are colloidal solutions made out of nanoparticles, particles between 1 and 100 nanometres in size with a surrounding interfacial layer, in some base fluids. These contemporary innovative dilute suspensions of nanoparticles, pioneered by Choi (1995) possess improved synergistic heat transfer enhancement characteristics as compared to the traditional base fluids. The type of nanoparticles determine the types of nanofluids and the distinction between them. The most common used nanoparticles are alumina ($AI_2O_3$), copper oxide (CuO) and copper (Cu). Examples of the base fluids commonly used are oils, water, ethylene glycol, bio fluids, lubricants and refrigerants. Advancement of technology is to a large extent dependent on heat transfer, and the advent of nanotechnology has greatly improved such advancement.

Peristalsis is an important mechanism of fluid transportation that involves area contraction or expansion of a progressive wave propagating along the flexible walls of a channel or tube. In physiology, the transport of urine from kidney to bladder, the swallowing of food through the oesophagus, ovum movement in the female fallopian tube, motion of chyme in various sizes of the intestine, blood circulation in arterioles and veins, etc, are all peristaltic processes (Abbasi *et al.*, 2015; Hayat et al., 2016; Nadeem *et al.*, 2009). Industrially, peristaltic transport is encountered in, for instance, roller and finger pumps, magnetohydrodynamic pumps, sanitary fluid transport, and transport of corrosive fluids (Vasudev *et al.*, 2011).

Due to the important role of nanofluids and peristalsis, this theoretical study is focussed on a detailed analysis of the dynamics of peristaltic nanofluid flow and heat transfer in a microchannel. Such a study has far reaching implications in, for instance, medical applications. In particular, peristaltic mechanism in presence of heat transfer is regarded very useful in the haemodialysis and oxygenation process (Hayat *et al.*, 2016). Further, nanofluids have been recommended as the heat transfer fluid in solar energy conversion systems and in many other industrial devices. In general, industrial productivity, sustainability, efficiency and competitiveness require engineering solutions, and these solutions are reliant on mathematical models.

Mathematical modelling, in particular modelling with differential equations, is a pertinent tool for engineering solutions. By transitivity, since engineering is the driver of advancement of technology, mathematical modelling therefore contributes significantly to civilisation. Most scientific and engineering problems are modelled mainly by nonlinear differential equations, and since these equations are solvable mostly by numerical methods, there is need for on-going efforts to refine and improve solution techniques to achieve computational efficiency. In this way, this work will contribute significantly to the body of knowledge in applied mathematics. Further, since nanofluid flow and heat transfer have pertinent applications as alluded to earlier, the investigation herein will also contribute to a systematic understanding of such flow systems as they are applied to the mentioned real life situations.

At a time when the world is fast moving towards complete decarbonisation of industry, South Africa is still highly reliant on fossil fuels for its energy needs (Tian and Zhao, 2013). While the country has already heeded the call to transform from fossil fuels (coal, petroleum and natural gas) to renewable energy sources for meeting electricity needs, to date not enough attention has been paid to the potential of renewable energy in industrial applications. The continued risk of ozone depletion has also placed sharp focus for South Africa and the world to reduce carbon emission significantly by 2030 (IPCC report, 2018). Alternative sustainable clean energy sources like wind and solar are currently considered. South Africa is endowed with some of the highest levels of solar irradiation in the world. The low thermal conductivity of the heat transfer fluid in solar energy conversion systems has been cited as the cause for their low thermal performance, among other shortfalls. Replacing the heat transfer fluid with nanofluid has been touted as a viable option owing to the improved heat transfer characteristic and thermal properties of nanofluids. In medicine, nanoparticles are also used for targeted treatment of cancerous cells in the body. The heat transfer enhancement capability of nanofluids has also seen them more suitable for use in heat pipes and compact heat exchangers for electronic equipment, spacecraft thermal control and automotive and residential air conditioning systems.

## 1.13 Aim of the Study

The aim of study is to investigate the dynamics of peristaltic nanofluid flow in a microchannel.

## 1.14 Objectives of the Study

The objectives of the study are to:

(i) Develop a mathematical model for peristaltic nanofluid flow in a microchannel.

(ii) Solve the model equations using the semi-analytic Adomian decomposition method .

(iii) Analyse the effects of the various thermophysical parameters embedded in the flow system on the velocity and temperature profiles and nanoparticle concentration profiles

(iv) Compare the results with those from similar studies by other methods in literature.

## 1.15 Research Methodology

Due to the nonlinear nature of the equations involved in this study, analytical solutions are not entirely possible. A myriad of numerical techniques can be applied to solve nonlinear differential equations. In this study we resort to semi-analytical Adomian decomposition method (ADM). This choice is informed by the desirable characteristics of ADM that we found in literature.

### 1.15.1 Adomian Decomposition Method

ADM is a semi-analytic method used to solve, effectively, a large class of linear and non-linear ordinary and partial differential equations. It was first established by George Adomian in the $1980's$ and is well addressed in literature (Tomaizeh, 2017; Wazwaz, 2009). The ADM consists of splitting the given equation into linear and nonlinear parts, inverting the highest-order derivative operator contained in the linear operator on both sides, identifying the initial and/or boundary conditions. The terms involving the independent variable alone as initial approximation, decomposing the unknown function into a series whose components are to be determined. Decomposing the nonlinear function into some special polynomials called Adomian polynomials. To find the successive terms of the series solution by recurrent relation using Adomian polynomials (Asha and Deepa, 2019). The advantages of using ADM over other methods is that firstly, it reduces the computational difficulties to the series solutions. Secondly, it provides an analytic, verifiable and fast convergence approximation. Thirdly, it is an efficient and accurate tool for obtaining analytical solutions for linear and nonlinear equations.

## Basics of ADM

Consider the equation

$$F(u(t)) = g(t),$$

where $F$ represents a general nonlinear ordinary or partial differential operator including both linear and nonlinear terms. The linear terms are decomposed into $L + R$, where $L$ is easily invertible (usually the highest order derivative) and $R$ is the remainder of the linear operator. Thus, the equation can be written as

$$Lu + Nu + Ru = g, \tag{1.22}$$

where $Nu$ indicates the nonlinear terms and $g$ is an inhomogeneous term. Applying the inverse operator $L^{-1}$ in equation (1.22) and re-arranging the terms, we get

$$L^{-1}Lu = L^{-1}g - L^{-1}Ru - L^{-1}Nu. \tag{1.23}$$

If $L$ is a second-order operator, $L^{-1}$ is a double indefinite integral. By solving equation (1.23) for $u$ we have

$$u = A + Bt + L^{-1}g - L^{-1}Ru - L^{-1}Nu, \tag{1.24}$$

where A and B are constants of integration and can be found by applying the boundary or initial conditions. ADM suggests that the solution of $u$ can be represented as the decomposition series

$$u = \sum_{n=0}^{\infty} u_n, \tag{1.25}$$

and the nonlinear term $Nu$ can be equated to an infinite series ploynomials

$$Nu = \sum_{n=0}^{\infty} A_n, \tag{1.26}$$

where $A_n$ are the Adomian polynomials. Substituting equation (1.25) and (1.26) into equation (1.24) yields

$$\sum_{n=0}^{\infty} u_n = A + Bt + L^{-1}g - L^{-1}R\left(\sum_{n=0}^{\infty} u_n\right) - L^{-1}\left(\sum_{n=0}^{\infty} A_n\right). \tag{1.27}$$

The various components $u_n$ of the solution $u$ can be determined easily by using the recursive relation

$$u_0 = A + Bt + L^{-1}g, \tag{1.28}$$

$$u_{k+1} = -L^{-1}(Ru_k) - L^{-1}(A_k), \quad k \geq 0. \tag{1.29}$$

The Adomian polynomials are calculated using the formula

$$A_n = \frac{1}{n!}\frac{d^n}{d\lambda^n}\left[N\left(\sum_{n=0}^{\infty} \lambda^i u_i\right)\right]_{\lambda=0}, \qquad n = 0, 1, 2, 3, \ldots \tag{1.30}$$

## 1.16 Outline of the Dissertation

The dissertation is organised as follows:

## Chapter One

This chapter presents a basic introduction, the definitions of terms, a review of nanofluids, applications of nanofluids, problem statement, aim and objectives of the study and research methodology. The chapter furthermore expresses the basic equations governing nanofluids flow such as continuity equation, momentum equation, energy equation, concentration transport equation and provides thermophysical properties of nanoparticles and base fluids.

## Chapter Two

This chapter presents the literature review and the significance of the study.

## Chapter Three

This chapter presents an analysis of peristaltic flow of a nanofluid through a two dimensional microchannel. The governing equations are non-dimensionalised and solved using ADM. The numerical results are obtained using Mathematica and are discussed.

## Chapter Four

This chapter investigates peristaltic flow of a nanofluid through a two dimensional microchannel with slip effects. The governing equations are non-dimensionalised and solved using ADM. The numerical results are obtained from Mathematica Software and are discussed.

## Chapter Five

This chapter concludes the dissertation with a general discussion, conclusions, recommendations and future research work.

# Chapter 2

# Literature Review

## 2.1 Literature Review

Nanofluids are potential heat transfer fluids with enhanced thermophysical properties and heat transfer performance and can be applied in many devices for better performance (Saidur *et al.*, 2011). Thermophysical properties like thermal conductivity, thermal diffusivity, viscosity and convective heat transfer coefficients are invariably boosted in nanofluids compared to those of base fluids (Wong and De Lean, 2010). Several experimental and theoretical investigations were conducted in order to establish the efficacy of nanofluids in dealing with various heat transfer problems emanating from engineering and industrial processes.

A mathematical model for mass, momentum and heat transport in nanofluids was developed by (Buongiorno, 2006). This ground breaking stride opened a whole new modelling landscape of the dynamics of nanofluid flow and heat transfer. Tripathi and Bég (2014) studied the peristaltic flow of nanofluid through a two-dimensional channel. The analysis was conducted based on the long wavelength and low Reynolds number approximations. In their investigations, the authors concluded that the nanoparticle fraction profile diminishes with increasing Brownian motion parameter while the thermophoretic parameter enhanced it. It was also revealed that both the Brownian motion parameter and thermophoresis parameter suppress the axial velocity profile but the temperature profile was enhanced. Bibi and Xu (2019) developed a mathematical model to examine the behaviour of a peristaltic flow with nanoparticles in a symmetric channel under the influence of a magnetic field. It was found that the temperature profile enhanced but the nanoparticles' volume fraction profiles lowered with increase in the Hartman number. Hayat *et al.* (2016) studied the impact of thermal radiation on peristaltic flow of nanofluid in a channel satisfying wall properties and convective conditions. It was observed that the thermal radiation parameter and the Biot number have opposing effects on the fluid temperature and concentration and that the heat transfer coefficient decreases when thermal radiation parameter is increased. Mallick and Misra (2019) studied electro-kinetic peristaltic flow Eyring-Powell nanofluid in an asymmetric wavy microchannel. The study showed that an increase in the volume fraction of the nanoparticles in the nanofluid can considerably enhance the momentum flow in the core region of the microchannel. Akbar *et al.* (2012) studied a peristaltic flow of a nanofluid in an asymmetric channel with slip conditions. The governing equations for the nanofluid were presented and simplified using long wave length and small Reynolds number approximations. The authors concluded that the nanoparticle concentration profile decreases with an increase in the concentration slip parameter and the thermophoresis parameter. It was also concluded that both the thermal slip parameter and the thermophoresis parameter enhanced the temperature profile and the Grashof number and the Brownian motion parameter have opposite effects on the velocity profile.

Modelling the dynamics of peristaltic nanofluid flow gives rise to nonlinear constitutive differential equations that are complex to solve analytically. Thus, although such flows have been studied, there is no conclusive understanding of the dynamics of peristaltic nanofluid flow. Research in this area is ongoing. For instance, although nanofluids offer better thermal behaviour to produce more uniform temperature distribution, the main concern of nanofluid is its stability at various temperatures, hence more investigations in this field are still needed. A form of fluid transport where the fluid flow is driven by a progressive wave of contraction or expansion which propagates along the length of a dilatable tube containing fluids is referred to as peristaltic pumping (Tripathi and Bég, 2014). The authors note that in such flows heat transfer plays an important role and peristalsis strongly influences heat transfer dynamics. The paper also states that although the influence of heat transfer on peristaltic flow of Newtonian and non-Newtonian fluids has been extensively studied, the same cannot be said for nanofluids. Despite the many applications of peristaltic nanofluid flow in biology, medical pharmacology, engineering and technology, very few studies have been undertaken.

The wide work that Tripathi has undertaken on peristaltic fluid transport includes the study of transient peristaltic heat flow through a finite porous channel (Tripathi, 2013). Mathematical modelling of heat transfer effects on swallowing dynamics of viscoelastic food bolus through the human oesophagus was studied by (Tripathi *et al.*, 2013). Tripathi and Bég (2012) investigated unsteady physiological magneto-fluid flow and heat transfer through a finite length channel by peristaltic pumping. The authors concluded that the magnetic parameter decreases the velocity and the temperature profiles. It was also observed that the temperature profile decreases with an increase in the Biot number and the Soret and the Schmidt numbers cause a drop in the concentration profiles.

# Chapter 3

# Adomian Decomposition Method for Peristaltic Flow of a Nanofluid Through a Two Dimensional Microchannel

In this chapter we consider the problem studied by Tripathi and Bég (2014) as stated in chapter 2. We non-dimensionalise the equations and apply the semi-analytic Adomian decomposition method to solve the non-dimensionalised equations. The method is implemented in symbolic package MATHEMATICA and the numerical solution for velocity, temperature and nanoprticle concentration is compared with the results obtained in Tripathi and Bég (2014) where an approximate analytic solution technique was applied.

## 3.1 Mathematical Model

The equation that constitutes the geometry of the wall (Fig. 3.1) due to wave propagation is defined as

$$\tilde{h}(\tilde{x},\tilde{t}) = d + b\sin\frac{2\pi}{\lambda}(\tilde{X} - c\tilde{t}), \tag{3.1}$$

where $\tilde{h}$ is the transverse vibration of the wall, $\tilde{x}$ is the axial coordinate, $\tilde{t}$ is the time, $d$ is the half width of the channel, $b$ is the amplitude of the wave, $\lambda$ is the wavelength and $c$ is the wave speed. We consider the peristaltic nanofluid flow in a channel where the wall surface has sine wave form as depicted in Fig. 3.1. The values of temperature ($T$) and the nanoparticle volume fraction ($C$) at the center line ($y = 0$) and the wall of the channel ($y = h$) are taken as $T_0,\ C_0$ and $T_1,\ C_1$ respectively.

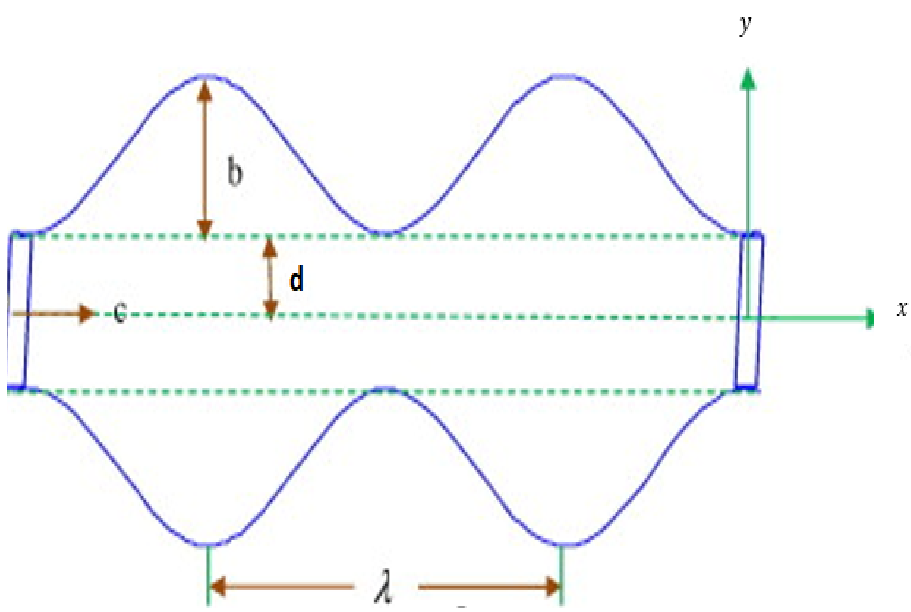


Figure 3.1: Geometry of the peristaltic nanofluid flow

Transformations between the fixed and moving frames are related as

$$\tilde{x} = \tilde{X} - c\tilde{t}, \quad \tilde{y} = \tilde{Y}, \quad \tilde{u} = \tilde{U} - c, \quad \tilde{v} = \tilde{V}, \quad \tilde{p}(\tilde{x}) = \tilde{P}(\tilde{X},\tilde{t}), \tag{3.2}$$

where $(\tilde{x},\tilde{y})$ are the coordinates in the moving frame, $(\tilde{u},\tilde{v})$ are the velocity components in the moving frame, $\tilde{P}(\tilde{X},\tilde{Y},\tilde{t})$ and $\tilde{p}(\tilde{x},\tilde{y})$ are the pressure in fixed and moving frames respectively, $(\tilde{X},\tilde{Y})$ are the coordinates in fixed frame and $(\tilde{U},\tilde{V})$ are the velocity components in fixed frame. The continuity, momentum, energy and nanoparticle concentration are given as Akbar *et al.* (2012),

$$\nabla.\tilde{V} = 0, \tag{3.3}$$

$$\rho_f\left[\frac{\partial \tilde{V}}{\partial \tilde{t}} + (\tilde{V}.\nabla)\tilde{V}\right] = -\nabla\tilde{P} + \mu\nabla^2\tilde{V} + \mathbf{f}, \tag{3.4}$$

$$(\rho c)_f\left[\frac{\partial \tilde{T}}{\partial \tilde{t}} + (\tilde{V}.\nabla)\tilde{T}\right] = k\nabla^2\tilde{T} + (\rho c)_p\left[D_B\nabla\tilde{C}\nabla\tilde{T} + \left(\frac{D_{\tilde{T}}}{\tilde{T}_0}\right)\nabla\tilde{T}\nabla\tilde{T}\right], \tag{3.5}$$

$$\frac{\partial \tilde{C}}{\partial \tilde{t}} + (\tilde{V}.\nabla)\tilde{C} = D_B\nabla^2\tilde{C} + \left(\frac{D_{\tilde{T}}}{\tilde{T}_0}\right)\nabla^2\tilde{T}. \tag{3.6}$$

where $\rho_f$ is the density of the fluid, $\rho_p$ is the density of the particle, $\mu$ is the viscosity, $c$ is the volumetric volume expansion coefficient, $\tilde{V}$ is the velocity vector, $\mathbf{f}$ is the body forces, $\tilde{P}$ is the pressure, $\tilde{C}$ is the nanoparticle volume fraction, $\tilde{T}$ is the temperature, $(\rho c)_f$ heat capacity of fluid, $(\rho c)_p$ is the effective heat capacity of nanoparticles, $k$ is the thermal conductivity, $D_B$ is the Brownian motion coefficient, $D_{\tilde{T}}$ is the thermophoretic diffusion coefficient and $\tilde{T}_0$ is the reference temperature.

The two-dimensional equations for nanofluid are as in Tripathi and Bég (2012) and are stated as

$$\frac{\partial \tilde{u}}{\partial \tilde{x}} + \frac{\partial \tilde{v}}{\partial \tilde{y}} = 0, \tag{3.7}$$

$$\rho_f\left[\frac{\partial \tilde{u}}{\partial \tilde{t}} + \tilde{u}\frac{\partial \tilde{u}}{\partial \tilde{x}} + \tilde{v}\frac{\partial \tilde{u}}{\partial \tilde{y}}\right] = -\frac{\partial \tilde{P}}{\partial \tilde{x}} + \mu\left[\frac{\partial^2 \tilde{u}}{\partial \tilde{x}^2} + \frac{\partial^2 \tilde{u}}{\partial \tilde{y}^2}\right] + g(1-C_0)\rho_{f0}\beta(T-T_0) - g(-\rho_{f0}+\rho_p)(C-C_0), \tag{3.8}$$

$$\rho_f\left[\frac{\partial \tilde{v}}{\partial \tilde{t}}+\tilde{u}\frac{\partial \tilde{v}}{\partial \tilde{x}}+\tilde{v}\frac{\partial \tilde{v}}{\partial \tilde{y}}\right]=-\frac{\partial \tilde{P}}{\partial \tilde{y}}+\mu\left[\frac{\partial^2 \tilde{v}}{\partial \tilde{x}^2}+\frac{\partial^2 \tilde{v}}{\partial \tilde{y}^2}\right]+g(1-C_0)\rho_{f0}\beta(T-T_0)-g(-\rho_{f0}+\rho_p)(C-C_0), \tag{3.9}$$

$$\left[\frac{\partial T}{\partial \tilde{t}}+\tilde{u}\frac{\partial T}{\partial \tilde{x}}+\tilde{v}\frac{\partial T}{\partial \tilde{y}}\right]=\alpha\left[\frac{\partial^2 T}{\partial \tilde{x}^2}+\frac{\partial^2 T}{\partial \tilde{y}^2}\right]+\tau\left[D_B\left(\frac{\partial C}{\partial \tilde{x}}\frac{\partial T}{\partial \tilde{x}}+\frac{\partial C}{\partial \tilde{y}}\frac{\partial T}{\partial \tilde{y}}\right)+\frac{D_T}{T_0}\left(\left(\frac{\partial T}{\partial \tilde{x}}\right)^2+\left(\frac{\partial T}{\partial \tilde{y}}\right)^2\right)\right], \tag{3.10}$$

$$\left[\frac{\partial C}{\partial \tilde{t}}+\tilde{u}\frac{\partial C}{\partial \tilde{x}}+\tilde{v}\frac{\partial C}{\partial \tilde{y}}\right]=D_B\left[\frac{\partial^2 C}{\partial \tilde{x}^2}+\frac{\partial^2 C}{\partial \tilde{y}^2}\right]+\frac{D_T}{T_0}\left[\frac{\partial^2 T}{\partial \tilde{x}^2}+\frac{\partial^2 T}{\partial \tilde{y}^2}\right], \tag{3.11}$$

where $\tilde{u}$ is the axial velocity, $\tilde{v}$ is the transverse velocity, $\tilde{p}$ is the pressure, $g$ is acceleration due to gravity, $\beta$ is the volumetric expansion coefficient of the fluid, $\rho_{f0}$ is the nanofluid density at the reference temperature, $\alpha = \dfrac{k}{(\rho c)_f}$ is the thermal diffusivity and $\tau = \dfrac{(\rho c)_p}{(\rho c)_f}$ is the ratio between the effective heat capacity of nanoparticle material and heat capacity of the fluid. The boundary conditions are

$$\frac{\partial \tilde{u}}{\partial \tilde{x}}=0, \quad at \quad \tilde{y}=0, \qquad \tilde{u}=0, \quad at \quad \tilde{y}=\tilde{h}, \tag{3.12}$$

$$T=T_0, \quad at \quad \tilde{y}=0, \qquad T=T_1, \quad at \quad \tilde{y}=\tilde{h}, \tag{3.13}$$

$$C=C_0, \quad at \quad \tilde{y}=0, \qquad C=C_1, \quad at \quad \tilde{y}=\tilde{h}. \tag{3.14}$$

In order to convert the governing equations and boundary conditions into dimensionless form, we introduce the dimensionless variables (Tripathi and Bég, 2012; Bibi and Xu, 2019)

$$\begin{gathered}
x=\frac{\tilde{x}}{\lambda}, \quad y=\frac{\tilde{y}}{d}, \quad t=\frac{c\tilde{t}}{\lambda}, \quad u=\frac{\tilde{u}}{c}, \quad \Phi=\frac{b}{d}, \quad p=\frac{\tilde{p}d^2}{\mu c\lambda}, \quad v=\frac{\tilde{v}}{c\delta}, \quad \delta=\frac{d}{\lambda}, \\
\nu=\frac{\mu}{\rho_{f_0}}, \quad h=\frac{\tilde{h}}{d}, \quad Re=\frac{\rho_f cd}{\mu}, \quad \theta=\frac{T-T_0}{T_1-T_0}, \quad \sigma=\frac{C-C_0}{C_1-C_0}, \\
N_b=\frac{\tau D_B(C_1-C_0)}{\alpha}, \quad N_t=\frac{\tau D_T(T_1-T_0)}{\alpha T_0}, \quad Pr=\frac{\nu}{\alpha}, \quad S_c=\frac{\mu}{\rho D_B}, \\
Gr_T=\frac{g\beta d^3(1-C_0)(T_1-T_0)}{\nu^2}, \quad Gr_C=\frac{gd^3(\rho_f-\rho_{f0})(C_1-C_0)}{\rho_{f0}\nu^2},
\end{gathered} \tag{3.15}$$

where $x$ is dimensionless axial coordinate, $y$ is the dimensionless transverse coordinate, $t$ is dimensionless time, $\delta$ is the dimensionless wave number, $c$ is the constant speed of channel walls, $u$ and $v$ are dimensionless axial and transverse velocity components, $\Phi$ is the amplitude ratio, $h$ is transverse vibration of the wall, $p$ is dimensionless pressure, $\nu$ is nanofluid kinematic viscosity, $Re$ is Reynolds number, $\theta$ is the dimensionless temperature, $\sigma$ is the dimensionless nanoparticle volume fraction, $Gr_T$ is the thermal Grashof number, $Gr_C$ is species Grashof number, $N_b$ is the Brownian motion parameter, $N_t$ is the thermophoresis parameter and $Pr$ is the Prandtl number.

Equation (3.7) in dimensionless form can be expressed as

$$\frac{\partial(cu)}{\partial(x\lambda)}+\frac{\partial(c\delta v)}{\partial(dy)}=0,$$

$$\implies \frac{c}{\lambda}\frac{\partial u}{\partial x}+\frac{c\delta}{d}\frac{\partial v}{\partial y}=0,$$

$$\implies \frac{c\delta}{d}\frac{\partial u}{\partial x}+\frac{c\delta}{d}\frac{\partial v}{\partial y}=0.$$

Multiplying by $\frac{d}{c\delta}$, we have

$$\frac{\partial u}{\partial x}+\frac{\partial v}{\partial y}=0. \tag{3.16}$$

Equation (3.8) in dimensionless form can be expressed as

$$\rho_f\left[c\frac{\partial(cu)}{\partial(\lambda t)}+cu\frac{\partial(cu)}{\partial(\lambda x)}+c\delta v\frac{\partial(cu)}{\partial(dy)}\right]=-\frac{\partial}{\partial(\lambda x)}\left(\frac{p\mu c\lambda}{d^2}\right)+\mu\left[\frac{\partial^2(cu)}{\partial(\lambda x)^2}+\frac{\partial^2(cu)}{\partial(dy)^2}\right]$$
$$+g(1-C_0)\rho_{f0}\beta(T_1-T_0)\theta-g(-\rho_{f0}+\rho_p)(C_1-C_0)\sigma,$$

$$\implies \rho_f\left[\frac{c^2}{\lambda}\frac{\partial u}{\partial t}+\frac{c^2}{\lambda}u\frac{\partial u}{\partial x}+\frac{c^2\delta}{d}v\frac{\partial u}{\partial y}\right]=-\frac{\mu c}{d^2}\frac{\partial p}{\partial x}+\mu\left[\frac{c}{\lambda^2}\frac{\partial^2 u}{\partial x^2}+\frac{c}{d^2}\frac{\partial^2 u}{\partial y^2}\right]+g(1-C_0)\rho_{f0}\beta(T_1-T_0)\theta$$
$$-g(-\rho_{f0}+\rho_p)(C_1-C_0)\sigma,$$

$$\implies \rho_f\left[\frac{c^2\delta}{d}\frac{\partial u}{\partial t}+\frac{c^2\delta}{d}u\frac{\partial u}{\partial x}+\frac{c^2\delta}{d}v\frac{\partial u}{\partial y}\right]=-\frac{\mu c}{d^2}\frac{\partial p}{\partial x}+\mu\left[\frac{c\delta^2}{d^2}\frac{\partial^2 u}{\partial x^2}+\frac{c}{d^2}\frac{\partial^2 u}{\partial y^2}\right]+g(1-C_0)\rho_{f0}\beta(T_1-T_0)\theta$$
$$-g(-\rho_{f0}+\rho_p)(C_1-C_0)\sigma,$$

$$\Longrightarrow \frac{c^2\rho_f}{d}\left[\delta\frac{\partial u}{\partial t}+u\delta\frac{\partial u}{\partial x}+v\delta\frac{\partial u}{\partial y}\right]=-\frac{\mu c}{d^2}\frac{\partial p}{\partial x}+\frac{c\mu}{d^2}\left[\delta^2\frac{\partial^2 u}{\partial x^2}+\frac{\partial^2 u}{\partial y^2}\right]+g(1-C_0)\rho_{f0}\beta(T_1-T_0)\theta$$
$$-g(-\rho_{f0}+\rho_p)(C_1-C_0)\sigma.$$

Multiplying by $\frac{d^2}{c\mu}$, yields

$$\frac{c\rho_f d}{\mu}\left[\delta\frac{\partial u}{\partial t}+u\delta\frac{\partial u}{\partial x}+v\delta\frac{\partial u}{\partial y}\right]=-\frac{\partial p}{\partial x}+\left[\delta^2\frac{\partial^2 u}{\partial x^2}+\frac{\partial^2 u}{\partial y^2}\right]+\frac{g\beta d^2(1-C_0)\rho_{f0}(T_1-T_0)}{c\mu}\theta$$
$$-\frac{gd^2(-\rho_{f0}+\rho_p)(C_1-C_0)}{c\mu}\sigma,$$

$$\Longrightarrow Re\delta\left[\frac{\partial u}{\partial t}+u\frac{\partial u}{\partial x}+v\frac{\partial u}{\partial y}\right]=-\frac{\partial p}{\partial x}+\left[\delta^2\frac{\partial^2 u}{\partial x^2}+\frac{\partial^2 u}{\partial y^2}\right]+\frac{g\beta d^3(1-C_0)(T_1-T_0)}{\nu^2}\theta$$
$$-\frac{gd^3(-\rho_{f0}+\rho_p)(C_1-C_0)}{\rho_{f0}\nu^2}\sigma,$$
$$\Longrightarrow Re\delta\left[\frac{\partial v}{\partial t}+u\frac{\partial v}{\partial x}+v\frac{\partial v}{\partial y}\right]=-\frac{\partial p}{\partial x}+\left[\delta^2\frac{\partial^2 v}{\partial x^2}+\frac{\partial^2 v}{\partial y^2}\right]+Gr_T\theta-Gr_C\sigma. \tag{3.17}$$

Equation (3.9) in dimensionless form can be expressed as

$$\rho_f\left[c\frac{\partial(c\delta v)}{\partial(\lambda t)}+cu\frac{\partial(c\delta v)}{\partial(\lambda x)}+c\delta v\frac{\partial(c\delta v)}{\partial(dy)}\right]=-\frac{\partial}{\partial(dx)}\left(\frac{p\mu c\lambda}{d^2}\right)+\mu\left[\frac{\partial^2(c\delta v)}{\partial(\lambda x)^2}+\frac{\partial^2(c\delta v)}{\partial(dy)^2}\right]$$
$$+g(1-C_0)\rho_{f0}\beta(T_1-T_0)\theta-g(-\rho_{f0}+\rho_p)(C_1-C_0)\sigma,$$

$$\Longrightarrow \rho_f\left[\frac{c^2\delta}{\lambda}\frac{\partial v}{\partial t}+\frac{c^2\delta}{\lambda}u\frac{\partial v}{\partial x}+\frac{c^2\delta^2}{d}v\frac{\partial v}{\partial y}\right]=-\frac{\mu c\lambda}{d^3}\frac{\partial p}{\partial y}+\mu\left[\frac{c\delta}{\lambda^2}\frac{\partial^2 v}{\partial x^2}+\frac{c\delta}{d^2}\frac{\partial^2 v}{\partial y^2}\right]+g(1-C_0)\rho_{f0}\beta(T_1-T_0)\theta$$
$$-g(-\rho_{f0}+\rho_p)(C_1-C_0)\sigma,$$

$$\Longrightarrow \rho_f\left[\frac{c^2\delta^2}{d}\frac{\partial v}{\partial t}+\frac{c^2\delta^2}{d}u\frac{\partial v}{\partial x}+\frac{c^2\delta^2}{d}v\frac{\partial v}{\partial y}\right]=-\frac{\mu c}{\delta d^2}\frac{\partial p}{\partial y}+\mu\left[\frac{c\delta^2}{d^2}\frac{\partial^2 v}{\partial x^2}+\frac{c\delta}{d^2}\frac{\partial^2 v}{\partial y^2}\right]+g(1-C_0)\rho_{f0}\beta(T_1-T_0)\theta$$
$$-g(-\rho_{f0}+\rho_p)(C_1-C_0)\sigma,$$

$$\Longrightarrow \frac{c^2\delta^2\rho_f}{d}\left[\frac{\partial v}{\partial t}+u\frac{\partial v}{\partial x}+v\frac{\partial v}{\partial y}\right]=-\frac{\mu c}{\delta d^2}\frac{\partial p}{\partial y}+\frac{\mu c\delta}{d^2}\left[\delta^2\frac{\partial^2 v}{\partial x^2}+\frac{\partial^2 v}{\partial y^2}\right]+g(1-C_0)\rho_{f0}\beta(T_1-T_0)\theta$$
$$-g(-\rho_{f0}+\rho_p)(C_1-C_0)\sigma.$$

Multiplying by $\frac{d^2}{\mu c\delta}$, we get

$$\frac{c\delta\rho_f d}{\mu}\left[\frac{\partial v}{\partial t}+u\frac{\partial v}{\partial x}+v\frac{\partial v}{\partial y}\right]=-\frac{1}{\delta^2}\frac{\partial p}{\partial y}+\left[\delta^2\frac{\partial^2 v}{\partial x^2}+\frac{\partial^2 v}{\partial y^2}\right]+\frac{g\beta d^2(1-C_0)\rho_{f0}(T_1-T_0)}{c\delta\mu}\theta$$
$$-\frac{gd^2(-\rho_{f0}+\rho_p)(C_1-C_0)}{c\delta\mu}\sigma.$$

Multiplying by $\delta^2$, yields

$$Re\delta^3\left[\frac{\partial v}{\partial t}+u\frac{\partial v}{\partial x}+v\frac{\partial v}{\partial y}\right]=-\frac{\partial p}{\partial y}+\delta^2\left[\delta^2\frac{\partial^2 v}{\partial x^2}+\frac{\partial^2 v}{\partial y^2}\right]+\frac{g\beta\delta d^3(1-C_0)(T_1-T_0)}{\nu^2}\theta$$
$$-\frac{g\delta d^3(-\rho_{f0}+\rho_p)(C_1-C_0)}{\rho_{f0}\nu^2}\sigma,$$
$$\Longrightarrow\ Re\delta^3\left[\frac{\partial v}{\partial t}+u\frac{\partial v}{\partial x}+v\frac{\partial v}{\partial y}\right]=-\frac{\partial p}{\partial y}+\delta^2\left[\delta^2\frac{\partial^2 v}{\partial x^2}+\frac{\partial^2 v}{\partial y^2}\right]+\delta Gr_T\theta-\delta Gr_C\sigma. \tag{3.18}$$

Equation (3.10) in dimensionless form can be expressed as

$$\left[c\frac{\partial(\theta(T_1-T_0)+T_0)}{\partial(\lambda t)}+cu\frac{\partial(\theta(T_1-T_0)+T_0)}{\partial(\lambda x)}+\delta cv\frac{\partial(\theta(T_1-T_0)+T_0)}{\partial(dy)}\right]=$$
$$\alpha\left[\frac{\partial^2(\theta(T_1-T_0)+T_0)}{\partial(\lambda x)^2}+\frac{\partial^2(\theta(T_1-T_0)+T_0)}{\partial(dy)^2}\right]$$
$$+\tau D_B\left(\frac{\partial(\sigma(C_1-C_0)+C_0)}{\partial(\lambda x)}\frac{\partial(\theta(T_1-T_0)+T_0)}{\partial(\lambda x)}+\frac{\partial(\sigma(C_1-C_0)+C_0)}{\partial(dy)}\frac{\partial(\theta(T_1-T_0)+T_0)}{\partial(dy)}\right)$$
$$+\tau\frac{D_T}{T_0}\left(\left(\frac{\partial(\theta(T_1-T_0)+T_0)}{\partial(\lambda x)}\right)^2+\left(\frac{\partial(\theta(T_1-T_0)+T_0)}{\partial(dy)}\right)^2\right),$$

$$\Longrightarrow\ \left[\frac{c(T_1-T_0)}{\lambda}\frac{\partial\theta}{\partial t}+\frac{c(T_1-T_0)}{\lambda}u\frac{\partial\theta}{\partial x}+\frac{\delta c(T_1-T_0)}{d}v\frac{\partial\theta}{\partial y}\right]=\alpha\left[\frac{(T_1-T_0)}{\lambda^2}\frac{\partial^2\theta}{\partial x^2}+\frac{(T_1-T_0)}{d^2}\frac{\partial^2\theta}{\partial y^2}\right]$$
$$+\tau D_B\left(\frac{(C_1-C_0)(T_1-T_0)}{\lambda^2}\frac{\partial\sigma}{\partial x}\frac{\partial\theta}{\partial x}+\frac{(C_1-C_0)(T_1-T_0)}{d^2}\frac{\partial\sigma}{\partial y}\frac{\partial\theta}{\partial y}\right)$$
$$+\tau\frac{D_T}{T_0}\left(\frac{(T_1-T_0)^2}{\lambda^2}\left(\frac{\partial\theta}{\partial x}\right)^2+\frac{(T_1-T_0)^2}{d^2}\left(\frac{\partial\theta}{\partial y}\right)^2\right),$$

$$\Longrightarrow \left[\frac{c\delta(T_1-T_0)}{d}\frac{\partial\theta}{\partial t}+\frac{c\delta(T_1-T_0)}{d}u\frac{\partial\theta}{\partial x}+\frac{\delta c(T_1-T_0)}{d}v\frac{\partial\theta}{\partial y}\right]=\alpha\left[\frac{\delta^2(T_1-T_0)}{d^2}\frac{\partial^2\theta}{\partial x^2}+\frac{(T_1-T_0)}{d^2}\frac{\partial^2\theta}{\partial y^2}\right]$$
$$+\tau D_B\left(\frac{(C_1-C_0)(T_1-T_0)\delta^2}{d^2}\frac{\partial\sigma}{\partial x}\frac{\partial\theta}{\partial x}+\frac{(C_1-C_0)(T_1-T_0)}{d^2}\frac{\partial\sigma}{\partial y}\frac{\partial\theta}{\partial y}\right)$$
$$+\tau\frac{D_T}{T_0}\left(\frac{(T_1-T_0)^2\delta^2}{d^2}\left(\frac{\partial\theta}{\partial x}\right)^2+\frac{(T_1-T_0)^2}{d^2}\left(\frac{\partial\theta}{\partial y}\right)^2\right),$$

$$\Longrightarrow \frac{c\delta(T_1-T_0)}{d}\left[\frac{\partial\theta}{\partial t}+u\frac{\partial\theta}{\partial x}+v\frac{\partial\theta}{\partial y}\right]=\alpha\frac{(T_1-T_0)}{d^2}\left[\delta^2\frac{\partial^2\theta}{\partial x^2}+\frac{\partial^2\theta}{\partial y^2}\right]$$
$$+\tau D_B\frac{(C_1-C_0)(T_1-T_0)}{d^2}\left(\delta^2\frac{\partial\sigma}{\partial x}\frac{\partial\theta}{\partial x}+\frac{\partial\sigma}{\partial y}\frac{\partial\theta}{\partial y}\right)$$
$$+\tau\frac{D_T}{T_0}\frac{(T_1-T_0)^2}{d^2}\left(\delta^2\left(\frac{\partial\theta}{\partial x}\right)^2+\left(\frac{\partial\theta}{\partial y}\right)^2\right).$$

Multiplying by $\dfrac{d^2}{\alpha(T_1-T_0)}$, we obtain

$$\frac{cd\delta}{\alpha}\left[\frac{\partial\theta}{\partial t}+u\frac{\partial\theta}{\partial x}+v\frac{\partial\theta}{\partial y}\right]=\left[\delta^2\frac{\partial^2\theta}{\partial x^2}+\frac{\partial^2\theta}{\partial y^2}\right]+\tau D_B\frac{(C_1-C_0)}{\alpha}\left(\delta^2\frac{\partial\sigma}{\partial x}\frac{\partial\theta}{\partial x}+\frac{\partial\sigma}{\partial y}\frac{\partial\theta}{\partial y}\right)$$
$$+\tau\frac{D_T}{T_0}\frac{(T_1-T_0)}{\alpha}\left(\delta^2\left(\frac{\partial\theta}{\partial x}\right)^2+\left(\frac{\partial\theta}{\partial y}\right)^2\right),$$

$$\Longrightarrow RePr\delta\left[\frac{\partial\theta}{\partial t}+u\frac{\partial\theta}{\partial x}+v\frac{\partial\theta}{\partial y}\right]=\left[\delta^2\frac{\partial^2\theta}{\partial x^2}+\frac{\partial^2\theta}{\partial y^2}\right]+N_b\left(\delta^2\frac{\partial\sigma}{\partial x}\frac{\partial\theta}{\partial x}+\frac{\partial\sigma}{\partial y}\frac{\partial\theta}{\partial y}\right)$$
$$+N_t\left(\delta^2\left(\frac{\partial\theta}{\partial x}\right)^2+\left(\frac{\partial\theta}{\partial y}\right)^2\right). \tag{3.19}$$

Equation (3.11) in dimensionless form can be expressed as

$$\left[c\frac{\partial(\sigma(C_1-C_0)+C_0)}{\partial(\lambda t)}+cu\frac{\partial(\sigma(C_1-C_0)+C_0)}{\partial(\lambda x)}+\delta cv\frac{\partial(\sigma(C_1-C_0)+C_0)}{\partial(dy)}\right]=$$
$$D_B\left[\frac{\partial^2(\sigma(C_1-C_0)+C_0)}{\partial(\lambda x)^2}+\frac{\partial^2(\sigma(C_1-C_0)+C_0)}{\partial(dy)^2}\right]+\frac{D_T}{T_0}\left[\frac{\partial^2(\sigma(T_1-T_0)+T_0)}{\partial(\lambda x)^2}+\frac{\partial^2(\sigma(T_1-T_0)+T_0)}{\partial(dy)^2}\right],$$

$$\Longrightarrow \left[\frac{c(C_1-C_0)}{\lambda}\frac{\partial\sigma}{\partial t}+\frac{c(C_1-C_0)}{\lambda}u\frac{\partial\sigma}{\partial x}+\frac{c\delta(C_1-C_0)}{d}v\frac{\partial\sigma}{\partial y}\right]=D_B\left[\frac{(C_1-C_0)}{\lambda^2}\frac{\partial^2\sigma}{\partial x^2}+\frac{(C_1-C_0)}{d^2}\frac{\partial^2\sigma}{\partial y^2}\right]$$
$$+\frac{D_T}{T_0}\left[\frac{(T_1-T_0)}{\lambda^2}\frac{\partial^2\theta}{\partial x^2}+\frac{(T_1-T_0)}{d^2}\frac{\partial^2\theta}{\partial y^2}\right],$$

$$\Longrightarrow \left[\frac{c\delta(C_1-C_0)}{d}\frac{\partial\sigma}{\partial t}+\frac{c\delta(C_1-C_0)}{d}u\frac{\partial\sigma}{\partial x}+\frac{c\delta(C_1-C_0)}{d}v\frac{\partial\sigma}{\partial y}\right]=$$
$$D_B\left[\frac{\delta^2(C_1-C_0)}{d^2}\frac{\partial^2\sigma}{\partial x^2}+\frac{(C_1-C_0)}{d^2}\frac{\partial^2\sigma}{\partial y^2}\right]+\frac{D_T}{T_0}\left[\frac{\delta^2(T_1-T_0)}{d^2}\frac{\partial^2\theta}{\partial x^2}+\frac{(T_1-T_0)}{d^2}\frac{\partial^2\theta}{\partial y^2}\right],$$

$$\Longrightarrow \frac{c\delta(C_1-C_0)}{d}\left[\frac{\partial\sigma}{\partial t}+u\frac{\partial\sigma}{\partial x}+v\frac{\partial\sigma}{\partial y}\right]=D_B\frac{(C_1-C_0)}{d^2}\left[\delta^2\frac{\partial^2\sigma}{\partial x^2}+\frac{\partial^2\sigma}{\partial y^2}\right]+\frac{D_T}{T_0}\frac{(T_1-T_0)}{d^2}\left[\delta^2\frac{\partial^2\theta}{\partial x^2}+\frac{\partial^2\theta}{\partial y^2}\right].$$

Multiplying by $\frac{d^2}{D_B(C_1-C_0)}$, we obtain

$$\frac{cd\delta}{D_B}\left[\frac{\partial\sigma}{\partial t}+u\frac{\partial\sigma}{\partial x}+v\frac{\partial\sigma}{\partial y}\right]=\left[\delta^2\frac{\partial^2\sigma}{\partial x^2}+\frac{\partial^2\sigma}{\partial y^2}\right]+\frac{D_T}{T_0}\frac{(T_1-T_0)}{(C_1-C_0)D_B}\left[\delta^2\frac{\partial^2\theta}{\partial x^2}+\frac{\partial^2\theta}{\partial y^2}\right],$$

$$\Longrightarrow ReS_c\delta\left[\frac{\partial\sigma}{\partial t}+u\frac{\partial\sigma}{\partial x}+v\frac{\partial\sigma}{\partial y}\right]=\left[\delta^2\frac{\partial^2\sigma}{\partial x^2}+\frac{\partial^2\sigma}{\partial y^2}\right]+\frac{N_t}{N_b}\left[\delta^2\frac{\partial^2\theta}{\partial x^2}+\frac{\partial^2\theta}{\partial y^2}\right]. \tag{3.20}$$

Substituting the dimensionless variables into the peristaltic wave equation (3.1)

$$yd=\tilde{h}=d+b\sin\frac{2\pi}{\lambda}(\lambda x),$$

and dividing by $d$, yields

$$y=\frac{\tilde{h}}{d}=1+\frac{b}{d}\sin(2\pi x),$$
$$\Longrightarrow y=h=1+\Phi\sin(2\pi x). \tag{3.21}$$

The boundary conditions in equation (3.12) in dimensionless form can be expressed as

$$\frac{\partial(uc)}{\partial(dy)}=0,$$
$$\Longrightarrow \frac{c}{d}\frac{\partial u}{\partial y}=0.$$

Multiplying by $\frac{d}{c}$ we get

$$\frac{\partial u}{\partial y} = 0. \tag{3.22}$$

Similarly

$$uc = 0,$$

$$\Longrightarrow u = 0. \tag{3.23}$$

The boundary conditions in equation (3.13) in dimensionless form can be expressed as

$$\theta(T_1 - T_0) + T_0 = T_0,$$

$$\Longrightarrow \theta(T_1 - T_0) = 0.$$

Dividing by $(T_1 - T_0)$, we get

$$\theta = 0. \tag{3.24}$$

Similarly

$$\theta(T_1 - T_0) + T_0 = T_1,$$

$$\Longrightarrow \theta(T_1 - T_0) = T_1 - T_0.$$

Dividing by $(T_1 - T_0)$, we get

$$\theta = 1. \tag{3.25}$$

The boundary conditions in equation (3.14) in dimensionless form can be expressed as

$$\sigma(C_1 - C_0) + C_0 = C_0,$$

$$\Longrightarrow \ \sigma(C_1 - C_0) = 0.$$

Dividing by $(C_1 - C_0)$, we get

$$\sigma = 0. \tag{3.26}$$

Similarly

$$\sigma(C_1 - C_0) + C_0 = C_1,$$
$$\implies \sigma(C_1 - C_0) = C_1 - C_0.$$

Dividing by $(C_1 - C_0)$, we get

$$\sigma = 1. \tag{3.27}$$

Using long wavelength and low Reynolds approximation, terms with $O(\delta)$ and higher tend to 0 and are ignored. So equations (3.16)-(3.20) are reduced to

$$\frac{\partial u}{\partial x} + \frac{\partial v}{\partial y} = 0, \tag{3.28}$$
$$\frac{\partial p}{\partial x} = \frac{\partial^2 u}{\partial y^2} + Gr_T\theta - Gr_C\sigma, \tag{3.29}$$
$$\frac{\partial p}{\partial y} = 0, \tag{3.30}$$
$$\frac{\partial^2 \theta}{\partial y^2} + N_b\frac{\partial \sigma}{\partial y}\frac{\partial \theta}{\partial y} + N_t\left(\frac{\partial \theta}{\partial y}\right)^2 = 0, \tag{3.31}$$
$$\frac{\partial^2 \sigma}{\partial y^2} + \frac{N_t}{N_b}\left(\frac{\partial^2 \theta}{\partial y^2}\right) = 0, \tag{3.32}$$

with the appropriate boundary conditions

$$\frac{\partial u}{\partial y} = 0 \quad at \quad y = 0, \quad u = 0 \quad at \quad y = h, \tag{3.33}$$
$$\theta = 0 \quad at \quad y = 0, \quad \theta = 1 \quad at \quad y = h, \tag{3.34}$$
$$\sigma = 0 \quad at \quad y = 0, \quad \sigma = 1 \quad at \quad y = h. \tag{3.35}$$

## 3.2 Method of Solution

We apply the Adomian decomposition method (ADM) to solve the dimensionless governing equations. Introducing the linear operator $L$ in equation (3.32) we get,

$$L\sigma + \frac{N_t}{N_b}\left(\frac{\partial^2 \theta}{\partial y^2}\right) = 0,$$

$$\implies L\sigma = -\frac{N_t}{N_b}\left(\frac{\partial^2\theta}{\partial y^2}\right), \tag{3.36}$$

where $L$ is the second order differential operator defined as $L = \frac{\partial^2}{\partial y^2}$. Applying the inverse operator $L^{-1}$ on both sides of equation (3.36)

$$L^{-1}L\sigma = -\frac{N_t}{N_b}L^{-1}\left(\frac{\partial^2\theta}{\partial y^2}\right), \tag{3.37}$$

where the inverse operator $L^{-1}$ is given by

$$L^{-1}(.) = \int_0^y \int_0^y (.)dydy,$$

we get

$$\int_0^y \int_0^y \frac{\partial^2\sigma}{\partial y^2}dydy = -\frac{N_t}{N_b}L^{-1}\left(\frac{\partial^2\theta}{\partial y^2}\right).$$

Double integrating the left hand side of the above equation and using the boundary conditions of equation (3.35) we obtain

$$\sigma(y) - y\sigma'(0) = -\frac{N_t}{N_b}L^{-1}\left(\frac{\partial^2\theta}{\partial y^2}\right). \tag{3.38}$$

Rearranging the terms and letting $\sigma'(0) = A$, we get

$$\sigma(y) = Ay - \frac{N_t}{N_b}L^{-1}\left(\frac{\partial^2\theta}{\partial y^2}\right), \tag{3.39}$$

where $A$ is a constant.

Using the ADM suggests that the solution $\sigma(y)$ can be expressed by the decomposition series

$$\sigma(y) = \sum_{n=0}^{\infty}\sigma_n(y). \tag{3.40}$$

Inserting (3.40) into (3.39) yields

$$\sum_{n=0}^{\infty}\sigma_n(y) = Ay - \frac{N_t}{N_b}L^{-1}\left(\sum_{n=0}^{\infty}\frac{\partial^2\theta_n}{\partial y^2}\right). \tag{3.41}$$

The zeroth component $\sigma_0(y)$ is usually defined by all terms that are not included under the operator $L^{-1}$. The remaining components can be determined recurrently such that each term is determined by using the previous component. Consequently, the components of $\sigma(y)$ can be elegantly determined by using the recursive relation

$$\begin{aligned} &\sigma_0(y) = Ay, \\ &\sigma_{k+1}(y) = -\frac{N_t}{N_b} L^{-1}\left(\frac{\partial^2\theta_k}{\partial y^2}\right), \qquad k \geq 0. \end{aligned} \tag{3.42}$$

In an operator form, equation (3.31) can be written as

$$L\theta + N_b \frac{\partial\sigma}{\partial y}\frac{\partial\theta}{\partial y} + N_t\left(\frac{\partial\theta}{\partial y}\right)^2 = 0,$$

$$\implies L\theta = -N_b \frac{\partial\sigma}{\partial y}\frac{\partial\theta}{\partial y} - N_t\left(\frac{\partial\theta}{\partial y}\right)^2. \tag{3.43}$$

Applying the inverse operator $L^{-1}$ on both sides of equation (3.43) yields

$$L^{-1}L\theta = -N_b L^{-1}\left(\frac{\partial\sigma}{\partial y}\frac{\partial\theta}{\partial y}\right) - N_t L^{-1}\left(\frac{\partial\theta}{\partial y}\right)^2. \tag{3.44}$$

This is equivalent to

$$\int_0^y \int_0^y \frac{\partial^2\theta}{\partial y^2} dy dy = -N_b L^{-1}\left(\frac{\partial\sigma}{\partial y}\frac{\partial\theta}{\partial y}\right) - N_t L^{-1}\left(\frac{\partial\theta}{\partial y}\right)^2. \tag{3.45}$$

Double integrating the left hand side of equation (3.45) and using the boundary conditions of equation (3.34) we obtain

$$\theta(y) - y\theta'(0) = -N_b L^{-1}\left(\frac{\partial\sigma}{\partial y}\frac{\partial\theta}{\partial y}\right) - N_t L^{-1}\left(\frac{\partial\theta}{\partial y}\right)^2. \tag{3.46}$$

Rearranging the terms and letting $\theta'(0) = B$ we get

$$\theta(y) = By - N_b L^{-1}\left(\frac{\partial\sigma}{\partial y}\frac{\partial\theta}{\partial y}\right) - N_t L^{-1}\left(\frac{\partial\theta}{\partial y}\right)^2, \tag{3.47}$$

where $B$ is a constant. Using the ADM suggests that the solution $\theta(y)$ can be expressed by the decomposition series

$$\theta(y) = \sum_{n=0}^{\infty} \theta_n(y), \tag{3.48}$$

and the nonlinear term $\left(\dfrac{\partial \theta}{\partial y}\right)^2$ is equated to

$$\left(\frac{\partial \theta}{\partial y}\right)^2 = \sum_{n=0}^{\infty} C_n. \tag{3.49}$$

where $C_n$ are called Adomian polynomials to be calculated.

Substituting equation (3.48) and equation (3.49) into equation (3.47) yields

$$\sum_{n=0}^{\infty} \theta_n(y) = By - N_b L^{-1}\left(\sum_{n=0}^{\infty} \frac{\partial \sigma_n}{\partial y}\frac{\partial \theta_n}{\partial y}\right) - N_t L^{-1}\left(\sum_{n=0}^{\infty} C_n\right). \tag{3.50}$$

We have the recursive relation

$$\begin{aligned} &\theta_0(y) = By, \\ &\theta_{k+1}(y) = -N_b L^{-1}\left(\frac{\partial \sigma_k}{\partial y}\frac{\partial \theta_k}{\partial y}\right) - N_t L^{-1}\left(C_k\right), \quad k \geq 0. \end{aligned} \tag{3.51}$$

We have formulated two recursive iterations for $\sigma$ and $\theta$. Now what is left is to find the $\sigma_{k+1}$ and $\theta_{k+1}$. For $k = 0$ we have

$$\begin{aligned} \sigma_1(y) &= -\frac{N_t}{N_b} L^{-1}\left(\frac{\partial^2 \theta_0}{\partial y^2}\right), \\ &= -\frac{N_t}{N_b} L^{-1}\left(\frac{\partial^2}{\partial y^2}(By)\right), \\ &= -\frac{N_t}{N_b} L^{-1}(0), \\ &= 0, \end{aligned} \tag{3.52}$$

$$\theta_1(y) = -N_b L^{-1}\left(\frac{\partial \sigma_0}{\partial y}\frac{\partial \theta_0}{\partial y}\right) - N_t L^{-1}\left(C_0\right).$$

The Adomian polynomial $C_0$ is given by

$$\begin{aligned} C_0 &= \left(\frac{\partial \theta}{\partial y}\right)^2, \\ &= \left(\frac{\partial}{\partial y}(By)\right)^2, \\ &= B^2. \end{aligned} \tag{3.53}$$

Then

$$\begin{aligned} \theta_1(y) &= -N_b L^{-1}\left(\frac{\partial}{\partial y}(By)\frac{\partial}{\partial y}(Ay)\right) - N_t L^{-1}\left(B^2\right), \\ &= -N_b L^{-1}(AB) - N_t L^{-1}\left(B^2\right), \\ &= -\frac{1}{2}N_b(AB)y^2 - \frac{1}{2}N_t B^2 y^2. \end{aligned} \tag{3.54}$$

For $k = 1$ we have

$$\begin{aligned} \sigma_2(y) &= -\frac{N_t}{N_b}L^{-1}\left(\frac{\partial^2 \theta_1}{\partial y^2}\right), \\ &= -\frac{N_t}{N_b}L^{-1}\left(\frac{\partial^2}{\partial y^2}(-\frac{1}{2}N_b(AB)y^2 - \frac{1}{2}N_t B^2 y^2)\right), \\ &= \frac{N_t}{N_b}L^{-1}\left(N_b(AB) + N_t B^2\right), \\ &= \frac{1}{2}N_t(AB)y^2 + \frac{1}{2}\frac{N_t^2}{N_b}B^2 y^2, \end{aligned} \tag{3.55}$$

$$\begin{aligned} \theta_2(y) &= -N_b L^{-1}\left(\frac{\partial \sigma_1}{\partial y}\frac{\partial \theta_1}{\partial y}\right) - N_t L^{-1}\left(C_1\right), \\ &= 0 - N_t L^{-1}\left(C_1\right), \\ &= -N_t L^{-1}\left(C_1\right). \end{aligned} \tag{3.56}$$

The Adomian polynomial $C_1$ is given by

$$\begin{aligned} C_1 &= 2\frac{\partial \theta_0}{\partial y}\frac{\partial \theta_1}{\partial y}, \\ &= 2\frac{\partial}{\partial y}(By)\frac{\partial}{\partial y}\left(-\frac{1}{2}N_b(AB)y^2 - \frac{1}{2}N_t B^2 y^2\right), \\ &= -2AB^2 N_b y - 2B^3 N_t y. \end{aligned} \tag{3.57}$$

Then

$$\begin{aligned}\theta_2 &= -N_t L^{-1}\left(-2AB^2N_b y - 2B^3N_t y\right),\\ &= \left(\frac{1}{3}N_b(AB^2)y^3 + \frac{1}{3}N_t B^3 y^3\right)N_t. \end{aligned}\tag{3.58}$$

For $k = 2$ we have

$$\begin{aligned}\sigma_3(y) &= -\frac{N_t}{N_b}L^{-1}\left(\frac{\partial^2\theta_2}{\partial y^2}\right),\\ &= -\frac{N_t}{N_b}L^{-1}\left(\frac{\partial^2}{\partial y^2}\left(\left(\frac{1}{3}N_b(AB^2)y^3 + \frac{1}{3}N_t B^3 y^3\right)N_t\right)\right),\\ &= -\frac{B^2y^3N_t^2(AN_b + BN_t)}{3N_b}. \end{aligned}\tag{3.59}$$

Now, the series solutions for $\sigma$ and $\theta$ are thus given by

$$\begin{aligned}\sigma(y) &= \sum_{n=0}^{\infty}\sigma_n(y)\\ &= Ay + \frac{1}{2}N_t(AB)y^2 + \frac{1}{2}\frac{N_t^2}{N_b}B^2y^2 - \frac{B^2y^3N_t^2(AN_b + BN_t)}{3N_b} + \dots, \qquad (3.60)\\ \theta(y) &= \sum_{n=0}^{\infty}\theta_n(y)\\ &= By - \frac{1}{2}N_b(AB)y^2 - \frac{1}{2}N_t B^2 y^2\left(\frac{1}{3}N_b(AB^2)y^3 + \frac{1}{3}N_t B^3 y^3\right)N_t + \dots \qquad (3.61)\end{aligned}$$

Introducing the linear operator $L$ in equation (3.29) we get

$$Lu(y) = \frac{\partial p}{\partial x} - Gr_T\theta + Gr_C\sigma.$$

Applying the inverse operator $L^{-1}$ on both sides of the above equation we obtain

$$L^{-1}Lu(y) = L^{-1}\frac{\partial p}{\partial x} - Gr_T L^{-1}\theta + Gr_C L^{-1}\sigma,$$

$$\implies \int_0^y\int_0^y \frac{\partial^2 u}{\partial y^2}dydy = L^{-1}\frac{\partial p}{\partial x} - Gr_T L^{-1}\theta + Gr_C L^{-1}\sigma. \tag{3.62}$$

Double integrating equation (3.62) and using the corresponding boundary conditions of (3.33) we get

$$u(y) - u(0) = L^{-1}\frac{\partial p}{\partial x} - Gr_T L^{-1}\theta + Gr_C L^{-1}\sigma,$$

$$\Longrightarrow u(y) = D + \frac{1}{2}\frac{\partial p}{\partial x}y^2 - Gr_T L^{-1}\theta + Gr_C L^{-1}\sigma, \tag{3.63}$$

where $D$ is a constant defined as $u(0) = D$. Using the ADM suggests that the solution $u(y)$ can be expressed by the decomposition series

$$u(y) = \sum_{n=0}^{\infty} u_n(y). \tag{3.64}$$

Substituting equation (4.40) into equation (4.39) we obtain

$$\sum_{n=0}^{\infty} u_n(y) = D + \frac{1}{2}\frac{\partial p}{\partial x}y^2 - Gr_T L^{-1}\left(\sum_{n=0}^{\infty}\theta_n(y)\right) + Gr_C L^{-1}\left(\sum_{n=0}^{\infty}\sigma_n(y)\right). \tag{3.65}$$

The recursive relation

$$\begin{aligned} u_0(y) &= D + \frac{1}{2}\frac{\partial p}{\partial x}y^2 \\ u_{k+1}(y) &= -Gr_T L^{-1}(\theta_k(y)) + Gr_C L^{-1}(\sigma_k(y)), \quad k \geq 0 \end{aligned} \tag{3.66}$$

is obtained. For $k = 0$ we have

$$\begin{aligned} u_1(y) &= Gr_C L^{-1}(\sigma_0) - Gr_T L^{-1}(\theta_0), \\ &= Gr_C L^{-1}(Ay) - Gr_T L^{-1}(By), \\ &= \frac{1}{3}AGr_C y^3 - \frac{1}{3}BGr_T y^3. \end{aligned} \tag{3.67}$$

For $k = 1$ we have

$$\begin{aligned} u_2(y) &= Gr_C L^{-1}(\sigma_1) - Gr_T L^{-1}(\theta_1), \\ &= Gr_C L^{-1}(0) - Gr_T L^{-1}\left(-\frac{1}{2}N_b(AB)y^2 - \frac{1}{2}N_t B^2 y^2\right), \\ &= Gr_T\left(\frac{1}{24}N_b(AB)y^4 + \frac{1}{24}N_t B^2 y^4\right). \end{aligned} \tag{3.68}$$

For $k=2$ we have

$$\begin{aligned}
u_3(y) &= Gr_C L^{-1}(\sigma_2) - Gr_T L^{-1}(\theta_2), \\
&= Gr_C L^{-1}\left(\frac{1}{2}N_t(AB)y^2 + \frac{1}{2}\frac{N_t^2}{N_b}B^2y^2\right) - Gr_T L^{-1}\left(\left(\frac{1}{3}N_b(AB^2)y^3 + \frac{1}{3}N_tB^3y^3\right)N_t\right), \\
&= Gr_C\left(\frac{1}{24}N_t(AB)y^4 + \frac{1}{24}\frac{N_t^2}{N_b}B^2y^4\right) - Gr_T\left(\left(\frac{1}{60}N_b(AB^2)y^5 + \frac{1}{60}N_tB^3y^5\right)N_t\right).
\end{aligned} \tag{3.69}$$

The series solution for $u$ is thus given by

$$\begin{aligned}
u(y) &= \sum_{n=0}^{\infty} u_n \\
&= D + \frac{1}{2}\frac{\partial p}{\partial x}y^2 + \frac{1}{3}AGr_Cy^3 - \frac{1}{3}BGr_Ty^3 + Gr_T\left(\frac{1}{24}N_b(AB)y^4 + \frac{1}{24}N_tB^2y^4\right) \\
&+ Gr_C\left(\frac{1}{24}N_t(AB)y^4 + \frac{1}{24}\frac{N_t^2}{N_b}B^2y^4\right) - Gr_T\left(\left(\frac{1}{60}N_b(AB^2)y^5 + \frac{1}{60}N_tB^3y^5\right)N_t\right) + \ldots
\end{aligned} \tag{3.70}$$

## 3.3 Results and Discussion

Equations (3.60), (3.61) and (3.70) are coded in symbolic package Mathematica for easy iteration of the numerical solution. Th numerical results from our ADM computations in MATHEMATICA are displayed in Figs 3.2-3.4. Thermophoresis is a phenomenon observed in mixtures of mobile particles where the different particle types exhibit different gradients. This phenomenon tend to move light molecules to elevated temperature regions and heavy molecules to depressed temperature regions. This is the so-called soret effect. Considering a nanofluid which comprises nanoparticles suspended in a base fluid, both the Brownian motion parameter $N_b$ and the thermophoresis parameter $N_t$ have significant influence on the nanoparticle species diffusion. Figures 3.2 and 3.3 show the variation of nanoparticle fraction profiles and nanofluid temperature profiles, respectively in response to the Brownian motion and the thermophoresis parameters. In Fig 3.2(a) the significant decrease in the nanoparticle fraction is noticed as the Brownian motion parameter $N_b$ is increased. A significant divergence of the profiles is more pronounced towards the channel walls as compared to the channel core region. These observations are consistent with the results of (Tripathi and Bég, 2014). In Fig 3.2(b) an increase in the thermophoresis parameter enhances the nanoparticle fraction profiles significantly. This shows that nanoparticle species diffusion is more noticeable or pronounced with thermophoresis. This is consistent with Tripathi and Bég (2014) and some references therein . The anormaly reported in Tripathi and Bég (2014), where nanoparticle concentrations are depressed closer to the channel core region is not observed in our study. Figures 3.3(a) and (b) depict similar effect of the Brownian motion and thermophoresis parameters on the nanofluid temperature distributions. The parameters show a pronounced cooling effect closer to the channel walls. Closer to the channel core region, both parameters enhance the nanofluid temperature, albeit marginally. In Tripathi and Bég (2014), this temperature enhancement effect around the channel core is more pronounced.

The variation of axial velocity ($u$) in response to increasing values of the Brownian motion parameter, the thermophoresis parameter, the thermal Grashof number $Gr_T$ and the species Grashof number $Gr_C$ is displayed in Figs 3.4(a)-(d). The graphs are plotted for channel half-space $0 \leq y \leq 1$. In this channel half-space, the axial velocity is shown to be generally negative, indicating that flow reversal or back flow is occurring . This result is consistent with (Tripathi and Bég, 2014). In all the four figures, maximum velocity is recorded at the channel core region and diminishing to zero at the channel walls. It is clear from Figs. 3.4(b) and 3.4(d) that the thermophoresis parameter and the thermal Grashof number both oppose the back-flow as they both decrease the magnitude of the axial velocity. The back-flow values of the axial velocity become more positive as these two parameters increase, $Gr_T = 4$ giving an almost entirely positive profile. The flow is therefore retarded by thermophoresis and Buoyancy forces. The Brownian motion parameter, $N_b$ and the nanoparticle species Grashof number, $Gr_C$ have the opposite effect. Figures 3.4(a) and 3.4(c) depict enhancement of back-flow values of the axial velocity. The back-flow phenomenon is thus worsened by the Brownian motion parameter and the species Grashof number $Gr_C$. These results are consistent with Tripathi and Bég (2014) except for the Brownian motion parameter which was observed to oppose the back-flow in their paper.

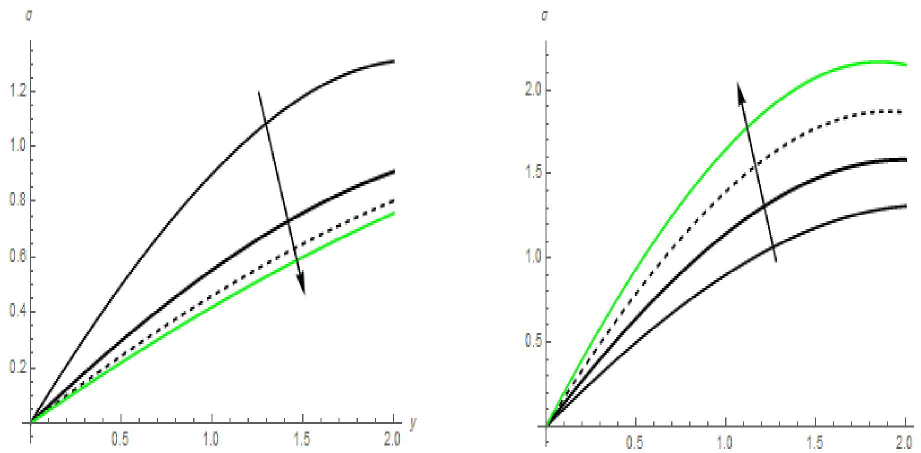


(a) $N_b = 1, 2, 3, 4$ (b) $N_t = 1, 2, 3, 4$

Figure 3.2: Nanoparticle concentration profiles

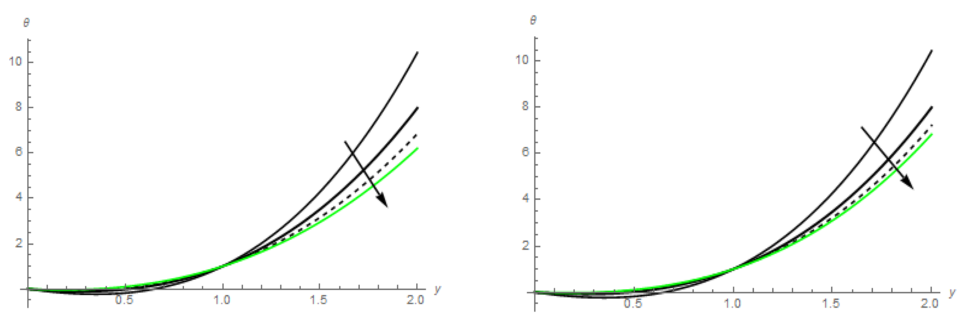


(a) $N_b = 1, 2, 3, 4$ (b) $N_t = 1, 2, 3, 4$

Figure 3.3: Temperature profiles

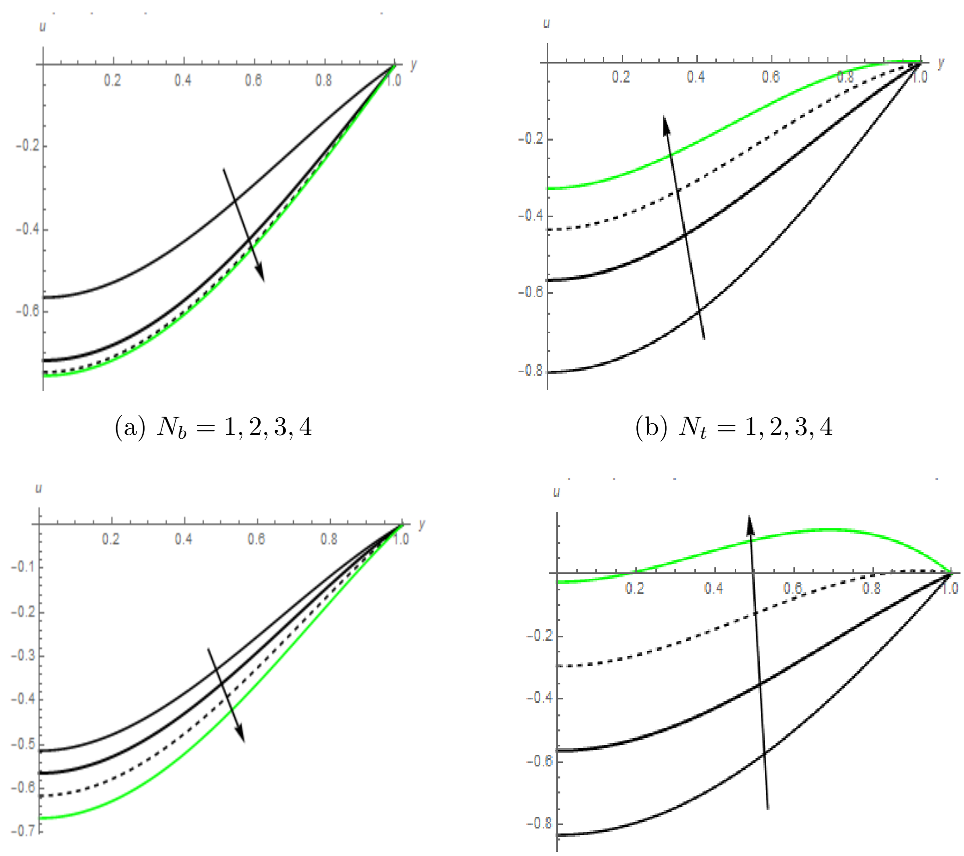


(a) $N_b = 1, 2, 3, 4$

(b) $N_t = 1, 2, 3, 4$

(c) $Gr_C = 1, 2, 3, 4$

(d) $Gr_T = 1, 2, 3, 4$

Figure 3.4: Velocity profiles

# Chapter 4

# Adomian Decomposition Method for Peristaltic Flow of a Nanofluid Through Two Dimensional Microchannel with Slip Effects

In this chapter we consider the problem studied by Akbar *et al.* (2012) as pointed out in chapter 2. The authors used the homotopy perturbation method to solve the non-dimensionalised governing equations. We, here, apply the ADM to solve the non-dimensionalised governing equations. We implement the method in symbolic package MATHEMATICA for easy computation of the numerical solutions. We compare the ADM results with those of the homotopy perturbation method.

## 4.1 Mathematical Model

We consider two dimensional incompressible nanofluid flow in an asymmetric channel of width $d_1 + d_2$. The flow is generated by a train of sinusoidal waves moving at a constant speed $c$ along the walls of the channel. The heat transfer and nanoparticle process is maintained by considering $T_0$, $T_1$ temperatures at the lower and upper walls respectively and $C_0$, $C_1$ nanoparticle concentrations at the lower and upper walls of the channel respectively. The peristaltic wave equations for the wall surfaces (see Fig 4.1) are given by

$$\tilde{Y} = H_1(\tilde{X}, \tilde{t}) = d_1 + a_1 \cos \frac{2\pi}{\lambda}(\tilde{X} - c\tilde{t}) \quad \text{upper wall}, \tag{4.1}$$

$$\tilde{Y} = H_2(\tilde{X}, \tilde{t}) = -d_2 - a_2 \cos \left[\frac{2\pi}{\lambda}(\tilde{X} - c\tilde{t}) + \Phi\right] \quad \text{lower wall}, \tag{4.2}$$

where $H_1$ and $H_2$ denote the peristaltic walls in the positive and negative $\tilde{Y}$ directions respectively, $a_1$ and $a_2$ are the amplitudes of the waves, $\tilde{t}$ is the time, $\lambda$ is the wavelength and $\Phi$ is the phase difference of the two waves.

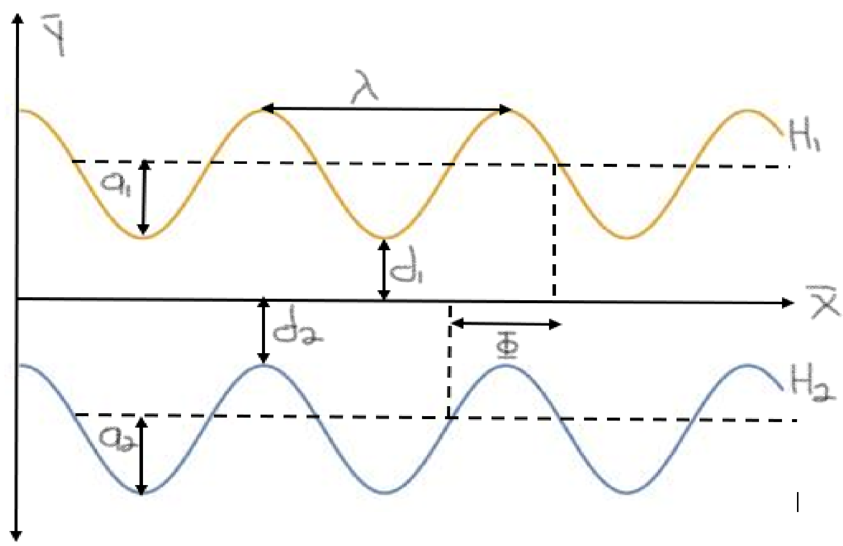


Figure 4.1: Schematic representation of the problem

We transform our problem from fixed frame to moving frame. Transformations between the fixed and moving frames are related as

$$\tilde{x} = \tilde{X} - c\tilde{t}, \quad \tilde{y} = \tilde{Y}, \quad \tilde{u} = \tilde{U} - c, \quad \tilde{v} = \tilde{V}, \quad \tilde{p}(\tilde{x}) = \tilde{P}(\tilde{X}, \tilde{t}), \quad H_1 = \tilde{h_1}, \quad H_2 = \tilde{h_2}, \tag{4.3}$$

where $(\tilde{x}, \tilde{y})$ are the coordinates in the moving frame, $(\tilde{u}, \tilde{v})$ are the velocity components in the moving frame, $\tilde{P}(\tilde{X}, \tilde{Y}, \tilde{t})$ and $\tilde{p}(\tilde{x}, \tilde{y})$ are the pressure in fixed and moving frames respectively, $(\tilde{X}, \tilde{Y})$ are the coordinates in fixed frame and $(\tilde{U}, \tilde{V})$ are the velocity components in the fixed frame.

The two-dimensional equations for an incompressible steady nanofluid are, as stated in Akbar *et al.*, (2012),

$$\frac{\partial \tilde{u}}{\partial \tilde{x}} + \frac{\partial \tilde{v}}{\partial \tilde{y}} = 0, \tag{4.4}$$

$$\rho \left[ \tilde{u} \frac{\partial \tilde{u}}{\partial \tilde{x}} + \tilde{v} \frac{\partial \tilde{v}}{\partial \tilde{y}} \right] = -\frac{\partial \tilde{P}}{\partial \tilde{x}} + \mu \left[ \frac{\partial^2 \tilde{u}}{\partial \tilde{x}^2} + \frac{\partial^2 \tilde{u}}{\partial \tilde{y}^2} \right] + \rho g \alpha (\tilde{T} - T_0) + \rho g \alpha (\tilde{C} - C_0), \tag{4.5}$$

$$\rho \left[ \tilde{u} \frac{\partial \tilde{v}}{\partial \tilde{x}} + \tilde{v} \frac{\partial \tilde{v}}{\partial \tilde{y}} \right] = -\frac{\partial \tilde{P}}{\partial \tilde{y}} + \mu \left[ \frac{\partial^2 \tilde{v}}{\partial \tilde{x}^2} + \frac{\partial^2 \tilde{v}}{\partial \tilde{y}^2} \right] + \rho g \alpha (\tilde{T} - T_0) + \rho g \alpha (\tilde{C} - C_0), \tag{4.6}$$

$$\left[ \tilde{u} \frac{\partial \tilde{T}}{\partial \tilde{x}} + \tilde{v} \frac{\partial \tilde{T}}{\partial \tilde{y}} \right] = \alpha \left[ \frac{\partial^2 \tilde{T}}{\partial \tilde{x}^2} + \frac{\partial^2 \tilde{T}}{\partial \tilde{y}^2} \right] + \tau \left[ D_B \left( \frac{\partial \tilde{C}}{\partial \tilde{x}} \frac{\partial \tilde{T}}{\partial \tilde{x}} + \frac{\partial \tilde{C}}{\partial \tilde{y}} \frac{\partial \tilde{T}}{\partial \tilde{y}} \right) + \frac{D_{\tilde{T}}}{\tilde{T}_0} \left( \left( \frac{\partial \tilde{T}}{\partial \tilde{x}} \right)^2 + \left( \frac{\partial \tilde{T}}{\partial \tilde{y}} \right)^2 \right) \right], \tag{4.7}$$

$$\left[ \tilde{u} \frac{\partial \tilde{C}}{\partial \tilde{x}} + \tilde{v} \frac{\partial \tilde{C}}{\partial \tilde{y}} \right] = D_B \left[ \frac{\partial^2 \tilde{C}}{\partial \tilde{x}^2} + \frac{\partial^2 \tilde{C}}{\partial \tilde{y}^2} \right] + \frac{D_{\tilde{T}}}{\tilde{T}_0} \left[ \frac{\partial^2 \tilde{T}}{\partial \tilde{x}^2} + \frac{\partial^2 \tilde{T}}{\partial \tilde{y}^2} \right], \tag{4.8}$$

where $\rho$ is the fluid density, $g$ is the acceleration due to gravity, $\mu$ is the viscosity, $\tilde{T}$ is the temperature, $\tilde{C}$ is the nanoparticle concentration, $\tau = \dfrac{(\rho c)_p}{(\rho c)_f}$ is the ratio between the effective heat capacity of nanoparticle material and heat capacity of the fluid, $D_B$ is the Brownian diffusion coefficient and $D_{\tilde{T}}$ is the thermophoretic diffusion coefficient. The boundary conditions for the particular problem are defined as

$$\tilde{u} = -\tilde{\beta} \frac{\partial \tilde{u}}{\partial \tilde{y}} - c \quad at \quad \tilde{y} = \tilde{h}_1, \quad \tilde{u} = \tilde{\beta} \frac{\partial \tilde{u}}{\partial \tilde{y}} - c \quad at \quad \tilde{y} = \tilde{h}_2, \tag{4.9}$$

$$\tilde{T} + \tilde{\gamma} \frac{\partial \tilde{T}}{\partial \tilde{y}} = T_0 \quad at \quad \tilde{y} = \tilde{h}_1, \quad \tilde{T} - \tilde{\gamma} \frac{\partial \tilde{T}}{\partial \tilde{y}} = T_1 \quad at \quad \tilde{y} = \tilde{h}_2, \tag{4.10}$$

$$\tilde{C} + \tilde{\eta} \frac{\partial \tilde{C}}{\partial \tilde{y}} = C_0 \quad at \quad \tilde{y} = \tilde{h}_1, \quad \tilde{C} - \tilde{\eta} \frac{\partial \tilde{C}}{\partial \tilde{y}} = C_1, \quad at \quad \tilde{y} = \tilde{h}_2, \tag{4.11}$$

where $\tilde{\beta}$ is the velocity slip parameter, $\tilde{\gamma}$ is the temperature slip parameter and $\tilde{\eta}$ is the concentration slip parameter.

In order to convert the governing equations and boundary conditions into dimensionless form, we introduce the dimensionless variables (Akbar *et al.*, 2012; Akbar and Nadeem, 2011)

$$\begin{aligned}
&x = \frac{2\pi\tilde{x}}{\lambda}, \quad y = \frac{\tilde{y}}{d_1}, \quad t = \frac{2\pi c\tilde{t}}{\lambda}, \quad u = \frac{\tilde{u}}{c}, \quad v = \frac{\tilde{v}}{c\delta}, \quad b = \frac{a_2}{d_1},\\
&p = \frac{2\pi d_1^2\tilde{p}}{\mu c\lambda}, \quad \delta = \frac{2\pi d_1}{\lambda}, \quad h_1 = \frac{\tilde{h}_1}{d_1}, \quad h_2 = \frac{\tilde{h}_2}{d_1}, \quad a = \frac{a_1}{d_1},\\
&\nu = \frac{\mu}{\rho}, \quad Re = \frac{\rho c d_1}{\mu}, \quad \theta = \frac{\tilde{T} - T_0}{T_1 - T_0}, \quad \phi = \frac{\tilde{C} - C_0}{C_1 - C_0}, \quad d = \frac{d_2}{d_1},\\
&\alpha = \frac{k}{(\rho c)_f}, \quad N_b = \frac{(\rho c)_p D_B (C_1 - C_0)}{k}, \quad N_t = \frac{(\rho c)_p D_{\tilde{T}} (T_1 - T_0)}{k T_0}, \quad Pr = \frac{v}{\alpha},\\
&Gr = \frac{g\alpha d_1^2 (T_1 - T_0)}{c\nu}, \quad Gr_\phi = \frac{g\alpha d_1^2 (C_1 - C_0)}{c\nu}, \quad \beta = \frac{\tilde{\beta}}{d_1}, \quad \gamma = \frac{\tilde{\gamma}}{d_1}, \quad \eta = \frac{\tilde{\eta}}{d_1},
\end{aligned} \tag{4.12}$$

where $x$ is the dimensionless axial coordinate, $y$ is the dimensionless transverse coordinate, $t$ is dimensionless time, $\delta$ is the dimensionless wave number, $c$ is the constant speed of channel walls, $u$ and $v$ are dimensionless axial and transverse velocity components, $p$ is dimensionless pressure, $\nu$ is nanofluid kinematic viscosity, $a$ and b are amplitude ratios, $Re$ is Reynolds number, $\theta$ is the dimensionless temperature, $\phi$ is the dimensionless nanoparticle concentration, $Gr$ is the local temperature Grashof number, $Gr_\phi$ is local nanoparticle Grashof number, $N_b$ is the Brownian motion parameter, $N_t$ is the thermophoresis parameter, $Pr$ is the Prandtl number, $\beta$ is the dimensionless velocity slip parameter, $\gamma$ is the dimensionless thermal slip parameter and $\eta$ is the dimensionless concentration slip parameter.

Equation (4.4) in dimensionless form can be expressed as

$$\frac{\partial(cu)}{\partial\left(\dfrac{x\lambda}{2\pi}\right)} + \frac{\partial(c\delta v)}{\partial(d_1 y)} = 0,$$

$$\Longrightarrow \quad \frac{2\pi c}{\lambda}\frac{\partial u}{\partial x} + \frac{c\delta}{d_1}\frac{\partial v}{\partial y} = 0,$$

$$\implies \frac{c\delta}{d_1}\frac{\partial u}{\partial x} + \frac{c\delta}{d_1}\frac{\partial v}{\partial y} = 0.$$

Multiplying by $\frac{d_1}{c\delta}$, we have

$$\frac{\partial u}{\partial x} + \frac{\partial v}{\partial y} = 0. \tag{4.13}$$

Equation (4.5) in dimensionless form can be expressed as

$$\rho\left[cu\frac{\partial(cu)}{\partial\left(\frac{\lambda x}{2\pi}\right)} + c\delta v\frac{\partial(cu)}{\partial(d_1 y)}\right] = -\frac{\partial}{\partial\left(\frac{\lambda x}{2\pi}\right)}\left(\frac{p\mu c\lambda}{2\pi d_1^2}\right) + \mu\left[\frac{\partial^2(cu)}{\partial\left(\frac{\lambda x}{2\pi}\right)^2} + \frac{\partial^2(cu)}{\partial(d_1 y)^2}\right] + \rho g\alpha(T_1 - T_0)\theta$$
$$+ \rho g\alpha(C_1 - C_0)\phi,$$

$$\implies \rho\left[\frac{2\pi c^2}{\lambda}u\frac{\partial u}{\partial x} + \frac{c^2\delta}{d_1}v\frac{\partial u}{\partial y}\right] = -\frac{\mu c}{d_1^2}\frac{\partial p}{\partial x} + \mu\left[\frac{4\pi^2 c}{\lambda^2}\frac{\partial^2 u}{\partial x^2} + \frac{c}{d_1^2}\frac{\partial^2 u}{\partial y^2}\right] + \rho g\alpha(T_1 - T_0)\theta + \rho g\alpha(C_1 - C_0)\phi,$$

$$\implies \rho\left[\frac{c^2\delta}{d_1}u\frac{\partial u}{\partial x} + \frac{c^2\delta}{d_1}v\frac{\partial u}{\partial y}\right] = -\frac{\mu c}{d_1^2}\frac{\partial p}{\partial x} + \mu\left[\frac{c\delta^2}{d_1^2}\frac{\partial^2 u}{\partial x^2} + \frac{c}{d_1^2}\frac{\partial^2 u}{\partial y^2}\right] + \rho g\alpha(T_1 - T_0)\theta + \rho g\alpha(C_1 - C_0)\phi,$$

$$\implies \frac{c^2\rho}{d_1}\left[u\delta\frac{\partial u}{\partial x} + v\delta\frac{\partial u}{\partial y}\right] = -\frac{\mu c}{d_1^2}\frac{\partial p}{\partial x} + \frac{c\mu}{d_1^2}\left[\delta^2\frac{\partial^2 u}{\partial x^2} + \frac{\partial^2 u}{\partial y^2}\right] + \rho g\alpha(T_1 - T_0)\theta + \rho g\alpha(C_1 - C_0)\phi.$$

Multiplying by $\frac{d_1^2}{c\mu}$, yields

$$\frac{c\rho d_1}{\mu}\left[u\delta\frac{\partial u}{\partial x} + v\delta\frac{\partial u}{\partial y}\right] = -\frac{\partial p}{\partial x} + \left[\delta^2\frac{\partial^2 u}{\partial x^2} + \frac{\partial^2 u}{\partial y^2}\right] + \frac{\rho g\alpha d_1^2(T_1 - T_0)}{c\mu}\theta + \frac{\rho g\alpha d_1^2(C_1 - C_0)}{c\mu}\phi,$$

$$\implies Re\delta\left[u\frac{\partial u}{\partial x} + v\frac{\partial u}{\partial y}\right] = -\frac{\partial p}{\partial x} + \left[\delta^2\frac{\partial^2 u}{\partial x^2} + \frac{\partial^2 u}{\partial y^2}\right] + \frac{g\alpha d_1^2(T_1 - T_0)}{c\nu}\theta + \frac{g\alpha d_1^2(C_1 - C_0)}{c\nu}\phi. \tag{4.14}$$

Equation (4.6) in dimensionless form can be expressed as

$$\rho\left[cu\frac{\partial(c\delta v)}{\partial\left(\frac{\lambda x}{2\pi}\right)} + c\delta v\frac{\partial(c\delta v)}{\partial(d_1 y)}\right] = -\frac{\partial}{\partial(d_1 y)}\left(\frac{p\mu c\lambda}{2\pi d_1^2}\right) + \mu\left[\frac{\partial^2(c\delta v)}{\partial\left(\frac{\lambda x}{2\pi}\right)^2} + \frac{\partial^2(c\delta v)}{\partial(d_1 y)^2}\right] + \rho g\alpha(T_1 - T_0)\theta$$
$$+ \rho g\alpha(C_1 - C_0)\phi,$$

$$\Longrightarrow\ \rho\left[\frac{2\pi c^2\delta}{\lambda}u\frac{\partial v}{\partial x}+\frac{c^2\delta^2}{d_1}v\frac{\partial v}{\partial y}\right]=-\frac{\mu c\lambda}{2\pi d_1^3}\frac{\partial p}{\partial y}+\mu\left[\frac{2\pi c\delta}{\lambda^2}\frac{\partial^2 v}{\partial x^2}+\frac{c\delta}{d_1^2}\frac{\partial^2 v}{\partial y^2}\right]+\rho g\alpha(T_1-T_0)\theta+\rho g\alpha(C_1-C_0)\phi,$$

$$\Longrightarrow\ \rho\left[\frac{c^2\delta^2}{d_1}u\frac{\partial v}{\partial x}+\frac{c^2\delta^2}{d_1}v\frac{\partial v}{\partial y}\right]=-\frac{\mu c}{\delta d_1^2}\frac{\partial p}{\partial y}+\mu\left[\frac{c\delta^2}{d_1^2}\frac{\partial^2 v}{\partial x^2}+\frac{c\delta}{d_1^2}\frac{\partial^2 v}{\partial y^2}\right]+\rho g\alpha(T_1-T_0)\theta+\rho g\alpha(C_1-C_0)\phi,$$

$$\Longrightarrow\ \frac{c^2\delta^2\rho}{d_1}\left[u\frac{\partial v}{\partial x}+v\frac{\partial v}{\partial y}\right]=-\frac{\mu c}{\delta d_1^2}\frac{\partial p}{\partial y}+\frac{\mu c\delta}{d_1^2}\left[\delta^2\frac{\partial^2 v}{\partial x^2}+\frac{\partial^2 v}{\partial y^2}\right]+\rho g\alpha(T_1-T_0)\theta+\rho g\alpha(C_1-C_0)\phi,$$

$$\Longrightarrow\ \frac{c^2\delta^2\rho}{d_1}\left[u\frac{\partial v}{\partial x}+v\frac{\partial v}{\partial y}\right]=-\frac{\mu c}{\delta d_1^2}\frac{\partial p}{\partial y}+\frac{\mu c\delta}{d_1^2}\left[\delta^2\frac{\partial^2 v}{\partial x^2}+\frac{\partial^2 v}{\partial y^2}\right]+\rho g\alpha(T_1-T_0)\theta+\rho g\alpha(C_1-C_0)\phi.$$

Multiplying by $\frac{d_1^2}{\mu c\delta}$, we get

$$\frac{c\delta\rho d_1}{\mu}\left[u\frac{\partial v}{\partial x}+v\frac{\partial v}{\partial y}\right]=-\frac{1}{\delta^2}\frac{\partial p}{\partial y}+\left[\delta^2\frac{\partial^2 v}{\partial x^2}+\frac{\partial^2 v}{\partial y^2}\right]+\frac{\rho g\alpha d_1^2(T_1-T_0)}{c\mu\delta}\theta+\frac{\rho g\alpha d_1^2(C_1-C_0)}{c\mu\delta}\phi.$$

Multiplying by $\delta^2$, yields

$$Re\delta^3\left[u\frac{\partial v}{\partial x}+v\frac{\partial v}{\partial y}\right]=-\frac{\partial p}{\partial y}+\delta^2\left[\delta^2\frac{\partial^2 v}{\partial x^2}+\frac{\partial^2 v}{\partial y^2}\right]+\frac{\delta g\alpha d_1^2(T_1-T_0)}{c\nu}\theta+\frac{\delta g\alpha d_1^2(C_1-C_0)}{c\nu}\phi. \quad (4.15)$$

Equation (4.7) in dimensionless form can be expressed as

$$\left[cu\frac{\partial(\theta(T_1-T_0)+T_0)}{\partial\left(\dfrac{\lambda x}{2\pi}\right)}+\delta cv\frac{\partial(\theta(T_1-T_0)+T_0)}{\partial(d_1 y)}\right]=\alpha\left[\frac{\partial^2(\theta(T_1-T_0)+T_0)}{\partial\left(\dfrac{\lambda x}{2\pi}\right)^2}+\frac{\partial^2(\theta(T_1-T_0)+T_0)}{\partial(d_1 y)^2}\right]$$
$$+\tau D_B\left(\frac{\partial(\sigma(C_1-C_0)+C_0)}{\partial\left(\dfrac{\lambda x}{2\pi}\right)}\frac{\partial(\theta(T_1-T_0)+T_0)}{\partial\left(\dfrac{\lambda x}{2\pi}\right)}+\frac{\partial(\sigma(C_1-C_0)+C_0)}{\partial(d_1 y)}\frac{\partial(\theta(T_1-T_0)+T_0)}{\partial(d_1 y)}\right)$$
$$+\tau\frac{D_{\tilde{T}}}{T_0}\left(\left(\frac{\partial(\theta(T_1-T_0)+T_0)}{\partial\left(\dfrac{\lambda x}{2\pi}\right)}\right)^2+\left(\frac{\partial(\theta(T_1-T_0)+T_0)}{\partial(d_1 y)}\right)^2\right),$$

$$\implies \left[\frac{2\pi c(T_1-T_0)}{\lambda}u\frac{\partial\theta}{\partial x}+\frac{\delta c(T_1-T_0)}{d_1}v\frac{\partial\theta}{\partial y}\right]=\alpha\left[\frac{4\pi^2(T_1-T_0)}{\lambda^2}\frac{\partial^2\theta}{\partial x^2}+\frac{(T_1-T_0)}{d_1^2}\frac{\partial^2\theta}{\partial y^2}\right]$$
$$+\tau D_B\left(\frac{4\pi^2(C_1-C_0)(T_1-T_0)}{\lambda^2}\frac{\partial\sigma}{\partial x}\frac{\partial\theta}{\partial x}+\frac{(C_1-C_0)(T_1-T_0)}{d_1^2}\frac{\partial\sigma}{\partial y}\frac{\partial\theta}{\partial y}\right)$$
$$+\tau\frac{D_{\tilde{T}}}{T_0}\left(\frac{4\pi^2(T_1-T_0)^2}{\lambda^2}\left(\frac{\partial\theta}{\partial x}\right)^2+\frac{(T_1-T_0)^2}{d_1^2}\left(\frac{\partial\theta}{\partial y}\right)^2\right),$$

$$\implies \left[\frac{c\delta(T_1-T_0)}{d_1}u\frac{\partial\theta}{\partial x}+\frac{\delta c(T_1-T_0)}{d_1}v\frac{\partial\theta}{\partial y}\right]=\alpha\left[\frac{\delta^2(T_1-T_0)}{d_1^2}\frac{\partial^2\theta}{\partial x^2}+\frac{(T_1-T_0)}{d_1^2}\frac{\partial^2\theta}{\partial y^2}\right]$$
$$+\tau D_B\left(\frac{(C_1-C_0)(T_1-T_0)\delta^2}{d_1^2}\frac{\partial\sigma}{\partial x}\frac{\partial\theta}{\partial x}+\frac{(C_1-C_0)(T_1-T_0)}{d_1^2}\frac{\partial\sigma}{\partial y}\frac{\partial\theta}{\partial y}\right)$$
$$+\tau\frac{D_{\tilde{T}}}{T_0}\left(\frac{(T_1-T_0)^2\delta^2}{d_1^2}\left(\frac{\partial\theta}{\partial x}\right)^2+\frac{(T_1-T_0)^2}{d_1^2}\left(\frac{\partial\theta}{\partial y}\right)^2\right),$$

$$\implies \frac{c\delta(T_1-T_0)}{d_1}\left[u\frac{\partial\theta}{\partial x}+v\frac{\partial\theta}{\partial y}\right]=\alpha\frac{(T_1-T_0)}{d_1^2}\left[\delta^2\frac{\partial^2\theta}{\partial x^2}+\frac{\partial^2\theta}{\partial y^2}\right]$$
$$+\tau D_B\frac{(C_1-C_0)(T_1-T_0)}{d_1^2}\left(\delta^2\frac{\partial\sigma}{\partial x}\frac{\partial\theta}{\partial x}+\frac{\partial\sigma}{\partial y}\frac{\partial\theta}{\partial y}\right)$$
$$+\tau\frac{D_{\tilde{T}}}{T_0}\frac{(T_1-T_0)^2}{d_1^2}\left(\delta^2\left(\frac{\partial\theta}{\partial x}\right)^2+\left(\frac{\partial\theta}{\partial y}\right)^2\right).$$

Multiplying by $\dfrac{d_1^2}{\alpha(T_1-T_0)}$, we obtain

$$\frac{cd_1\delta}{\alpha}\left[u\frac{\partial\theta}{\partial x}+v\frac{\partial\theta}{\partial y}\right]=\left[\delta^2\frac{\partial^2\theta}{\partial x^2}+\frac{\partial^2\theta}{\partial y^2}\right]+\tau D_B\frac{(C_1-C_0)}{\alpha}\left(\delta^2\frac{\partial\sigma}{\partial x}\frac{\partial\theta}{\partial x}+\frac{\partial\sigma}{\partial y}\frac{\partial\theta}{\partial y}\right)$$
$$+\tau\frac{D_{\tilde{T}}}{T_0}\frac{(T_1-T_0)}{\alpha}\left(\delta^2\left(\frac{\partial\theta}{\partial x}\right)^2+\left(\frac{\partial\theta}{\partial y}\right)^2\right),$$

$$\implies RePr\delta\left[u\frac{\partial\theta}{\partial x}+v\frac{\partial\theta}{\partial y}\right]=\left[\delta^2\frac{\partial^2\theta}{\partial x^2}+\frac{\partial^2\theta}{\partial y^2}\right]+N_b\left(\delta^2\frac{\partial\sigma}{\partial x}\frac{\partial\theta}{\partial x}+\frac{\partial\sigma}{\partial y}\frac{\partial\theta}{\partial y}\right)+N_t\left(\delta^2\left(\frac{\partial\theta}{\partial x}\right)^2+\left(\frac{\partial\theta}{\partial y}\right)^2\right). \tag{4.16}$$

Equation (4.8) in dimensionless form can be expressed as

$$\left[cu\frac{\partial(\phi(C_1-C_0)+C_0)}{\partial\left(\frac{\lambda x}{2\pi}\right)}+\delta cv\frac{\partial(\phi(C_1-C_0)+C_0)}{\partial(d_1y)}\right]=D_B\left[\frac{\partial^2(\phi(C_1-C_0)+C_0)}{\partial\left(\frac{\lambda x}{2\pi}\right)^2}+\frac{\partial^2(\phi(C_1-C_0)+C_0)}{\partial(d_1y)^2}\right]$$
$$+\frac{D_{\tilde{T}}}{T_0}\left[\frac{\partial^2(\theta(T_1-T_0)+T_0)}{\partial\left(\frac{\lambda x}{2\pi}\right)^2}+\frac{\partial^2(\theta(T_1-T_0)+T_0)}{\partial(d_1y)^2}\right],$$

$$\Longrightarrow\left[\frac{2\pi c(C_1-C_0)}{\lambda}u\frac{\partial\phi}{\partial x}+\frac{c\delta(C_1-C_0)}{d_1}v\frac{\partial\phi}{\partial y}\right]=D_B\left[\frac{4\pi^2(C_1-C_0)}{\lambda^2}\frac{\partial^2\phi}{\partial x^2}+\frac{(C_1-C_0)}{d_1^2}\frac{\partial^2\phi}{\partial y^2}\right]$$
$$+\frac{D_{\tilde{T}}}{T_0}\left[\frac{4\pi^2(T_1-T_0)}{\lambda^2}\frac{\partial^2\theta}{\partial x^2}+\frac{(T_1-T_0)}{d_1^2}\frac{\partial^2\theta}{\partial y^2}\right],$$

$$\Longrightarrow\left[\frac{c\delta(C_1-C_0)}{d_1}u\frac{\partial\phi}{\partial x}+\frac{c\delta(C_1-C_0)}{d_1}v\frac{\partial\phi}{\partial y}\right]=D_B\left[\frac{\delta^2(C_1-C_0)}{d_1^2}\frac{\partial^2\phi}{\partial x^2}+\frac{(C_1-C_0)}{d_1^2}\frac{\partial^2\phi}{\partial y^2}\right]$$
$$+\frac{D_{\tilde{T}}}{T_0}\left[\frac{\delta^2(T_1-T_0)}{d_1^2}\frac{\partial^2\theta}{\partial x^2}+\frac{(T_1-T_0)}{d_1^2}\frac{\partial^2\theta}{\partial y^2}\right],$$

$$\Longrightarrow\frac{c\delta(C_1-C_0)}{d_1}\left[u\frac{\partial\phi}{\partial x}+v\frac{\partial\phi}{\partial y}\right]=D_B\frac{(C_1-C_0)}{d_1^2}\left[\delta^2\frac{\partial^2\phi}{\partial x^2}+\frac{\partial^2\phi}{\partial y^2}\right]+\frac{D_{\tilde{T}}}{T_0}\frac{(T_1-T_0)}{d_1^2}\left[\delta^2\frac{\partial^2\theta}{\partial x^2}+\frac{\partial^2\theta}{\partial y^2}\right].$$

Multiplying by $\frac{d_1^2}{D_B(C_1-C_0)}$, we obtain

$$\frac{cd_1\delta}{D_B}\left[u\frac{\partial\phi}{\partial x}+v\frac{\partial\phi}{\partial y}\right]=\left[\delta^2\frac{\partial^2\phi}{\partial x^2}+\frac{\partial^2\phi}{\partial y^2}\right]+\frac{D_T}{T_0}\frac{(T_1-T_0)}{D_B(C_1-C_0)}\left[\delta^2\frac{\partial^2\theta}{\partial x^2}+\frac{\partial^2\theta}{\partial y^2}\right],$$

$$\Longrightarrow ReS_c\delta\left[u\frac{\partial\phi}{\partial x}+v\frac{\partial\phi}{\partial y}\right]=\left[\delta^2\frac{\partial^2\phi}{\partial x^2}+\frac{\partial^2\phi}{\partial y^2}\right]+\frac{N_t}{N_b}\left[\delta^2\frac{\partial^2\theta}{\partial x^2}+\frac{\partial^2\theta}{\partial y^2}\right].\tag{4.17}$$

Substituting non-dimensional variables in equation (4.1) we obtain

$$yd_1=\tilde{h}_1=d_1+a_1\cos\frac{2\pi}{\lambda}\left(\frac{x\lambda}{2\pi}\right).$$

Dividing by $d_1$ yields

$$y = \frac{\tilde{h}_1}{d_1} = 1 + \frac{a_1}{d_1}\cos(x),$$

$$\Longrightarrow \; y = h_1 = 1 + a\cos(x). \tag{4.18}$$

Similarly for equation (4.2), substituting non-dimensional variables yields

$$yd_1 = \tilde{h}_2 = -d_2 - a_2\cos\left[\frac{2\pi}{\lambda}\left(\frac{x\lambda}{2\pi}\right) + \Phi\right].$$

Dividing by $d_1$ gives

$$y = \frac{\tilde{h}_2}{d_1} = -\frac{d_2}{d_1} + \frac{a_2}{d_1}\cos(x + \Phi),$$

$$\Longrightarrow y = h_2 = -d - b\cos(x + \Phi). \tag{4.19}$$

The boundary conditions of equation (4.9) in dimensionless form become

$$uc = -\tilde{\beta}\frac{\partial(uc)}{\partial(d_1 y)} - c,$$
$$\Longrightarrow uc = -\frac{\tilde{\beta}c}{d_1}\frac{\partial u}{\partial y} - c.$$

Dividing by $c$ we obtain,

$$u = -\frac{\tilde{\beta}}{d_1}\frac{\partial u}{\partial y} - 1,$$
$$u = -\beta\frac{\partial u}{\partial y} - 1. \tag{4.20}$$

$$uc = \tilde{\beta}\frac{\partial(uc)}{\partial(d_1 y)} - c,$$
$$\Longrightarrow uc = \frac{\tilde{\beta}c}{d_1}\frac{\partial u}{\partial y} - c,$$

$$u = \frac{\tilde{\beta}}{d_1}\frac{\partial u}{\partial y} - 1,$$
$$u = \beta\frac{\partial u}{\partial y} - 1. \tag{4.21}$$

The boundary conditions of equation (4.10) in dimensionless form become

$$\theta(T_1 - T_0) + T_0 + \tilde{\gamma}\frac{\partial(\theta(T_1 - T_0) + T_0)}{\partial(d_1 y)} = T_0,$$
$$\theta(T_1 - T_0) + \frac{\tilde{\gamma}(T_1 - T_0)}{d_1}\frac{\partial\theta}{\partial y} = 0.$$

Dividing by $(T_1 - T_0)$, we get

$$\theta + \frac{\tilde{\gamma}}{d_1}\frac{\partial\theta}{\partial y} = 0,$$
$$\theta + \gamma\frac{\partial\theta}{\partial y} = 0. \tag{4.22}$$

$$\theta(T_1 - T_0) + T_0 - \tilde{\gamma}\frac{\partial(\theta(T_1 - T_0) + T_0)}{\partial(d_1 y)} = T_1,$$
$$\theta(T_1 - T_0) - \frac{\tilde{\gamma}(T_1 - T_0)}{d_1}\frac{\partial\theta}{\partial y} = (T_1 - T_0),$$

$$\theta - \frac{\tilde{\gamma}}{d_1}\frac{\partial\theta}{\partial y} = 1,$$
$$\theta - \gamma\frac{\partial\theta}{\partial y} = 1. \tag{4.23}$$

The boundary conditions of equation (4.11) in dimensionless form become

$$\phi(C_1 - C_0) + C_0 + \tilde{\eta}\frac{\partial(\phi(C_1 - C_0))}{\partial(d_1 y)} = C_0,$$
$$\phi(C_1 - C_0) + \frac{\tilde{\eta}(C_1 - C_0)}{d_1}\frac{\partial\phi}{\partial y} = 0.$$

Dividing by $(C_1 - C_0)$, we get

$$\phi + \frac{\tilde{\eta}}{d_1}\frac{\partial\phi}{\partial y} = 0,$$
$$\phi + \eta\frac{\partial\phi}{\partial y} = 0. \tag{4.24}$$

$$\phi(C_1 - C_0) + C_0 - \tilde{\eta}\frac{\partial(\phi(C_1 - C_0))}{\partial(d_1 y)} = C_1,$$
$$\phi(C_1 - C_0) - \frac{\tilde{\eta}(C_1 - C_0)}{d_1}\frac{\partial \phi}{\partial y} = (C_1 - C_0),$$

$$\phi - \frac{\tilde{\eta}}{d_1}\frac{\partial \phi}{\partial y} = 1,$$
$$\phi - \eta\frac{\partial \phi}{\partial y} = 1. \tag{4.25}$$

Using long wavelength approximation, terms with $O(\delta)$ and higher tend to 0 and are ignored. So equations (4.13)-(4.17) are reduced to

$$\frac{\partial u}{\partial x} + \frac{\partial v}{\partial y} = 0, \tag{4.26}$$
$$\frac{\partial p}{\partial x} = \frac{\partial^2 u}{\partial y^2} + Gr\theta + Gr_\phi \phi, \tag{4.27}$$
$$\frac{\partial p}{\partial y} = 0, \tag{4.28}$$
$$\frac{\partial^2 \theta}{\partial y^2} + N_b \frac{\partial \phi}{\partial y}\frac{\partial \theta}{\partial y} + N_t\left(\frac{\partial \theta}{\partial y}\right)^2 = 0, \tag{4.29}$$
$$\frac{\partial^2 \phi}{\partial y^2} + \frac{N_t}{N_b}\left(\frac{\partial^2 \theta}{\partial y^2}\right) = 0, \tag{4.30}$$

with the appropriate boundary conditions

$$u = -\beta\frac{\partial u}{\partial y} - 1 \quad at \quad y = h_1, \quad u = \beta\frac{\partial u}{\partial y} - 1 \quad at \quad y = h_2, \tag{4.31}$$
$$\theta + \gamma\frac{\partial \theta}{\partial y} = 0 \quad at \quad y = h_1, \quad \theta - \gamma\frac{\partial \theta}{\partial y} = 1 \quad at \quad y = h_2, \tag{4.32}$$
$$\phi + \eta\frac{\partial \phi}{\partial y} = 0 \quad at \quad y = h_1, \quad \phi - \eta\frac{\partial \phi}{\partial y} = 1 \quad at \quad y = h_2, \tag{4.33}$$

where $\beta$ is the dimensionless velocity slip parameter, $\gamma$ is the dimensionless thermal slip parameter and $\eta$ is the dimensionless concentration slip parameter.

## 4.2 Method of Solution

We implement the ADM to solve the dimensionless governing equations. Introducing the linear operator $L$ in equation (4.30) we get,

$$L\phi + \frac{N_t}{N_b}\left(\frac{\partial^2\theta}{\partial y^2}\right) = 0,$$

$$\implies L\phi = -\frac{N_t}{N_b}\left(\frac{\partial^2\theta}{\partial y^2}\right). \tag{4.34}$$

Applying the inverse operator $L^{-1}$ on both sides of equation (4.34) gives

$$L^{-1}L\phi = -\frac{N_t}{N_b}L^{-1}\left(\frac{\partial^2\theta}{\partial y^2}\right), \tag{4.35}$$

$$\implies \int_0^y\int_0^y \frac{\partial^2\phi}{\partial y^2}dydy = -\frac{N_t}{N_b}L^{-1}\left(\frac{\partial^2\theta}{\partial y^2}\right). \tag{4.36}$$

Double integrating the left hand side of equation (4.36) we obtain

$$\phi(y) - \phi(0) - \phi'(0)y = -\frac{N_t}{N_b}L^{-1}\left(\frac{\partial^2\theta}{\partial y^2}\right). \tag{4.37}$$

Rearranging the terms and letting $\phi(0) = \alpha_1$ and $\phi'(0) = \alpha_2$ we get

$$\phi(y) = \alpha_1 + \alpha_2 y - \frac{N_t}{N_b}L^{-1}\left(\frac{\partial^2\theta}{\partial y^2}\right), \tag{4.38}$$

where $\alpha_1$ and $\alpha_2$ are constants. Using the ADM suggests that the solution $\phi(y)$ can be expressed by the decomposition series

$$\phi(y) = \sum_{n=0}^{\infty}\phi_n(y). \tag{4.39}$$

Inserting (4.39) into (4.38) yields

$$\sum_{n=0}^{\infty}\phi_n(y) = \alpha_1 + \alpha_2 y - \frac{N_t}{N_b}L^{-1}\left(\sum_{n=0}^{\infty}\frac{\partial^2\theta_n}{\partial y^2}\right). \tag{4.40}$$

We get the recursive relation

$$\phi_0(y) = \alpha_1 + \alpha_2 y,$$
$$\phi_{k+1}(y) = -\frac{N_t}{N_b} L^{-1}\left(\frac{\partial^2 \theta_k}{\partial y^2}\right), \qquad k \geq 0. \tag{4.41}$$

In an operator form, equation (4.29) can be written as

$$L\theta + N_b \frac{\partial \phi}{\partial y}\frac{\partial \theta}{\partial y} + N_t \left(\frac{\partial \theta}{\partial y}\right)^2 = 0,$$

$$\Longrightarrow \; L\theta = -N_b \frac{\partial \phi}{\partial y}\frac{\partial \theta}{\partial y} - N_t \left(\frac{\partial \theta}{\partial y}\right)^2. \tag{4.42}$$

Applying the inverse operator $L^{-1}$ on both sides of equation (4.42) yields

$$L^{-1}L\theta = -N_b L^{-1}\left(\frac{\partial \phi}{\partial y}\frac{\partial \theta}{\partial y}\right) - N_t L^{-1}\left(\frac{\partial \theta}{\partial y}\right)^2. \tag{4.43}$$

$$\Longrightarrow \; \int_0^y \int_0^y \frac{\partial^2 \theta}{\partial y^2} dy dy = -N_b L^{-1}\left(\frac{\partial \phi}{\partial y}\frac{\partial \theta}{\partial y}\right) - N_t L^{-1}\left(\frac{\partial \theta}{\partial y}\right)^2. \tag{4.44}$$

Double integrating the left hand side of equation (4.44), we obtain

$$\theta(y) - \theta(0) - \theta'(0)y = -N_b L^{-1}\left(\frac{\partial \phi}{\partial y}\frac{\partial \theta}{\partial y}\right) - N_t L^{-1}\left(\frac{\partial \theta}{\partial y}\right)^2. \tag{4.45}$$

Rearranging the terms and letting $\theta(0) = \alpha_3$ and $\theta'(0) = \alpha_4$ we get

$$\theta(y) = \alpha_3 + \alpha_4 y - N_b L^{-1}\left(\frac{\partial \phi}{\partial y}\frac{\partial \theta}{\partial y}\right) - N_t L^{-1}\left(\frac{\partial \theta}{\partial y}\right)^2, \tag{4.46}$$

where $\alpha_3$ and $\alpha_4$ are constants. The ADM suggests that the solution $\theta(y)$ can be expressed by the decomposition series

$$\theta(y) = \sum_{n=0}^{\infty} \theta_n(y), \tag{4.47}$$

and the nonlinear term $\left(\frac{\partial \theta}{\partial y}\right)^2$ is decomposed as

$$\left(\frac{\partial \theta}{\partial y}\right)^2 = \sum_{n=0}^{\infty} \omega_n. \tag{4.48}$$

where $\omega_n$ are called Adomian polynomials to be calculated.

Substituting equation (4.47) and equation (4.48) into equation (4.46) yields

$$\sum_{n=0}^{\infty} \theta_n(y) = \alpha_3 + \alpha_4 y - N_b L^{-1} \left( \sum_{n=0}^{\infty} \frac{\partial \phi_n}{\partial y} \frac{\partial \theta_n}{\partial y} \right) - N_t L^{-1} \left( \sum_{n=0}^{\infty} \omega_n \right). \tag{4.49}$$

We get the recursive relation

$$\begin{aligned} \theta_0(y) &= \alpha_3 + \alpha_4 y, \\ \theta_{k+1}(y) &= -N_b L^{-1} \left( \frac{\partial \phi_k}{\partial y} \frac{\partial \theta_k}{\partial y} \right) - N_t L^{-1} \left( \omega_k \right), \qquad k \geq 0. \end{aligned} \tag{4.50}$$

We have formulated two recursive iterations for $\phi$ and $\theta$. Now what is left is to find $\phi_{k+1}$ and $\theta_{k+1}$. For $k = 0$ we have

$$\begin{aligned} \phi_1(y) &= -\frac{N_t}{N_b} L^{-1} \left( \frac{\partial^2 \theta_0}{\partial y^2} \right), \\ &= -\frac{N_t}{N_b} L^{-1} \left( \frac{\partial^2}{\partial y^2} (\alpha_3 + \alpha_4 y) \right), \\ &= -\frac{N_t}{N_b} L^{-1}(0), \\ &= 0, \end{aligned} \tag{4.51}$$

$$\theta_1(y) = -N_b L^{-1} \left( \frac{\partial \phi_0}{\partial y} \frac{\partial \theta_0}{\partial y} \right) - N_t L^{-1} \left( \omega_0 \right).$$

The Adomian polynomial $\omega_0$ is given by

$$\begin{aligned} \omega_0 &= \left( \frac{\partial \theta_0}{\partial y} \right)^2, \\ &= \left( \frac{\partial}{\partial y} (\alpha_3 + \alpha_4 y) \right)^2, \\ &= \alpha_4^2, \end{aligned} \tag{4.52}$$

so that

$$\begin{aligned} \theta_1(y) &= -N_b L^{-1} \left( \frac{\partial}{\partial y} (\alpha_1 + \alpha_2 y) \frac{\partial}{\partial y} (\alpha_3 + \alpha_4 y) \right) - N_t L^{-1} \left( \alpha_4^2 \right), \\ &= -N_b L^{-1} (\alpha_2 \alpha_4) - N_t L^{-1} \left( \alpha_4^2 \right), \\ &= -\frac{1}{2} N_b (\alpha_2 \alpha_4) y^2 - \frac{1}{2} N_t \alpha_4^2 y^2. \end{aligned} \tag{4.53}$$

For $k = 1$ we have

$$\begin{aligned}
\phi_2(y) &= -\frac{N_t}{N_b} L^{-1}\left(\frac{\partial^2\theta_1}{\partial y^2}\right), \\
&= -\frac{N_t}{N_b} L^{-1}\left(\frac{\partial^2}{\partial y^2}(-\frac{1}{2}N_b(\alpha_2\alpha_4)y^2 - \frac{1}{2}N_t\alpha_4^2 y^2)\right), \\
&= \frac{N_t}{N_b} L^{-1}\left(N_b(\alpha_2\alpha_4) + N_t\alpha_4^2\right), \\
&= \frac{1}{2}N_t(\alpha_2\alpha_4)y^2 + \frac{1}{2}\frac{N_t^2}{N_b}\alpha_4^2 y^2,
\end{aligned} \tag{4.54}$$

$$\begin{aligned}
\theta_2(y) &= -N_b L^{-1}\left(\frac{\partial\phi_1}{\partial y}\frac{\partial\theta_1}{\partial y}\right) - N_t L^{-1}(\omega_1), \\
&= 0 - N_t L^{-1}(\omega_1), \\
&= -N_t L^{-1}(\omega_1).
\end{aligned} \tag{4.55}$$

The Adomian polynomial $\omega_1$ is given by

$$\begin{aligned}
\omega_1 &= 2\frac{\partial\theta_0}{\partial y}\frac{\partial\theta_1}{\partial y}, \\
&= 2\frac{\partial}{\partial y}(By)\frac{\partial}{\partial y}\left(-\frac{1}{2}N_b(\alpha_2\alpha_4)y^2 - \frac{1}{2}N_t\alpha_2^2 y^2\right), \\
&= -2\alpha_2\alpha_4^2 N_b y - 2\alpha_4^3 N_t y
\end{aligned} \tag{4.56}$$

so that

$$\begin{aligned}
\theta_2 &= -N_t L^{-1}\left(-2\alpha_2\alpha_4^2 N_b y - 2\alpha_4^3 N_t y\right), \\
&= \left(\frac{1}{3}N_b(\alpha_2\alpha_4^2)y^3 + \frac{1}{3}N_t\alpha_4^3 y^3\right) N_t.
\end{aligned} \tag{4.57}$$

For $k = 2$ we have

$$\begin{aligned}
\phi_3(y) &= -\frac{N_t}{N_b} L^{-1}\left(\frac{\partial^2\theta_2}{\partial y^2}\right), \\
&= -\frac{N_t}{N_b} L^{-1}\left(\frac{\partial^2}{\partial y^2}\left(\left(\frac{1}{3}N_b(\alpha_2\alpha_4^2)y^3 + \frac{1}{3}N_t\alpha_4^3 y^3\right) N_t\right)\right), \\
&= -\frac{\alpha_4^2 y^3 N_t^2(\alpha_2 N_b + \alpha_4 N_t)}{3N_b}.
\end{aligned} \tag{4.58}$$

The series solutions for $\phi$ and $\theta$ are thus given by

$$
\begin{aligned}
\phi &= \sum_{n=0}^{\infty} \phi_n \\
&= \phi_0 + \phi_1 + \phi_2 + \phi_3 + \dots \\
&= \alpha_1 + \alpha_2 y + \frac{1}{2} N_t(\alpha_2\alpha_4) y^2 + \frac{1}{2}\frac{N_t^2}{N_b}\alpha_4^2 y^2 - \frac{\alpha_4^2 y^3 N_t^2(\alpha_2 N_b + \alpha_4 N_t)}{3N_b} + \dots, \qquad (4.59) \\
\theta &= \sum_{n=0}^{\infty} \theta_n \\
&= \theta_0 + \theta_1 + \theta_2 + \dots \\
&= \alpha_3 + \alpha_4 y - \frac{1}{2} N_b(\alpha_2\alpha_4) y^2 - \frac{1}{2} N_t \alpha_4^2 y^2 + \left(\frac{1}{3} N_b(\alpha_2\alpha_4^2) y^3 + \frac{1}{3} N_t \alpha_4^3 y^3\right) N_t + \dots \qquad (4.60)
\end{aligned}
$$

Introducing the linear operator $L$ in equation (4.27) we get

$$Lu(y) = \frac{\partial p}{\partial x} - Gr\theta - Gr_\phi(\phi).$$

Applying the inverse operator $L^{-1}$ on both sides of the equation we obtain

$$L^{-1}Lu(y) = L^{-1}\frac{\partial p}{\partial x} - GrL^{-1}\theta - Gr_\phi L^{-1}\phi,$$

$$\implies \int_0^y \int_0^y \frac{\partial^2 u}{\partial y^2} dy dy = L^{-1}\frac{\partial p}{\partial x} - GrL^{-1}\theta - Gr_\phi L^{-1}\phi. \qquad (4.61)$$

Double integrating equation (4.61), we get

$$u(y) - u(0) - u'(0)y = L^{-1}\frac{\partial p}{\partial x} - GrL^{-1}\theta - Gr_\phi L^{-1}\phi.$$

Rearranging the terms and letting $u(0) = \alpha_5$ and $u'(0) = \alpha_6$

$$\implies u(y) = \alpha_5 + \alpha_6 y + \frac{1}{2}\frac{\partial p}{\partial x} y^2 - GrL^{-1}\theta - Gr_\phi L^{-1}\phi \qquad (4.62)$$

where $\alpha_5$ and $\alpha_6$ are constants. ADM suggests that the solution $u(y)$ can be expressed by the decomposition series

$$u(y) = \sum_{n=0}^{\infty} u_n(y). \qquad (4.63)$$

Substituting equation (4.63) into equation (4.62) we obtain

$$\sum_{n=0}^{\infty} u_n(y) = \alpha_5 + \alpha_6 y + \frac{1}{2}\frac{\partial p}{\partial x} y^2 - GrL^{-1}\left(\sum_{n=0}^{\infty}\theta_n(y)\right) - Gr_\phi L^{-1}\left(\sum_{n=0}^{\infty}\phi_n(y)\right). \tag{4.64}$$

The recursive relation

$$\begin{aligned} u_0(y) &= \alpha_5 + \alpha_6 y + \frac{1}{2}\frac{\partial p}{\partial x} y^2, \\ u_{k+1}(y) &= -GrL^{-1}\left(\theta_k(y)\right) - Gr_\phi L^{-1}\left(\phi_k(y)\right), \quad k \geq 0, \end{aligned} \tag{4.65}$$

is obtained. For $k = 0$ we have

$$\begin{aligned} u_1(y) &= -GrL^{-1}\left(\theta_0\right) - Gr_\phi L^{-1}\left(\phi_0\right), \\ &= -GrL^{-1}\left(\alpha_3 + \alpha_4 y\right) - Gr_\phi L^{-1}\left(\alpha_1 + \alpha_2 y\right), \\ &= -Gr\left(\frac{1}{2}\alpha_3 y^2 + \frac{1}{6}\alpha_4 y^3\right) - Gr_\phi\left(\frac{1}{2}\alpha_1 y^2 + \frac{1}{6}\alpha_2 y^3\right). \end{aligned} \tag{4.66}$$

For $k = 1$ we have

$$\begin{aligned} u_2(y) &= -GrL^{-1}\left(\theta_1\right) - Gr_\phi L^{-1}\left(\phi_1\right), \\ &= -GrL^{-1}\left(-\frac{1}{2}N_b(\alpha_2\alpha_4)y^2 - \frac{1}{2}N_t\alpha_4^2 y^2\right) - Gr_\phi L^{-1}\left(0\right), \\ &= Gr\left(\frac{1}{24}N_b(\alpha_2\alpha_4)y^4 + \frac{1}{24}N_t\alpha_4^2 y^4\right). \end{aligned} \tag{4.67}$$

For $k = 2$ we have

$$\begin{aligned} u_3(y) &= -GrL^{-1}\left(\theta_2\right) - Gr_\phi L^{-1}\left(\phi_2\right), \\ &= -GrL^{-1}\left(\left(\frac{1}{3}N_b(\alpha_2\alpha_4^2)y^3 + \frac{1}{3}N_t\alpha_4^3 y^3\right)N_t\right) - Gr_\phi L^{-1}\left(\frac{1}{2}N_t(\alpha_2\alpha_4)y^2 + \frac{1}{2}\frac{N_t^2}{N_b}\alpha_4^2 y^2\right), \\ &= -Gr\left(\frac{1}{60}N_b(\alpha_2\alpha_4^2)y^5 + \frac{1}{60}N_t\alpha_4^3 y^5\right)N_t - Gr_\phi\left(\frac{1}{24}N_t(\alpha_2\alpha_4)y^4 + \frac{1}{24}\frac{N_t^2}{N_b}\alpha_4^2 y^4\right). \end{aligned} \tag{4.68}$$

The series solution for $u$ is thus given as

$$
\begin{aligned}
u(y) =& \sum_{n=0}^{\infty} u_n \\
=& u_0 + u_1 + u_2 + u_3 + \dots \\
=& \alpha_5 + \alpha_6 y + \frac{1}{2}\frac{\partial p}{\partial x} y^2 - Gr\left(\frac{1}{2}\alpha_3 y^2 + \frac{1}{6}\alpha_4 y^3\right) - Gr_\phi\left(\frac{1}{2}\alpha_1 y^2 + \frac{1}{6}\alpha_2 y^3\right) \\
&+ Gr\left(\frac{1}{24}N_b(\alpha_2\alpha_4)y^4 + \frac{1}{24}N_t\alpha_4^2 y^4\right) - Gr\left(\frac{1}{60}N_b(\alpha_2\alpha_4^2)y^5 + \frac{1}{60}N_t\alpha_4^3 y^5\right) N_t \\
&- Gr_\phi\left(\frac{1}{24}N_t(\alpha_2\alpha_4)y^4 + \frac{1}{24}\frac{N_t^2}{N_b}\alpha_4^2 y^4\right) + \dots. \qquad (4.69)
\end{aligned}
$$

## 4.3 Results and Discussion

In this section we present the graphical solution of peristaltic flow of a nanofluid through a two dimensional microchannel with slip effects. Numerical solution showing the influence of the various parameters on the axial velocity, temperature and nanoparticle concentration profile are displayed in Figs 4.2-4.16. Unless a parameter is being varied, the default values $N_b = 3$, $Gr = 5$, $N_t = 1$, $\beta = 0.2$, $\gamma = 0.2$, $\eta = 0.2$ and $Gr_\phi = 5$ are used in the ADM computations. As we pointed out in chapter 3, both the Brownian motion parameter and the thermophoresis parameter have significant influence on the nanoparticle species diffusion. Further, thermophoresis tends to move light molecules to elevated temperature regions and heavy molecules to depressed temperature regions.

Figures 4.2-4.5 show the influence of the Brownian motion parameter $N_b$, the thermophoresis parameter $N_t$, the concentration slip parameter $\eta$ and the thermal slip parameter $\gamma$ on the nanoparticle concentration profile. Figure 4.2 shows slight enhancement of the nanoparticle concentration profile with increasing values of the Brownian motion parameter. On the other hand, in Fig 4.3 the thermophoresis parameter is observed to cause a significant reduction in the nanoparticle concentration profile. The most significant reduction is from the channel core region to the upper wall. A possible reason for the behaviour in Fig 4.2 is that by increasing the Brownian motion, the random motion of particles increases causing increased concentration in some specific channel regions. The concentration slip parameter $\eta$, Fig 4.4, is observed to reduce the nanoparticle concentration profile in the bulk of the fluid, but closer to the upper channel wall the concentration slip parameter enhances it. In Fig 4.5, the thermal slip parameter causes a slight increase in the nanoparticle concentration profile in the bulk of the fluid away from the lower channel wall. The response of the nanofluid temperature profile to the parameter variations is depicted in Figs 4.6-4.9. Both the Brownian motion parameter and the thermophoresis parameter have an enhancement effect on the temperature profile (see Figs 4.6-4.7). One can see that the effects of the two parameters are, physically, mirror images of each other. In Fig 4.8, the thermal slip parameter increases the fluid temperature in the bulk of the fluid in the region $-0.6 < y \leq 1$. Closer to the lower wall, the thermal slip parameter decreases the fluid temperature marginally. The concentration slip parameter $\eta$ has a cooling effect on the fluid (see Fig 4.9).

Figures 4.10-4.16 display the effects of the fluid parameters on the axial velocity profile $u$. In Figs 4.10, 4.12, 4.14, 4.15 and 4.16, the Brownian motion parameter $N_b$, the velocity slip parameter $\beta$, the thermal Grashof number $Gr$, the thermal slip parameter $\gamma$ and the nanoparticle Grashof number $Gr_\phi$, respectively are all observed to increase the axial velocity profile significantly. The physical interpretation of this phenomenon is that an increase in Brownian motion enhances the random movement of the fluid particles and thereby increasing the velocity. Further, since the thermal slip parameter increases the fluid temperature in the bulk of the fluid (Fig 4.8), it inevitably enhances the motion of the fluid particles as depicted in Fig 4.15. In Fig 4.14 and 4.16, the Grashof numbers enhancement of the axial velocity profile is a result of the effects of buoyancy sources terms that raise the fluid temperature, and due to coupling, the axial velocity increases as a result. The retardation of the axial velocity due to an increase in the concentration slip parameter, Fig 4.13, is explained by the fact that the concentration slip parameter diminishes the fluid temperature (Fig 4.9). In Fig 4.11, the thermophoresis parameter is observed to have a significant retardation effect on fluid axial velocity.

This phenomenon is somewhat peculiar because the thermophoresis parameter was observed to increase the fluid temperature in Fig 4.7. Finally, our results are consistent with those of Akbar *et al.* (2012), where the same type of flow was investigated using the homotopy perturbation method . We, however, must point out that Akbar *et al.* (2012) did not investigate the effect of thermophoresis on axial velocity.

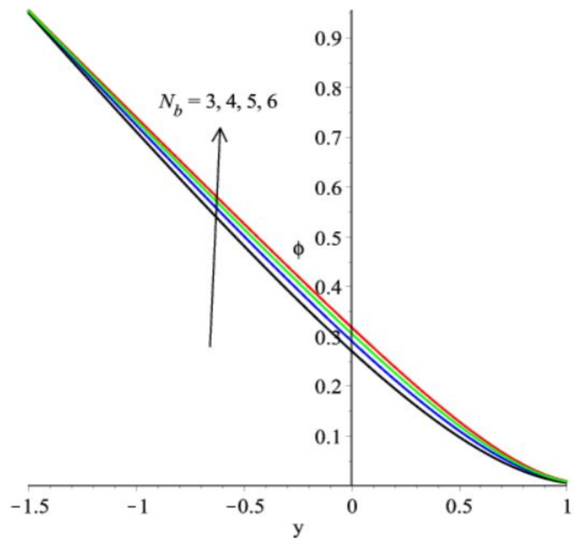


Figure 4.2: Effects of Brownian motion parameter $N_b$ on nanoparticle concentration profile

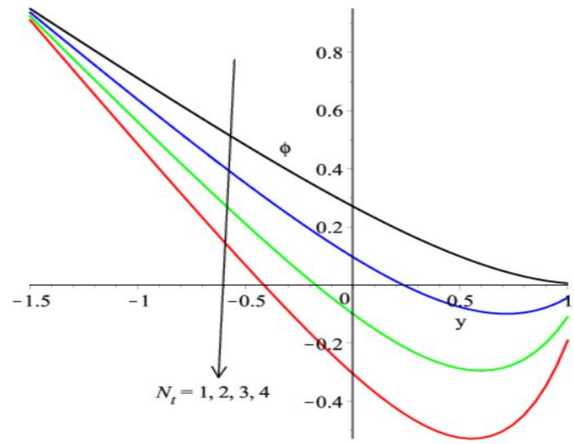


Figure 4.3: Effects of thermophoresis parameter $N_t$ on nanoparticle concentration profile

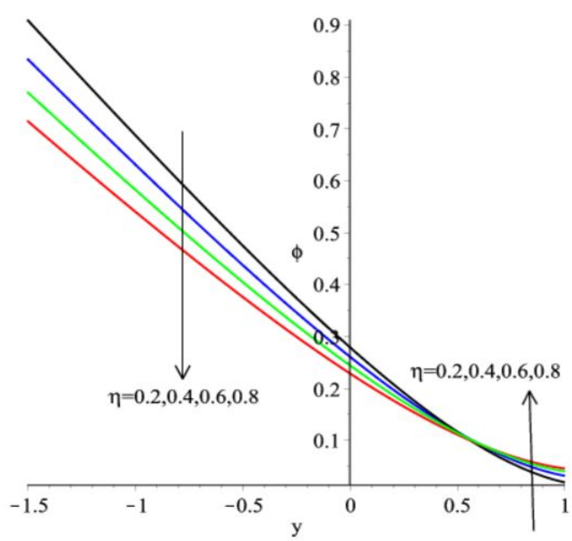


Figure 4.4: Effects of concentration slip parameter $\eta$ on nanoparticle concentration profile

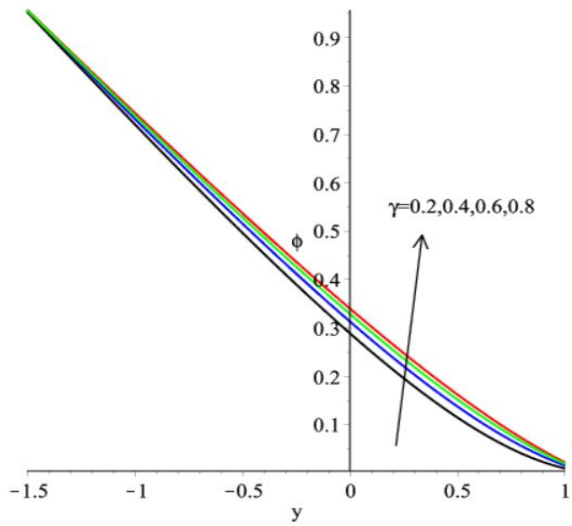


Figure 4.5: Effects of thermal slip parameter $\gamma$ on nanoparticle concentration profile

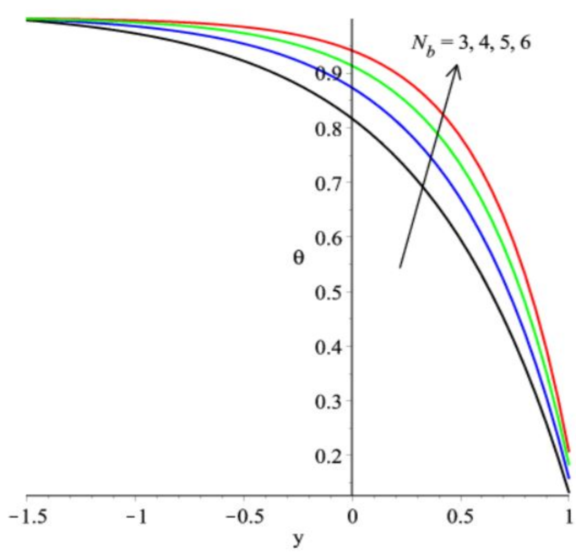


Figure 4.6: Effects of Brownian motion parameter $N_b$ on temperature profile

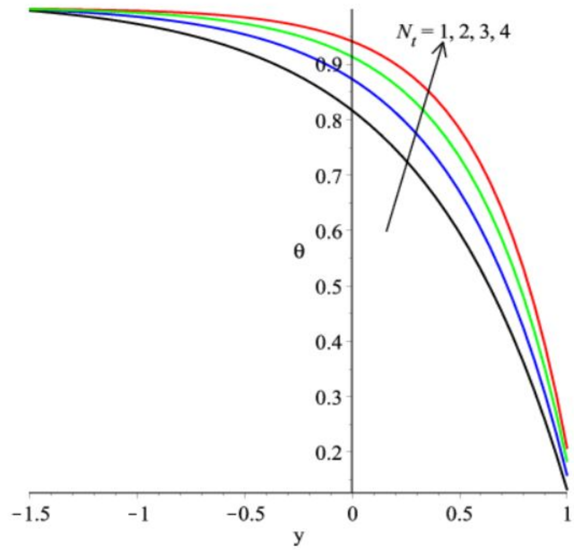


Figure 4.7: Effects of thermophoresis parameter $N_t$ on temperature profile

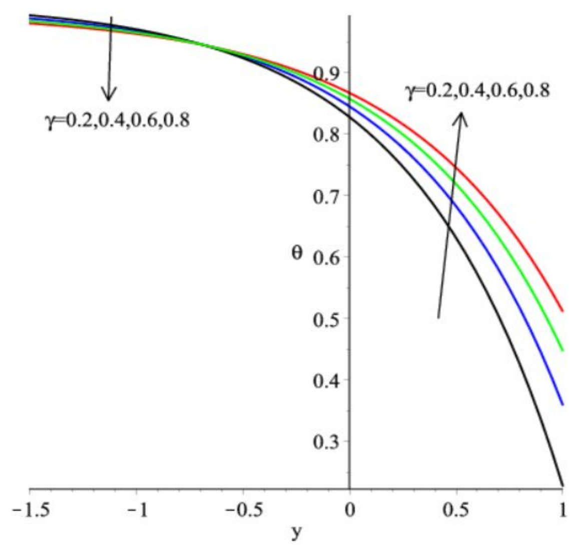


Figure 4.8: Effects of thermal slip parameter $\gamma$ on temperature profile

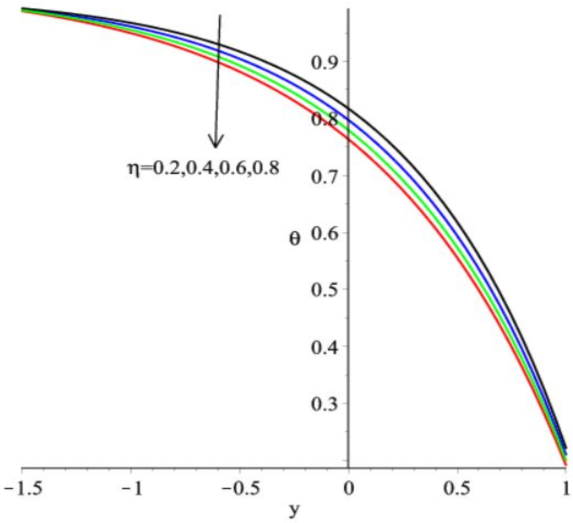


Figure 4.9: Effects of concentration slip parameter $\eta$ on temperature profile

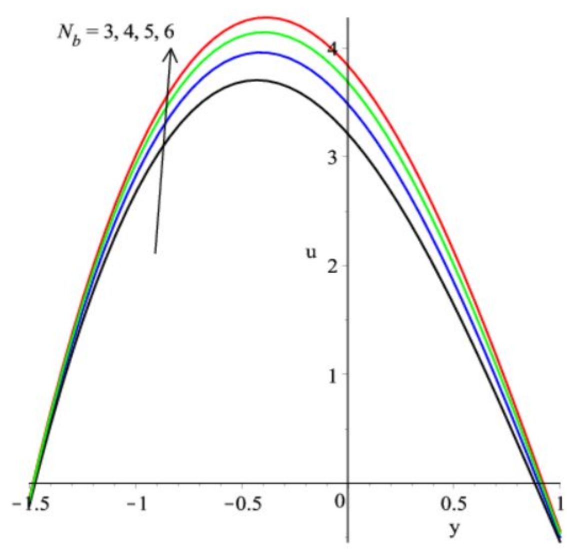


Figure 4.10: Effects of Brownian motion parameter $N_b$ on velocity profile

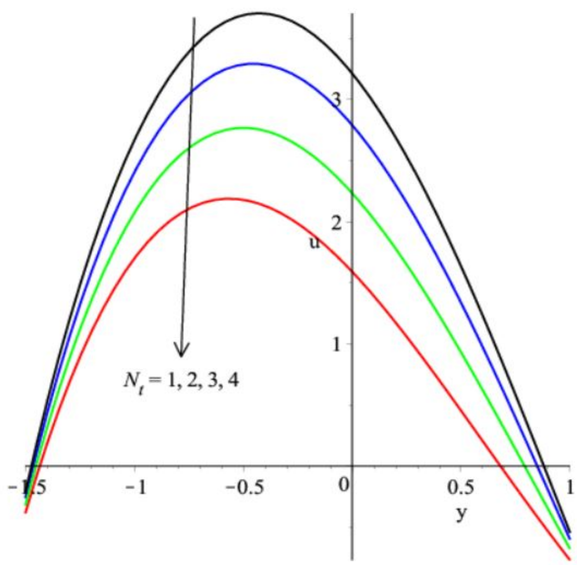


Figure 4.11: Effects of thermophoresis parameter $N_t$ on velocity profile

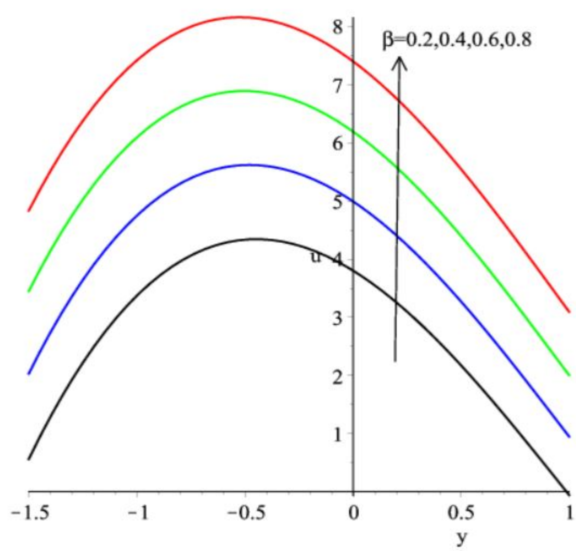


Figure 4.12: Effects of velocity slip parameter $\beta$ on velocity profile

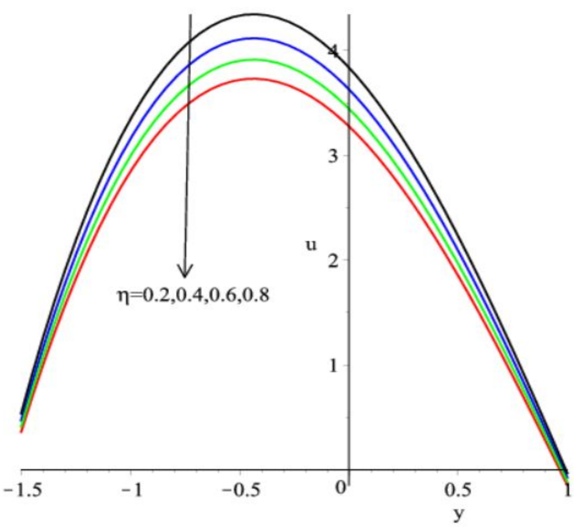


Figure 4.13: Effects of concentration slip parameter $\eta$ on velocity profile

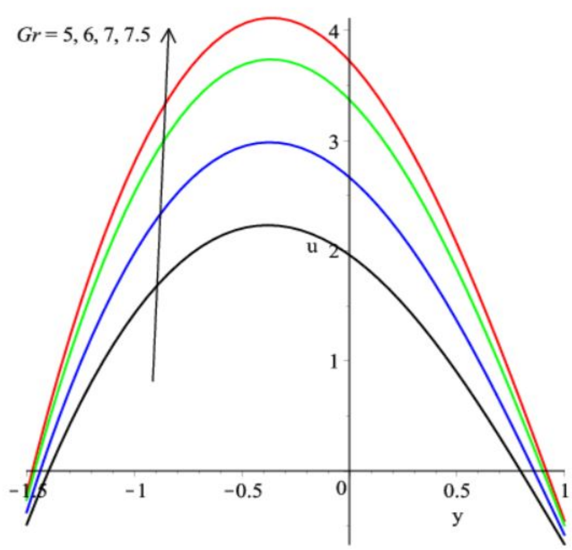


Figure 4.14: Effects of local thermal Grashof number $Gr$ on velocity profile

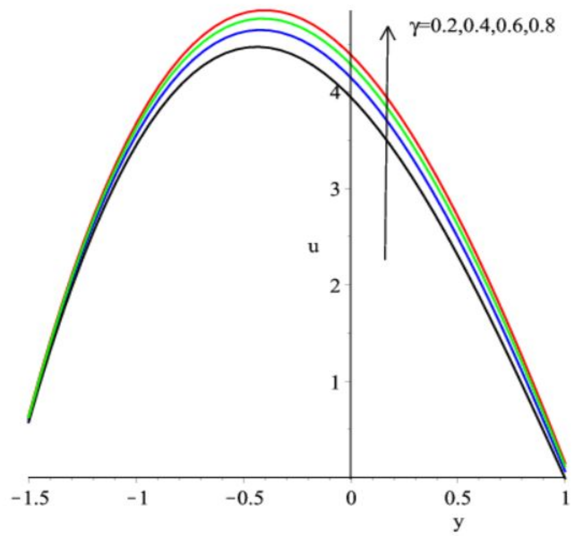


Figure 4.15: Effects of thermal slip parameter $\gamma$ on velocity profile

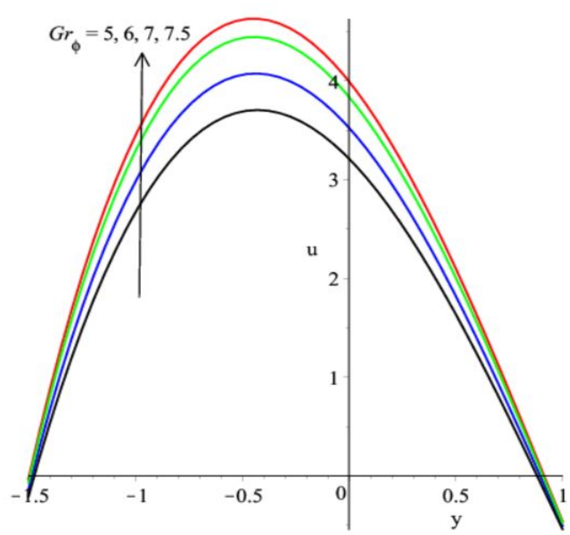


Figure 4.16: Effects of local nanoparticle Grashof number $Gr_\phi$ on velocity profile

# Chapter 5

# General Discussion, Conclusions and Recommendations

## 5.1 General Discussion

In this theoretical study, a survey of nanofluids as important heat transfer fluids is carried out. The Buongiorno model formulation was utilized for peristaltic flow of a nanofluid in a two dimensional microchannel with and without slip effects. The Adomian decomposition method was applied to solve the governing equations, obtaining the series solutions for axial velocity, temperature and nanoparticle concentration profiles. Variations of these flow field variables with the embedded thermophysical parameters were analyzed graphically and discussed quantitatively and qualitatively. The results were compared with those in literature.

## 5.2 Conclusions

Peristaltic flow of a nanofluid in a two dimensional microchannel was investigated by employing the Buongiorno model formulation. Brownian motion, thermophoresis, buoyancy and slip parameters were observed to impact the flow axial velocity, temperature and nanoparticle concentration profiles significantly.

In the flow without slip effects, significant flow reversal was observed in the channel half-space and maximum axial velocity was record around the channel core region, diminishing to zero at the channel walls. The thermophoresis parameter and the thermal Grashof number were observed to have an opposing effect on the backflow and, on the other hand, Brownian motion parameter and the nanoparticle species Grashof number enhanced it. The Brownian motion and the thermophoresis parameters depicted similar effects on the nanofluid temperature distribution. The parameters reveal a cooling effect around the channel walls and marginal increase in the fluid temperature in the channel core region. The nanoparticle concentration profile is enhanced by thermophoresis.

In the flow with slip effects, both the Brownian motion and thermophoresis parameters had a diminishing effect on the nanoparticle concentration profile. The concentration slip parameter was also observed to reduce the nanoparticle concentration profile in the bulk of the fluid, but closer to the upper channel wall, the opposite effect was noticed. The thermal slip parameter was observed to cause a marginal increase in the nanoparticle concentration profile in the bulk of the fluid. The nanofluid temperature profile was enhanced with both the Brownian motion and thermophoresis parameters. The concentration slip parameter had a cooling effect on the nanofluid, whereas the thermal slip parameter increased the temperature in the bulk of the fluid but decreases it marginally closer to the lower channel wall.

The axial velocity profile increased with the Brownian motion parameter, the velocity slip parameter, the thermal Grashof number, the thermal slip parameter and the nanoparticle Grashof number. On the other hand, the axial velocity profile was retarded by the concentration slip parameter. The thermophoresis parameter was observed to have significant retardation effect on the axial velocity in the slip flow.

In general, the obtained results compared very well with those obtained by Triphathi and Bég (2014) and Akbar *et al.* (2012) where the same flows were studied by an approximate analytical method and the homotopy analysis method, respectively. The results of this study have profound impact on real life as peristaltic nanofluid flow has wide applications as documented in the earlier survey chapter.

## 5.3 Recommendations

The ADM was implemented effectively in solving nonlinear equations modelling peristaltic nanofluid flow. Generally, agreement with results of the methods in literature confirms that ADM is also a pertinent tool in solving nonlinear models.

## 5.4 Future Research Work

Future work involves extending the model by considering different flow geometries subjected to various physical effects like magnetic field, chemical reaction, porous media and convective boundary conditions. Exploration of the application of other numerical methods is also a possibility.

# List of References

Abbasi, F.M., Hayat, T. and Alsaedi, A., 2015. Peristaltic transport of magneto-nanoparticles submerged in water: model for drug delivery system. Physica E: Low-dimensional Systems and Nanostructures, 68, pp.123-132.

Ahmadi, M., 2015. Heat transfer mechanisms in water-based nanofluids (Doctoral dissertation, University of Louisville).

Ahmed, S.E., Hussein, A.K., Mansour, M.A., Raizah, Z.A. and Zhang, X., 2018. MHD mixed convection in trapezoidal enclosures filled with micropolar nanofluids. Nanoscience and Technology: An International Journal, 9(4), pp 343-372.

Akbar, N.S. and Nadeem, S., 2011. Endoscopic effects on peristaltic flow of a nanofluid. Communications in Theoretical Physics, 56(4), p.761.

Akbar, N.S., Nadeem, S., Hayat, T. and Hendi, A.A., 2012. Peristaltic flow of a nanofluid with slip effects. Meccanica, 47(5), pp.1283-1294.

Ali, H.M., Sajid, M.U. and Arshad, A., 2017. Heat transfer applications of TiO2 nanofluids. Application of titanium dioxide.

Alonso, M. and Finn, E.J., 1967. Fundamental university physics. Reading, MA: Addison-Wesley.

Asha, S.K. and Deepa, C.K., 2019. Entropy generation for peristaltic blood flow of a magneto-micropolar fluid with thermal radiation in a tapered asymmetric channel. Results in Engineering, 3, p.100024.

Bahiraei, M. and Heshmatian, S., 2018. Electronics cooling with nanofluids: a critical review.

Energy Conversion and Management, 172, pp.438-456.

Bairwa, D.K., Upman, K.K. and Kantak, G., 2015. Nanofluids and its Applications. International Journal of Engineering, Management and Sciences, 2, pp.7-14.

Bibi, A. and Xu, H., 2019. Entropy generation analysis of peristaltic flow and heat transfer of a Jeffery nanofluid in a horizontal channel under magnetic environment. Mathematical Problems in Engineering, https://doi.org/10.1155/2019/2405986, Article ID 2405986 13 pages.

Buongiorno, J. 2006. Convective transport in nanofluids, ASME, Journal of Heat Transfer, 128, pp.240-250.

Chamsa-Ard, W., Brundavanam, S., Fung, C.C., Fawcett, D. and Poinern, G., 2017. Nanofluid types, their synthesis, properties and incorporation in direct solar thermal collectors: A review. Nanomaterials, 7(6), p.131.

Chein, R., and Chuang, J., 2007, Experimental Microchannel Heat Sink Performance Studies using Nanofluids, Int. J. Therm. Sci., 46(1), pp. 57-66.

Choi, S.U.S.: Enhancing thermal conductivity of fluids with nanoparticles, in: D.A. Siginer, H.P. Wang (Eds.), developments and applications of non-Newtonian flows FED-vol. 231/MD-66, ASME, New York, 1995, 99–105.

Choi, S.U. and Eastman, J.A., 1995. Enhancing thermal conductivity of fluids with nanoparticles (No. ANL/MSD/CP-84938; CONF-951135-29). Argonne National Lab.(ANL), Argonne, IL (United States).

Deshmukh G., Jose N., Shidhav R., Suryawanshi A., Datir R. and Ravindra M.R, 2019. Nanofluids: An Introduction to New Generation Heat Transfer Fluids; vol 3 Acta Scientific Agriculture 3.2 p.p 41-48.

El-Mistikawy, T., 2018. Couette-Poiseuille flow with partial slip and uniform cross flow for power-law fluids. arXiv preprint arXiv:1803.07606.

en.wikiversity.org/wiki, Retrived on 25 February 2022.

Fanchi, J.R. and Christiansen, R.L., 2016. Introduction to petroleum engineering. John Wiley and Sons, New York.

Feynman, R.P., Leighton, R.B. and Sands, M., 1965. The feynman lectures on physics; vol. i. American Journal of Physics, 33(9), pp.750-752.

Fox, R.W., McDonald, A.T. and Mitchell, J.W., 2020. Fox and McDonald's introduction to fluid mechanics. John Wiley and Sons, New York.

Hayat, T., Nisar, Z., Yasmin, H. and Alsaedi, A., 2016. Peristaltic transport of nanofluid in a compliant wall channel with convective conditions and thermal radiation. Journal of Molecular Liquids, 220, pp.448-453.

Intergovernmental Panel on Climate Change (IPCC). 2018. Global Warming of 1.5°C. 11-15.

Iborra Rubio, J., 2012. Nanofluids: Thermophysical Analysis and Heat Transfer Performance (Masters dissertation, KTH School of Industrial Engineering and Management Energy Technology)

Ibragimov, M.H., 2011. Channel Flow. In Thermopedia. Begel House Inc, United States.

Incropera, F.P., DeWitt, D.P., Bergman, T.L. and Lavine, A.S., 1996. Fundamentals of heat and mass. New York: Wiley.

Jordan, A., Scholz, R., Wust, P., Fähling, H. and Felix, R., 1999. Magnetic fluid hyperthermia (MFH): Cancer treatment with AC magnetic field induced excitation of biocompatible superparamagnetic nanoparticles. Journal of Magnetism and Magnetic materials, 201(1-3), pp.413-419.

Lai, W.M., Rubin, D.H., Rubin, D. and Krempl, E., 2009. Introduction to continuum mechanics. Butterworth-Heinemann, United Kingdom.

Lee, J., and Mudawar, I., 2007, "Assessment of the Effectiveness of Nanofluids for Single-Phase and Two-Phase Heat Transfer in MicroChannels," Int. J. Heat Mass Tran., 50(3-4), pp. 452-463.

Li, J. and Yu, B., 2022. Gas properties, fundamental equations of state and phase relationships. In Sustainable Natural Gas Reservoir and Production Engineering (pp. 1-28). Gulf Professional Publishing, London, UK.

Lo, C.H., Tsung, T.T., Chen, L.C., Su, C.H. and Lin, H.M., 2005. Fabrication of copper oxide nanofluid using submerged arc nanoparticle synthesis system (SANSS). Journal of Nanoparticle Research, 7(2), pp.313-320.

Mallick, B. and Misra, J.C., 2019. Peristaltic flow of Eyring-Powell nanofluid under the action of an electromagnetic field. Engineering Science and Technology, an International Journal, 22(1), pp.266-281.

Mamut, E., 2006. Characterization of heat and mass transfer properties of nanofluids. Romanian Journal of Physics, 51(1/2), p.5.

Mishra, A., 2014. Analysis of nanofluids. International Journal of Mechanical Engineering and Robotics Research, 3(3), p.557.

Molana, M., 2017. On the nanofluids application in the automotive radiator to reach the enhanced thermal performance: a review. Am. J. Heat Mass Transf, 4(4), pp.168-187.

Monaledi, R., 2020. Theoretical study of variable viscosity nanofluids flow in microchannels (Doctoral dissertation, Stellenbosch: Stellenbosch University).

Mutuku-Njane, W.N., 2014. Analysis of hydromagnetic boundary layer flow and heat transfer of nanofluids (Doctoral dissertation, Cape Peninsula University of Technology).

Nadeem, S. and Akbar, N.S., 2009. Influence of heat transfer on a peristaltic transport of Herschel–Bulkley fluid in a non-uniform inclined tube. Communications in Nonlinear Science and Numerical Simulation, 14(12), pp.4100-4113.

Nakayama, Y., 2018. Introduction to fluid mechanics. Butterworth-Heinemann, United Kingdom.

Nave, R., 2000. HyperPhysics. Georgia State University, Department of Physics and Astronomy.

Özerinç, S., 2010. Heat transfer enhancement with nanofluids (Masters dissertation, Middle East Technical University).

Prasad, A.R., Singh, D.S. and Nagar, D.H., 2017. A Review on Nano fluids: properties and applications. Int. J. Adv. Res. Innov. Ideas. Educ, 3(3), pp.3185-3209.

Rapp, B.E., 2016. Microfluidics: modeling, mechanics and mathematics. William Andrew, Norwich, New York.

Rehm, B., Haghshenas, A., Paknejad, A.S. and Schubert, J., 2008. Situational problems in MPD. In Managed Pressure Drilling (pp. 39-80). Gulf Publishing Company, London, UK.

Saidur, R., Leong, K.Y. and Mohammed, H.A., 2011. A review on applications and challenges of nanofluids. Renewable and sustainable energy reviews, 15(3), pp.1646-1668.

Saini, D.K. and Agarwal, G.D., 2016. Thermo-physical properties of nano fluids—a review. Int. J. Adv. Eng. Sci. Technol, 5(1), pp.39-45.

Saleh, H., Alali, E. and Ebaid, A., 2017. Medical applications for the flow of carbon-nanotubes suspended nanofluids in the presence of convective condition using Laplace transform. Journal of the association of Arab universities for basic and applied sciences, 24, pp.206-212.

Sheikholeslami, M. and Ganji, D.D., 2017. Applications of nanofluid for heat transfer enhancement. William Andrew, Norwich, New Yok.

Smith, R., Inomata, H. and Peters, C., 2013. Introduction to supercritical fluids: a spreadsheet-based approach. Newnes, Australia.

Speiser, D., 2008. Discovering the principles of mechanics 1600-1800: essays by David Speiser (Vol. 1). Springer Science and Business Media, Berlin, Germany.

Srinivasacharya, D., Mallikarjuna, B. and Bhuvanavijaya, R., 2015. Soret and Dufour effects on mixed convection along a vertical wavy surface in a porous medium with variable properties. Ain Shams Engineering Journal, 6(2), pp.553-564.

Study.com/academy/answer, Retrieved on 05 March 2022.

Tian, Y. and Zhao, C. Y. 2013. A review of solar collectors and thermal energy storage in solar thermal applications. Applied Energy, 104, pp.538-553.

Tomaizeh, H., 2017. Modified Adomian Decomposition Method For Differential Equations (Masters dissertation, Hebron University)

Tripathi, D. and Bég, O.A., 2014. A study on peristaltic flow of nanofluids: Application in drug delivery systems. International Journal of Heat and Mass Transfer, 70, pp.61-70.

Vasudev, C., Rajeswara Rao, U., Prabhakara Rao, G. and Subba Reddy, M.V., 2011. Peristaltic flow of a Newtonian fluid through a porous medium in a vertical tube under the effect of a magnetic field, International Journal of Current Scientific Research, 1(3), pp. 105-110.

Wang, X.Q. and Mujumdar, A.S., 2008. A review on nanofluids-part I: theoretical and numerical investigations. Brazilian Journal of Chemical Engineering, 25(4), pp.613-630.

Wazwaz, A.M., 2009. Solitary Waves Theory. In Partial Differential Equations and Solitary Waves Theory (pp. 479-502). Springer, Berlin, Heidelberg.

White, F.M., 1979. Fluid mechanics. Tata McGraw-Hill Education, United States.

Wong, K.V. and De Leon, O., 2010. Applications of nanofluids: current and future. Advances in Mechanical Engineering, 2, pp.519-659.

# Appendix: Mathematica code used for the computations

```
   DSolve[{ D[ D[ \[Sigma][y], y], y] +
     Subscript[N, t]/Subscript[N, b] D[ D[\[Theta][y], y], y] ==
   0, \[Sigma][0] == 0,
  D[ \[Sigma][0], y] == 0, \[Sigma][h] == 1}, \[Sigma], y]
  Subscript[\[Sigma], 0][y] = A y
  Subscript[\[Theta], 0][y] = B y
  Subscript[\[Sigma], 1][y] = -( Subscript[N, t]/Subscript[N, b]) \!\(
\*SubsuperscriptBox[\(\[Integral]\), \(0\), \(y\)]\(
\*SubsuperscriptBox[\(\[Integral]\), \(0\), \(y\)]\ D[\ D[
\(\*SubscriptBox[\(\[Theta]\), \(0\)]\)[y], \ y],
      y] \[DifferentialD]y \[DifferentialD]y\)\)=0
Subscript[\[Theta], 1][y] = -(1/2) y^2 (A B) Subscript[N, b] -
  1/2 y^2 B^2 Subscript[N, t]
      =-(1/2) A B y^2 Subscript[N, b] - 1/2 B^2 y^2 Subscript[N, t]
      =Subscript[\[Sigma], 2][y] = - ( Subscript[N, t]/Subscript[N, b]) \!\(
\*SubsuperscriptBox[\(\[Integral]\), \(0\), \(y\)]\(
\*SubsuperscriptBox[\(\[Integral]\), \(0\), \(y\)]\ D[\ D[
\(\*SubscriptBox[\(\[Theta]\), \(1\)]\)[y], \ y],
```

```
      y] \[DifferentialD]y \[DifferentialD]y\)\)
      =-((y^2 Subscript[N, t] (-A B Subscript[N, b] - B^2 Subscript[N, t]))/(
 2 Subscript[N, b]))
 Subscript[\[Theta], 2][y] =
 Subscript[N,
  t] (1/3  y^3 B (A B) Subscript[N, b] + 1/3 B^3 y^3 Subscript[N, t])
  =Subscript[N, t] (1/3 A B^2 y^3 Subscript[N, b] +
   1/3 B^3 y^3 Subscript[N, t])
   Subscript[\[Sigma], 3][y] = - ( Subscript[N, t]/Subscript[N, b]) \!\(
\*SubsuperscriptBox[\(\[Integral]\), \(0\), \(y\)]\(
\*SubsuperscriptBox[\(\[Integral]\), \(0\), \(y\)]\ D[\ D[
\(\*SubscriptBox[\(\[Theta]\), \(2\)]\)[y], \ y],
      y] \[DifferentialD]y \[DifferentialD]y\)\)
      =-((B^2 y^3
\!\(\*SubsuperscriptBox[\(N\), \(t\), \(2\)]\) (A Subscript[N, b] +
    B Subscript[N, t]))/(3 Subscript[N, b]))
    B = (-6 h + 3 h Subscript[N, b] + 3 h Subscript[N, t] +
  Sqrt[(-6 h + 3 h Subscript[N, b] + 3 h Subscript[N, t])^2 -
   24 (-2 h^2 Subscript[N, b] Subscript[N, t] - 2 h^2
\!\(\*SubsuperscriptBox[\(N\), \(t\), \(2\)]\))])/(
 4 (h^2 Subscript[N, b] Subscript[N, t] + h^2
\!\(\*SubsuperscriptBox[\(N\), \(t\), \(2\)]\)))
A = (6 - 6 B h + 3 B^2 h^2 Subscript[N, t] - 2 B^3 h^3
\!\(\*SubsuperscriptBox[\(N\), \(t\), \(2\)]\))/(
 B h^2 Subscript[N, b] (-3 + 2 B h Subscript[N, t]))
 =(4 (h^2 Subscript[N, b] Subscript[N, t] + h^2
\!\(\*SubsuperscriptBox[\(N\), \(t\), \(2\)]\)) (6 - (
```

```
   3 h (-6 h + 3 h Subscript[N, b] + 3 h Subscript[N, t] +
      Sqrt[(-6 h + 3 h Subscript[N, b] + 3 h Subscript[N, t])^2 -
       24 (-2 h^2 Subscript[N, b] Subscript[N, t] - 2 h^2
\!\(\*SubsuperscriptBox[\(N\), \(t\), \(2\)]\))]))/(
   2 (h^2 Subscript[N, b] Subscript[N, t] + h^2
\!\(\*SubsuperscriptBox[\(N\), \(t\), \(2\)]\))) + (
   3 h^2 Subscript[N,
    t] (-6 h + 3 h Subscript[N, b] + 3 h Subscript[N, t] +
      Sqrt[(-6 h + 3 h Subscript[N, b] + 3 h Subscript[N, t])^2 -
       24 (-2 h^2 Subscript[N, b] Subscript[N, t] - 2 h^2
\!\(\*SubsuperscriptBox[\(N\), \(t\), \(2\)]\))])^2)/(
   16 (h^2 Subscript[N, b] Subscript[N, t] + h^2
\!\(\*SubsuperscriptBox[\(N\), \(t\), \(2\)]\))^2) - (h^3
\!\(\*SubsuperscriptBox[\(N\), \(t\), \(2\)]\) (-6 h +
      3 h Subscript[N, b] + 3 h Subscript[N, t] +
      Sqrt[(-6 h + 3 h Subscript[N, b] + 3 h Subscript[N, t])^2 -
       24 (-2 h^2 Subscript[N, b] Subscript[N, t] - 2 h^2
\!\(\*SubsuperscriptBox[\(N\), \(t\), \(2\)]\))])^3)/(
   32 (h^2 Subscript[N, b] Subscript[N, t] + h^2
\!\(\*SubsuperscriptBox[\(N\), \(t\), \(2\)]\))^3)))/(h^2 \
Subscript[N, b] (-6 h + 3 h Subscript[N, b] + 3 h Subscript[N, t] +
   Sqrt[(-6 h + 3 h Subscript[N, b] + 3 h Subscript[N, t])^2 -
    24 (-2 h^2 Subscript[N, b] Subscript[N, t] - 2 h^2
\!\(\*SubsuperscriptBox[\(N\), \(t\), \(2\)]\))]) (-3 + (
   h Subscript[N,
    t] (-6 h + 3 h Subscript[N, b] + 3 h Subscript[N, t] +
      Sqrt[(-6 h + 3 h Subscript[N, b] + 3 h Subscript[N, t])^2 -
```

```
      24 (-2 h^2 Subscript[N, b] Subscript[N, t] - 2 h^2
\!\(\*SubsuperscriptBox[\(N\), \(t\), \(2\)]\))]))/(
    2 (h^2 Subscript[N, b] Subscript[N, t] + h^2
\!\(\*SubsuperscriptBox[\(N\), \(t\), \(2\)]\))))
\[Sigma][y] = \!\(
\*UnderoverscriptBox[\(\[Sum]\), \(n = 0\), \(3\)]\(
\(\*SubscriptBox[\(\[Sigma]\), \(n\)]\)[y]\)\)
=(4 y (h^2 Subscript[N, b] Subscript[N, t] + h^2
\!\(\*SubsuperscriptBox[\(N\), \(t\), \(2\)]\)) (6 - (
    3 h (-6 h + 3 h Subscript[N, b] + 3 h Subscript[N, t] +
       Sqrt[(-6 h + 3 h Subscript[N, b] + 3 h Subscript[N, t])^2 -
        24 (-2 h^2 Subscript[N, b] Subscript[N, t] - 2 h^2
\!\(\*SubsuperscriptBox[\(N\), \(t\), \(2\)]\))]))/(
    2 (h^2 Subscript[N, b] Subscript[N, t] + h^2
\!\(\*SubsuperscriptBox[\(N\), \(t\), \(2\)]\))) + (
    3 h^2 Subscript[N,
     t] (-6 h + 3 h Subscript[N, b] + 3 h Subscript[N, t] +
       Sqrt[(-6 h + 3 h Subscript[N, b] + 3 h Subscript[N, t])^2 -
        24 (-2 h^2 Subscript[N, b] Subscript[N, t] - 2 h^2
\!\(\*SubsuperscriptBox[\(N\), \(t\), \(2\)]\))])^2)/(
    16 (h^2 Subscript[N, b] Subscript[N, t] + h^2
\!\(\*SubsuperscriptBox[\(N\), \(t\), \(2\)]\))^2) - (h^3
\!\(\*SubsuperscriptBox[\(N\), \(t\), \(2\)]\) (-6 h +
       3 h Subscript[N, b] + 3 h Subscript[N, t] +
       Sqrt[(-6 h + 3 h Subscript[N, b] + 3 h Subscript[N, t])^2 -
        24 (-2 h^2 Subscript[N, b] Subscript[N, t] - 2 h^2
\!\(\*SubsuperscriptBox[\(N\), \(t\), \(2\)]\))])^3)/(
```

```
    32 (h^2 Subscript[N, b] Subscript[N, t] + h^2
\!\(\*SubsuperscriptBox[\(N\), \(t\), \(2\)]\))^3)))/(
 h^2 Subscript[N,
  b] (-6 h + 3 h Subscript[N, b] + 3 h Subscript[N, t] +
    Sqrt[(-6 h + 3 h Subscript[N, b] + 3 h Subscript[N, t])^2 -
     24 (-2 h^2 Subscript[N, b] Subscript[N, t] - 2 h^2
\!\(\*SubsuperscriptBox[\(N\), \(t\), \(2\)]\))]) (-3 + (
    h Subscript[N,
     t] (-6 h + 3 h Subscript[N, b] + 3 h Subscript[N, t] +
       Sqrt[(-6 h + 3 h Subscript[N, b] + 3 h Subscript[N, t])^2 -
        24 (-2 h^2 Subscript[N, b] Subscript[N, t] - 2 h^2
\!\(\*SubsuperscriptBox[\(N\), \(t\), \(2\)]\))]))/(
    2 (h^2 Subscript[N, b] Subscript[N, t] + h^2
\!\(\*SubsuperscriptBox[\(N\), \(t\), \(2\)]\))))) -
 1/(2 Subscript[N, b])
   y^2 Subscript[N,
   t] (-((Subscript[N,
       t] (-6 h + 3 h Subscript[N, b] + 3 h Subscript[N, t] +
         Sqrt[(-6 h + 3 h Subscript[N, b] + 3 h Subscript[N, t])^2 -
          24 (-2 h^2 Subscript[N, b] Subscript[N, t] - 2 h^2
\!\(\*SubsuperscriptBox[\(N\), \(t\), \(2\)]\))])^2)/(
      16 (h^2 Subscript[N, b] Subscript[N, t] + h^2
\!\(\*SubsuperscriptBox[\(N\), \(t\), \(2\)]\))^2)) - (
     6 - (3 h (-6 h + 3 h Subscript[N, b] + 3 h Subscript[N, t] +
         Sqrt[(-6 h + 3 h Subscript[N, b] + 3 h Subscript[N, t])^2 -
          24 (-2 h^2 Subscript[N, b] Subscript[N, t] - 2 h^2
\!\(\*SubsuperscriptBox[\(N\), \(t\), \(2\)]\))]))/(
```

```
      2 (h^2 Subscript[N, b] Subscript[N, t] + h^2
\!\(\*SubsuperscriptBox[\(N\), \(t\), \(2\)]\))) + (
      3 h^2 Subscript[N,
       t] (-6 h + 3 h Subscript[N, b] + 3 h Subscript[N, t] +
         Sqrt[(-6 h + 3 h Subscript[N, b] + 3 h Subscript[N, t])^2 -
          24 (-2 h^2 Subscript[N, b] Subscript[N, t] - 2 h^2
\!\(\*SubsuperscriptBox[\(N\), \(t\), \(2\)]\))])^2)/(
      16 (h^2 Subscript[N, b] Subscript[N, t] + h^2
\!\(\*SubsuperscriptBox[\(N\), \(t\), \(2\)]\))^2) - (h^3
\!\(\*SubsuperscriptBox[\(N\), \(t\), \(2\)]\) (-6 h +
         3 h Subscript[N, b] + 3 h Subscript[N, t] +
         Sqrt[(-6 h + 3 h Subscript[N, b] + 3 h Subscript[N, t])^2 -
          24 (-2 h^2 Subscript[N, b] Subscript[N, t] - 2 h^2
\!\(\*SubsuperscriptBox[\(N\), \(t\), \(2\)]\))])^3)/(
      32 (h^2 Subscript[N, b] Subscript[N, t] + h^2
\!\(\*SubsuperscriptBox[\(N\), \(t\), \(2\)]\))^3))/(
     h^2 (-3 + (
        h Subscript[N,
         t] (-6 h + 3 h Subscript[N, b] + 3 h Subscript[N, t] +
           Sqrt[(-6 h + 3 h Subscript[N, b] +
              3 h Subscript[N, t])^2 -
            24 (-2 h^2 Subscript[N, b] Subscript[N, t] - 2 h^2
\!\(\*SubsuperscriptBox[\(N\), \(t\), \(2\)]\))]))/(
        2 (h^2 Subscript[N, b] Subscript[N, t] + h^2
\!\(\*SubsuperscriptBox[\(N\), \(t\), \(2\)]\))))) -
 1/(48 Subscript[N, b] (h^2 Subscript[N, b] Subscript[N, t] + h^2
\!\(\*SubsuperscriptBox[\(N\), \(t\), \(2\)]\))^2) y^3
```

```
\!\(\*SubsuperscriptBox[\(N\), \(t\), \(2\)]\) (-6 h +
     3 h Subscript[N, b] + 3 h Subscript[N, t] +
     Sqrt[(-6 h + 3 h Subscript[N, b] + 3 h Subscript[N, t])^2 -
      24 (-2 h^2 Subscript[N, b] Subscript[N, t] - 2 h^2
\!\(\*SubsuperscriptBox[\(N\), \(t\), \(2\)]\))])^2 ((
     Subscript[N,
      t] (-6 h + 3 h Subscript[N, b] + 3 h Subscript[N, t] +
        Sqrt[(-6 h + 3 h Subscript[N, b] + 3 h Subscript[N, t])^2 -
         24 (-2 h^2 Subscript[N, b] Subscript[N, t] - 2 h^2
\!\(\*SubsuperscriptBox[\(N\), \(t\), \(2\)]\))]))/(
     4 (h^2 Subscript[N, b] Subscript[N, t] + h^2
\!\(\*SubsuperscriptBox[\(N\), \(t\), \(2\)]\))) + (4 (h^2 Subscript[
           N, b] Subscript[N, t] + h^2
\!\(\*SubsuperscriptBox[\(N\), \(t\), \(2\)]\)) (6 - (
          3 h (-6 h + 3 h Subscript[N, b] + 3 h Subscript[N, t] +
             Sqrt[(-6 h + 3 h Subscript[N, b] +
                3 h Subscript[N, t])^2 -
              24 (-2 h^2 Subscript[N, b] Subscript[N, t] - 2 h^2
\!\(\*SubsuperscriptBox[\(N\), \(t\), \(2\)]\))]))/(
          2 (h^2 Subscript[N, b] Subscript[N, t] + h^2
\!\(\*SubsuperscriptBox[\(N\), \(t\), \(2\)]\))) + (
          3 h^2 Subscript[N,
           t] (-6 h + 3 h Subscript[N, b] + 3 h Subscript[N, t] +
             Sqrt[(-6 h + 3 h Subscript[N, b] +
                3 h Subscript[N, t])^2 -
              24 (-2 h^2 Subscript[N, b] Subscript[N, t] - 2 h^2
\!\(\*SubsuperscriptBox[\(N\), \(t\), \(2\)]\))])^2)/(
```

```
          16 (h^2 Subscript[N, b] Subscript[N, t] + h^2
\!\(\*SubsuperscriptBox[\(N\), \(t\), \(2\)]\))^2) - (h^3
\!\(\*SubsuperscriptBox[\(N\), \(t\), \(2\)]\) (-6 h +
             3 h Subscript[N, b] + 3 h Subscript[N, t] +
             Sqrt[(-6 h + 3 h Subscript[N, b] +
                3 h Subscript[N, t])^2 -
              24 (-2 h^2 Subscript[N, b] Subscript[N, t] - 2 h^2
\!\(\*SubsuperscriptBox[\(N\), \(t\), \(2\)]\))])^3)/(
          32 (h^2 Subscript[N, b] Subscript[N, t] + h^2
\!\(\*SubsuperscriptBox[\(N\), \(t\), \(2\)]\))^3)))/(h^2 (-6 h +
          3 h Subscript[N, b] + 3 h Subscript[N, t] +
          Sqrt[(-6 h + 3 h Subscript[N, b] + 3 h Subscript[N, t])^2 -
           24 (-2 h^2 Subscript[N, b] Subscript[N, t] - 2 h^2
\!\(\*SubsuperscriptBox[\(N\), \(t\), \(2\)]\))]) (-3 + (
          h Subscript[N,
           t] (-6 h + 3 h Subscript[N, b] + 3 h Subscript[N, t] +
             Sqrt[(-6 h + 3 h Subscript[N, b] +
                3 h Subscript[N, t])^2 -
              24 (-2 h^2 Subscript[N, b] Subscript[N, t] - 2 h^2
\!\(\*SubsuperscriptBox[\(N\), \(t\), \(2\)]\))]))/(
          2 (h^2 Subscript[N, b] Subscript[N, t] + h^2
\!\(\*SubsuperscriptBox[\(N\), \(t\), \(2\)]\))))))
QP31[x] = \[Sigma][y] /. Subscript[N, t] -> {1, 2, 3, 4} /.
   Subscript[N, b] -> 1 /. h -> 3
   {(Sqrt[2/3] (21/2 - 3 Sqrt[3/2] - 3 Sqrt[6]) y)/(3 (-3 + Sqrt[6])) -
  1/2 (-(1/6) - (21/2 - 3 Sqrt[3/2] - 3 Sqrt[6])/(
     9 (-3 + Sqrt[6]))) y^2 -
```

```
1/18 (1/Sqrt[6] + (Sqrt[2/3] (21/2 - 3 Sqrt[3/2] - 3 Sqrt[6]))/(
   3 (-3 + Sqrt[6]))) y^3, (
24 (6 + 1/12 (-9 - 9 Sqrt[33]) +
   1/864 (9 + 9 Sqrt[33])^2 - (9 + 9 Sqrt[33])^3/46656) y)/((9 +
   9 Sqrt[33]) (-3 +
   1/18 (9 + 9 Sqrt[33]))) - (-((9 + 9 Sqrt[33])^2/23328) - (
   6 + 1/12 (-9 - 9 Sqrt[33]) +
    1/864 (9 + 9 Sqrt[33])^2 - (9 + 9 Sqrt[33])^3/46656)/(
   9 (-3 + 1/18 (9 + 9 Sqrt[33])))) y^2 - ((9 +
   9 Sqrt[33])^2 (1/108 (9 + 9 Sqrt[33]) + (
   24 (6 + 1/12 (-9 - 9 Sqrt[33]) +
      1/864 (9 + 9 Sqrt[33])^2 - (9 + 9 Sqrt[33])^3/46656))/((9 +
      9 Sqrt[33]) (-3 + 1/18 (9 + 9 Sqrt[33])))) y^3)/34992, (
48 (6 + 1/24 (-18 - 18 Sqrt[17]) + (18 + 18 Sqrt[17])^2/
   2304 - (18 + 18 Sqrt[17])^3/165888) y)/((18 + 18 Sqrt[17]) (-3 +
   1/24 (18 + 18 Sqrt[17]))) -
3/2 (-((18 + 18 Sqrt[17])^2/62208) - (
   6 + 1/24 (-18 - 18 Sqrt[17]) + (18 + 18 Sqrt[17])^2/
    2304 - (18 + 18 Sqrt[17])^3/165888)/(
   9 (-3 + 1/24 (18 + 18 Sqrt[17])))) y^2 - ((18 +
   18 Sqrt[17])^2 (1/144 (18 + 18 Sqrt[17]) + (
   48 (6 + 1/24 (-18 - 18 Sqrt[17]) + (18 + 18 Sqrt[17])^2/
      2304 - (18 + 18 Sqrt[17])^3/165888))/((18 +
      18 Sqrt[17]) (-3 + 1/24 (18 + 18 Sqrt[17])))) y^3)/62208, (
80 (6 + 1/40 (-27 - 3 Sqrt[1041]) + (27 + 3 Sqrt[1041])^2/
   4800 - (27 + 3 Sqrt[1041])^3/432000) y)/((27 +
   3 Sqrt[1041]) (-3 + 1/30 (27 + 3 Sqrt[1041]))) -
```

```
 2 (-((27 + 3 Sqrt[1041])^2/129600) - (
    6 + 1/40 (-27 - 3 Sqrt[1041]) + (27 + 3 Sqrt[1041])^2/
     4800 - (27 + 3 Sqrt[1041])^3/432000)/(
    9 (-3 + 1/30 (27 + 3 Sqrt[1041])))) y^2 - ((27 +
    3 Sqrt[1041])^2 (1/180 (27 + 3 Sqrt[1041]) + (
    80 (6 + 1/40 (-27 - 3 Sqrt[1041]) + (27 + 3 Sqrt[1041])^2/
       4800 - (27 + 3 Sqrt[1041])^3/432000))/((27 +
       3 Sqrt[1041]) (-3 + 1/30 (27 + 3 Sqrt[1041])))) y^3)/97200}
       Plot[%, {y, 0, 2}, AxesLabel -> {y, \[Sigma]},
PlotStyle -> {{Black}, {Black, Thick}, {Black, Dashed}, {Green}},
PlotLabel -> {Subscript[N, t] == {1, 2, 3, 4} ,
  Subscript[N, b] == 1, h == 3}]
  QP31[x] = \[Sigma][y] /. Subscript[N, b] -> {1, 2, 3, 4} /.
  Subscript[N, t] -> 1 /. h -> 3
  (Sqrt[2/3] (21/2 - 3 Sqrt[3/2] - 3 Sqrt[6]) y)/(3 (-3 + Sqrt[6])) -
 1/2 (-(1/6) - (21/2 - 3 Sqrt[3/2] - 3 Sqrt[6])/(
    9 (-3 + Sqrt[6]))) y^2 -
 1/18 (1/Sqrt[6] + (Sqrt[2/3] (21/2 - 3 Sqrt[3/2] - 3 Sqrt[6]))/(
    3 (-3 + Sqrt[6]))) y^3, (
 6 (6 + 1/6 (-9 - 9 Sqrt[17]) +
    1/432 (9 + 9 Sqrt[17])^2 - (9 + 9 Sqrt[17])^3/23328) y)/((9 +
    9 Sqrt[17]) (-3 + 1/18 (9 + 9 Sqrt[17]))) -
 1/4 (-((9 + 9 Sqrt[17])^2/11664) - (
    6 + 1/6 (-9 - 9 Sqrt[17]) +
     1/432 (9 + 9 Sqrt[17])^2 - (9 + 9 Sqrt[17])^3/23328)/(
    9 (-3 + 1/18 (9 + 9 Sqrt[17])))) y^2 - ((9 +
    9 Sqrt[17])^2 (1/108 (9 + 9 Sqrt[17]) + (
```

```
   12 (6 + 1/6 (-9 - 9 Sqrt[17]) +
      1/432 (9 + 9 Sqrt[17])^2 - (9 + 9 Sqrt[17])^3/23328))/((9 +
      9 Sqrt[17]) (-3 + 1/18 (9 + 9 Sqrt[17])))) y^3)/69984, (
16 (6 + 1/8 (-18 - 6 Sqrt[57]) +
   1/768 (18 + 6 Sqrt[57])^2 - (18 + 6 Sqrt[57])^3/55296) y)/(
3 (18 + 6 Sqrt[57]) (-3 + 1/24 (18 + 6 Sqrt[57]))) -
1/6 (-((18 + 6 Sqrt[57])^2/20736) - (
   6 + 1/8 (-18 - 6 Sqrt[57]) +
    1/768 (18 + 6 Sqrt[57])^2 - (18 + 6 Sqrt[57])^3/55296)/(
   9 (-3 + 1/24 (18 + 6 Sqrt[57])))) y^2 - ((18 +
   6 Sqrt[57])^2 (1/144 (18 + 6 Sqrt[57]) + (
   16 (6 + 1/8 (-18 - 6 Sqrt[57]) +
      1/768 (18 + 6 Sqrt[57])^2 - (18 + 6 Sqrt[57])^3/
      55296))/((18 + 6 Sqrt[57]) (-3 +
      1/24 (18 + 6 Sqrt[57])))) y^3)/186624, (
5 (6 + 1/10 (-27 - 3 Sqrt[321]) + (27 + 3 Sqrt[321])^2/
   1200 - (27 + 3 Sqrt[321])^3/108000) y)/((27 + 3 Sqrt[321]) (-3 +
   1/30 (27 + 3 Sqrt[321]))) -
1/8 (-((27 + 3 Sqrt[321])^2/32400) - (
   6 + 1/10 (-27 - 3 Sqrt[321]) + (27 + 3 Sqrt[321])^2/
    1200 - (27 + 3 Sqrt[321])^3/108000)/(
   9 (-3 + 1/30 (27 + 3 Sqrt[321])))) y^2 - ((27 +
   3 Sqrt[321])^2 (1/180 (27 + 3 Sqrt[321]) + (
   20 (6 + 1/10 (-27 - 3 Sqrt[321]) + (27 + 3 Sqrt[321])^2/
      1200 - (27 + 3 Sqrt[321])^3/108000))/((27 +
      3 Sqrt[321]) (-3 + 1/30 (27 + 3 Sqrt[321])))) y^3)/388800}
      Plot[%, {y, 0, 2}, AxesLabel -> {y, \[Sigma]},
```

```
 PlotStyle -> {{Black}, {Black, Thick}, {Black, Dashed}, {Green}},
 PlotLabel -> {Subscript[N, b] == {1, 2, 3, 4} ,
   Subscript[N, t] == 1, h == 3}]
   DSolve[{ D[  D[\[Theta][y], y], y] +
    Subscript[N, b] D[\[Theta][y], y] D[\[Sigma][y], y] +
    Subscript[N, t] ( D[\[Theta][y], y ])^2 == 0,
  D[ \[Theta][0], y] == 0, \[Theta][h] == 1}, \[Theta], y]
  \[Theta][y] = \!\(
\*UnderoverscriptBox[\(\[Sum]\), \(n = 0\), \(2\)]\(
\(\*SubscriptBox[\(\[Theta]\), \(n\)]\)[y]\)\)
(y (6 h - 3 h Subscript[N, b] - 3 h Subscript[N, t] +
    Sqrt[(-6 h + 3 h Subscript[N, b] + 3 h Subscript[N, t])^2 -
     24 (-2 h^2 Subscript[N, b] Subscript[N, t] - 2 h^2
\!\(\*SubsuperscriptBox[\(N\), \(t\), \(2\)]\))]))/(
 2 (-2 h^2 Subscript[N, b] Subscript[N, t] - 2 h^2
\!\(\*SubsuperscriptBox[\(N\), \(t\), \(2\)]\))) - (
 y^2 Subscript[N,
  t] (6 h - 3 h Subscript[N, b] - 3 h Subscript[N, t] +
    Sqrt[(-6 h + 3 h Subscript[N, b] + 3 h Subscript[N, t])^2 -
     24 (-2 h^2 Subscript[N, b] Subscript[N, t] - 2 h^2
\!\(\*SubsuperscriptBox[\(N\), \(t\), \(2\)]\))])^2)/(
 8 (-2 h^2 Subscript[N, b] Subscript[N, t] - 2 h^2
\!\(\*SubsuperscriptBox[\(N\), \(t\), \(2\)]\))^2) - (y^2 (6 h -
      3 h Subscript[N, b] - 3 h Subscript[N, t] +
      Sqrt[(-6 h + 3 h Subscript[N, b] + 3 h Subscript[N, t])^2 -
       24 (-2 h^2 Subscript[N, b] Subscript[N, t] - 2 h^2
\!\(\*SubsuperscriptBox[\(N\), \(t\), \(2\)]\))]) (-6 Subscript[N,
```

```
       b] + (3 h^2
\!\(\*SubsuperscriptBox[\(N\), \(t\), \(2\)]\) (6 h -
         3 h Subscript[N, b] - 3 h Subscript[N, t] +
         Sqrt[(-6 h + 3 h Subscript[N, b] + 3 h Subscript[N, t])^2 -
          24 (-2 h^2 Subscript[N, b] Subscript[N, t] - 2 h^2
\!\(\*SubsuperscriptBox[\(N\), \(t\), \(2\)]\))])^2)/(
      4 (-2 h^2 Subscript[N, b] Subscript[N, t] - 2 h^2
\!\(\*SubsuperscriptBox[\(N\), \(t\), \(2\)]\))^2) - (h^3
\!\(\*SubsuperscriptBox[\(N\), \(t\), \(3\)]\) (6 h -
         3 h Subscript[N, b] - 3 h Subscript[N, t] +
         Sqrt[(-6 h + 3 h Subscript[N, b] + 3 h Subscript[N, t])^2 -
          24 (-2 h^2 Subscript[N, b] Subscript[N, t] - 2 h^2
\!\(\*SubsuperscriptBox[\(N\), \(t\), \(2\)]\))])^3)/(
      4 (-2 h^2 Subscript[N, b] Subscript[N, t] - 2 h^2
\!\(\*SubsuperscriptBox[\(N\), \(t\), \(2\)]\))^3)))/(4 h (-2 h^2 \
Subscript[N, b] Subscript[N, t] - 2 h^2
\!\(\*SubsuperscriptBox[\(N\), \(t\), \(2\)]\)) (-6 - (
      3 h Subscript[N,
       t] (6 h - 3 h Subscript[N, b] - 3 h Subscript[N, t] +
         Sqrt[(-6 h + 3 h Subscript[N, b] + 3 h Subscript[N, t])^2 -
          24 (-2 h^2 Subscript[N, b] Subscript[N, t] - 2 h^2
\!\(\*SubsuperscriptBox[\(N\), \(t\), \(2\)]\))]))/(
      2 (-2 h^2 Subscript[N, b] Subscript[N, t] - 2 h^2
\!\(\*SubsuperscriptBox[\(N\), \(t\), \(2\)]\))) + (h^2
\!\(\*SubsuperscriptBox[\(N\), \(t\), \(2\)]\) (6 h -
         3 h Subscript[N, b] - 3 h Subscript[N, t] +
         Sqrt[(-6 h + 3 h Subscript[N, b] + 3 h Subscript[N, t])^2 -
```

```
          24 (-2 h^2 Subscript[N, b] Subscript[N, t] - 2 h^2
\!\(\*SubsuperscriptBox[\(N\), \(t\), \(2\)]\))])^2)/(
      2 (-2 h^2 Subscript[N, b] Subscript[N, t] - 2 h^2
\!\(\*SubsuperscriptBox[\(N\), \(t\), \(2\)]\))^2))) +
 1/(12 (-2 h^2 Subscript[N, b] Subscript[N, t] - 2 h^2
\!\(\*SubsuperscriptBox[\(N\), \(t\), \(2\)]\))^2)
   y^3 Subscript[N,
   t] (6 h - 3 h Subscript[N, b] - 3 h Subscript[N, t] +
     Sqrt[(-6 h + 3 h Subscript[N, b] + 3 h Subscript[N, t])^2 -
      24 (-2 h^2 Subscript[N, b] Subscript[N, t] - 2 h^2
\!\(\*SubsuperscriptBox[\(N\), \(t\), \(2\)]\))])^2 ((
     Subscript[N,
      t] (6 h - 3 h Subscript[N, b] - 3 h Subscript[N, t] +
        Sqrt[(-6 h + 3 h Subscript[N, b] + 3 h Subscript[N, t])^2 -
         24 (-2 h^2 Subscript[N, b] Subscript[N, t] - 2 h^2
\!\(\*SubsuperscriptBox[\(N\), \(t\), \(2\)]\))]))/(
     2 (-2 h^2 Subscript[N, b] Subscript[N, t] - 2 h^2
\!\(\*SubsuperscriptBox[\(N\), \(t\), \(2\)]\))) + (-6 Subscript[N,
         b] + (3 h^2
\!\(\*SubsuperscriptBox[\(N\), \(t\), \(2\)]\) (6 h -
           3 h Subscript[N, b] - 3 h Subscript[N, t] +
           Sqrt[(-6 h + 3 h Subscript[N, b] +
              3 h Subscript[N, t])^2 -
            24 (-2 h^2 Subscript[N, b] Subscript[N, t] - 2 h^2
\!\(\*SubsuperscriptBox[\(N\), \(t\), \(2\)]\))])^2)/(
        4 (-2 h^2 Subscript[N, b] Subscript[N, t] - 2 h^2
\!\(\*SubsuperscriptBox[\(N\), \(t\), \(2\)]\))^2) - (h^3
```

```
\!\(\*SubsuperscriptBox[\(N\), \(t\), \(3\)]\) (6 h -
           3 h Subscript[N, b] - 3 h Subscript[N, t] +
           Sqrt[(-6 h + 3 h Subscript[N, b] +
              3 h Subscript[N, t])^2 -
            24 (-2 h^2 Subscript[N, b] Subscript[N, t] - 2 h^2
\!\(\*SubsuperscriptBox[\(N\), \(t\), \(2\)]\))])^3)/(
        4 (-2 h^2 Subscript[N, b] Subscript[N, t] - 2 h^2
\!\(\*SubsuperscriptBox[\(N\), \(t\), \(2\)]\))^3))/(h (-6 - (
          3 h Subscript[N,
           t] (6 h - 3 h Subscript[N, b] - 3 h Subscript[N, t] +
             Sqrt[(-6 h + 3 h Subscript[N, b] +
                3 h Subscript[N, t])^2 -
              24 (-2 h^2 Subscript[N, b] Subscript[N, t] - 2 h^2
\!\(\*SubsuperscriptBox[\(N\), \(t\), \(2\)]\))]))/(
          2 (-2 h^2 Subscript[N, b] Subscript[N, t] - 2 h^2
\!\(\*SubsuperscriptBox[\(N\), \(t\), \(2\)]\))) + (h^2
\!\(\*SubsuperscriptBox[\(N\), \(t\), \(2\)]\) (6 h -
             3 h Subscript[N, b] - 3 h Subscript[N, t] +
             Sqrt[(-6 h + 3 h Subscript[N, b] +
                3 h Subscript[N, t])^2 -
              24 (-2 h^2 Subscript[N, b] Subscript[N, t] - 2 h^2
\!\(\*SubsuperscriptBox[\(N\), \(t\), \(2\)]\))])^2)/(
          2 (-2 h^2 Subscript[N, b] Subscript[N, t] - 2 h^2
\!\(\*SubsuperscriptBox[\(N\), \(t\), \(2\)]\))^2))))
QP31[x] = \[Theta][y] /. Subscript[N, t] -> {1, 2, 3, 4} /.
   Subscript[N, b] -> 1 /. h -> 1
   {-Sqrt[(3/2)] y - (3 y^2)/4 + (Sqrt[3/2] (-(3/2) + 3 Sqrt[3/2]) y^2)/(
```

```
2 (-3 + 3 Sqrt[3/2])) +
1/2 (-Sqrt[(3/2)] + (-(3/2) + 3 Sqrt[3/2])/(-3 +
    3 Sqrt[3/2])) y^3, -(1/24) (-3 + 3 Sqrt[33]) y -
1/576 (-3 + 3 Sqrt[33])^2 y^2 + ((-3 + 3 Sqrt[33]) (-6 +
   1/48 (-3 + 3 Sqrt[33])^2 + 1/864 (-3 + 3 Sqrt[33])^3) y^2)/(
48 (-6 + 1/4 (-3 + 3 Sqrt[33]) + 1/72 (-3 + 3 Sqrt[33])^2)) +
1/864 (-3 +
   3 Sqrt[33])^2 (1/12 (3 - 3 Sqrt[33]) + (-6 +
    1/48 (-3 + 3 Sqrt[33])^2 + 1/864 (-3 + 3 Sqrt[33])^3)/(-6 +
    1/4 (-3 + 3 Sqrt[33]) + 1/72 (-3 + 3 Sqrt[33])^2)) y^3, -(1/
  48) (-6 + 6 Sqrt[17]) y - ((-6 + 6 Sqrt[17])^2 y^2)/
1536 + ((-6 + 6 Sqrt[17]) (-6 +
   3/256 (-6 + 6 Sqrt[17])^2 + (-6 + 6 Sqrt[17])^3/2048) y^2)/(
96 (-6 + 3/16 (-6 + 6 Sqrt[17]) +
   1/128 (-6 + 6 Sqrt[17])^2)) + ((-6 +
   6 Sqrt[17])^2 (1/16 (6 - 6 Sqrt[17]) + (-6 +
    3/256 (-6 + 6 Sqrt[17])^2 + (-6 + 6 Sqrt[17])^3/2048)/(-6 +
    3/16 (-6 + 6 Sqrt[17]) + 1/128 (-6 + 6 Sqrt[17])^2)) y^3)/
2304, -(1/80) (-9 + Sqrt[1041]) y - ((-9 + Sqrt[1041])^2 y^2)/
3200 + ((-9 + Sqrt[1041]) (-6 +
   3/400 (-9 + Sqrt[1041])^2 + (-9 + Sqrt[1041])^3/4000) y^2)/(
160 (-6 + 3/20 (-9 + Sqrt[1041]) +
   1/200 (-9 + Sqrt[1041])^2)) + ((-9 + Sqrt[
   1041])^2 (1/20 (9 - Sqrt[1041]) + (-6 +
    3/400 (-9 + Sqrt[1041])^2 + (-9 + Sqrt[1041])^3/4000)/(-6 +
    3/20 (-9 + Sqrt[1041]) + 1/200 (-9 + Sqrt[1041])^2)) y^3)/4800}
    Plot[%, {y, 0, 2}, AxesLabel -> {y, \[Theta]},
```

```
PlotStyle -> {{Black}, {Black, Thick}, {Black, Dashed}, {Green}},
PlotLabel -> {Subscript[N, t] == {1, 2, 3, 4} ,
  Subscript[N, b] == 1, h == 1}]
  QP31[x] = \[Theta][y] /. Subscript[N, b] -> {1, 2, 3, 4} /.
  Subscript[N, t] -> 1 /. h -> 1
  {-Sqrt[(3/2)] y - (3 y^2)/4 + (Sqrt[3/2] (-(3/2) + 3 Sqrt[3/2]) y^2)/(
 2 (-3 + 3 Sqrt[3/2])) +
 1/2 (-Sqrt[(3/2)] + (-(3/2) + 3 Sqrt[3/2])/(-3 +
     3 Sqrt[3/2])) y^3, -(1/12) (-3 + 3 Sqrt[17]) y -
 1/288 (-3 + 3 Sqrt[17])^2 y^2 + ((-3 + 3 Sqrt[17]) (-12 +
    1/48 (-3 + 3 Sqrt[17])^2 + 1/864 (-3 + 3 Sqrt[17])^3) y^2)/(
 24 (-6 + 1/4 (-3 + 3 Sqrt[17]) + 1/72 (-3 + 3 Sqrt[17])^2)) +
 1/432 (-3 +
    3 Sqrt[17])^2 (1/12 (3 - 3 Sqrt[17]) + (-12 +
     1/48 (-3 + 3 Sqrt[17])^2 + 1/864 (-3 + 3 Sqrt[17])^3)/(-6 +
     1/4 (-3 + 3 Sqrt[17]) + 1/72 (-3 + 3 Sqrt[17])^2)) y^3, -(1/
   16) (-6 + 2 Sqrt[57]) y -
 1/512 (-6 + 2 Sqrt[57])^2 y^2 + ((-6 + 2 Sqrt[57]) (-18 +
    3/256 (-6 + 2 Sqrt[57])^2 + (-6 + 2 Sqrt[57])^3/2048) y^2)/(
 32 (-6 + 3/16 (-6 + 2 Sqrt[57]) + 1/128 (-6 + 2 Sqrt[57])^2)) +
 1/768 (-6 +
    2 Sqrt[57])^2 (1/16 (6 - 2 Sqrt[57]) + (-18 +
     3/256 (-6 + 2 Sqrt[57])^2 + (-6 + 2 Sqrt[57])^3/2048)/(-6 +
     3/16 (-6 + 2 Sqrt[57]) + 1/128 (-6 + 2 Sqrt[57])^2)) y^3, -(1/
   20) (-9 + Sqrt[321]) y -
 1/800 (-9 + Sqrt[321])^2 y^2 + ((-9 + Sqrt[321]) (-24 +
    3/400 (-9 + Sqrt[321])^2 + (-9 + Sqrt[321])^3/4000) y^2)/(
```

```
 40 (-6 + 3/20 (-9 + Sqrt[321]) + 1/200 (-9 + Sqrt[321])^2)) + ((-9 +
     Sqrt[321])^2 (1/20 (9 - Sqrt[321]) + (-24 +
     3/400 (-9 + Sqrt[321])^2 + (-9 + Sqrt[321])^3/4000)/(-6 +
     3/20 (-9 + Sqrt[321]) + 1/200 (-9 + Sqrt[321])^2)) y^3)/1200}
   Plot[%, {y, 0, 2}, AxesLabel -> {y, \[Theta]},
 PlotStyle -> {{Black}, {Black, Thick}, {Black, Dashed}, {Green}},
 PlotLabel -> {Subscript[N, b] == {1, 2, 3, 4} ,
   Subscript[N, t] == 1, h == 1}]
  DSolve[{ D[  D[u[y], y], y] + Subscript[G, r] \[Theta] +
    Subscript[B, r] \[Sigma] - D[P[x], x] == 0, D[ u[h], y] == 0,
  D[u[0], y] == 0}, u, y]
  Subscript[u, 1][y] = \!\(
\*SubsuperscriptBox[\(\[Integral]\), \(0\), \(y\)]\(
\*SubsuperscriptBox[\(\[Integral]\), \(0\), \(y\)]D[P[x], \
     x] \[DifferentialD]y \[DifferentialD]y\)\) - \!\(
\*SubsuperscriptBox[\(\[Integral]\), \(0\), \(y\)]\(
\*SubsuperscriptBox[\(\[Integral]\), \(0\), \(y\)]
\*SubscriptBox[\(G\), \(r\)]\
\(\*SubscriptBox[\(\[Theta]\), \(0\)]\)[
     y] \[DifferentialD]y \[DifferentialD]y\)\) - \!\(
\*SubsuperscriptBox[\(\[Integral]\), \(0\), \(y\)]\(
\*SubsuperscriptBox[\(\[Integral]\), \(0\), \(y\)]
\*SubscriptBox[\(B\), \(r\)]\
\(\*SubscriptBox[\(\[Sigma]\), \(0\)]\)[
     y] \[DifferentialD]y \[DifferentialD]y\)\)
     =-((y^3 Subscript[G,
  r] (-6 + 3 Subscript[N, b] + 3 Subscript[N, t] - Sqrt[36 + 9
```

```
\!\(\*SubsuperscriptBox[\(N\), \(b\), \(2\)]\) - 36 Subscript[N, t] +
      57
\!\(\*SubsuperscriptBox[\(N\), \(t\), \(2\)]\) +
      6 Subscript[N, b] (-6 + 11 Subscript[N, t])]))/(
  24 h Subscript[N, t] (Subscript[N, b] + Subscript[N, t]))) - (y^3 (8
\!\(\*SubsuperscriptBox[\(N\), \(b\), \(4\)]\) + 24
\!\(\*SubsuperscriptBox[\(N\), \(b\), \(3\)]\) Subscript[N, t] + 6
\!\(\*SubsuperscriptBox[\(N\), \(t\), \(3\)]\) + 3
\!\(\*SubsuperscriptBox[\(N\), \(b\), \(2\)]\) (-3 +
         2 Subscript[N, t] + 8
\!\(\*SubsuperscriptBox[\(N\), \(t\), \(2\)]\)) - 6 (6 + Sqrt[36 + 9
\!\(\*SubsuperscriptBox[\(N\), \(b\), \(2\)]\) - 36 Subscript[N, t] +
          57
\!\(\*SubsuperscriptBox[\(N\), \(t\), \(2\)]\) +
          6 Subscript[N, b] (-6 + 11 Subscript[N, t])]) +
      3 Subscript[N, t] (12 + Sqrt[36 + 9
\!\(\*SubsuperscriptBox[\(N\), \(b\), \(2\)]\) - 36 Subscript[N, t] +
          57
\!\(\*SubsuperscriptBox[\(N\), \(t\), \(2\)]\) +
          6 Subscript[N, b] (-6 + 11 Subscript[N, t])]) - \!\(
\*SubsuperscriptBox[\(N\), \(t\), \(2\)]\ \((45 + 2\
\*SqrtBox[\(36 + 9\
\*SubsuperscriptBox[\(N\), \(b\), \(2\)] - 36\
\*SubscriptBox[\(N\), \(t\)] + 57\
\*SubsuperscriptBox[\(N\), \(t\), \(2\)] + 6\
\*SubscriptBox[\(N\), \(b\)]\ \((\(-6\) + 11\
\*SubscriptBox[\(N\), \(t\)])\)\)])\)\) + Subscript[N, b] (36 + 12
```

```
\!\(\*SubsuperscriptBox[\(N\), \(t\), \(2\)]\) + 8
\!\(\*SubsuperscriptBox[\(N\), \(t\), \(3\)]\) + 3 Sqrt[36 + 9
\!\(\*SubsuperscriptBox[\(N\), \(b\), \(2\)]\) - 36 Subscript[N, t] +
           57
\!\(\*SubsuperscriptBox[\(N\), \(t\), \(2\)]\) +
           6 Subscript[N, b] (-6 + 11 Subscript[N, t])] -
         2 Subscript[N, t] (27 + Sqrt[36 + 9
\!\(\*SubsuperscriptBox[\(N\), \(b\), \(2\)]\) - 36 Subscript[N, t] +
             57
\!\(\*SubsuperscriptBox[\(N\), \(t\), \(2\)]\) +
             6 Subscript[N,
              b] (-6 + 11 Subscript[N, t])]))) (Subscript[-((
      6 - 3 Subscript[N, b] - 3 Subscript[N, t] + Sqrt[36 + 9
\!\(\*SubsuperscriptBox[\(N\), \(b\), \(2\)]\) - 36 Subscript[N, t] +
        57
\!\(\*SubsuperscriptBox[\(N\), \(t\), \(2\)]\) +
        6 Subscript[N, b] (-6 + 11 Subscript[N, t])])/(
      4 h Subscript[N, t] (Subscript[N, b] + Subscript[N, t]))),
     r]))/(12 h Subscript[N,
    b] (Subscript[N, b] + Subscript[N, t]) (-6 + 4
\!\(\*SubsuperscriptBox[\(N\), \(b\), \(2\)]\) + 3 Subscript[N, t] +
      Subscript[N, b] (3 + 4 Subscript[N, t]) - Sqrt[36 + 9
\!\(\*SubsuperscriptBox[\(N\), \(b\), \(2\)]\) - 36 Subscript[N, t] +
       57
\!\(\*SubsuperscriptBox[\(N\), \(t\), \(2\)]\) +
       6 Subscript[N, b] (-6 + 11 Subscript[N, t])])) +
 1/2 y^2 Derivative[1][P][x]
```

```
 Subscript[u, 2][y] = \!\(
\*SubsuperscriptBox[\(\[Integral]\), \(0\), \(y\)]\(
\*SubsuperscriptBox[\(\[Integral]\), \(0\), \(y\)]D[P[x], \
      x] \[DifferentialD]y \[DifferentialD]y\)\) - \!\(
\*SubsuperscriptBox[\(\[Integral]\), \(0\), \(y\)]\(
\*SubsuperscriptBox[\(\[Integral]\), \(0\), \(y\)]
\*SubscriptBox[\(G\), \(r\)]\
\(\*SubscriptBox[\(\[Theta]\), \(1\)]\)[
      y] \[DifferentialD]y \[DifferentialD]y\)\) - \!\(
\*SubsuperscriptBox[\(\[Integral]\), \(0\), \(y\)]\(
\*SubsuperscriptBox[\(\[Integral]\), \(0\), \(y\)]
\*SubscriptBox[\(B\), \(r\)]\
\(\*SubscriptBox[\(\[Sigma]\), \(1\)]\)[
      y] \[DifferentialD]y \[DifferentialD]y\)\)
      =-((y^4 Subscript[G,
   r] (6 - 3 Subscript[N, b] - 3 Subscript[N, t] + Sqrt[36 + 9
\!\(\*SubsuperscriptBox[\(N\), \(b\), \(2\)]\) - 36 Subscript[N, t] +
      57
\!\(\*SubsuperscriptBox[\(N\), \(t\), \(2\)]\) +
      6 Subscript[N, b] (-6 + 11 Subscript[N, t])]))/(
  96 h^2 Subscript[N, t])) + 1/2 y^2 Derivative[1][P][x]
  QP31[x] =
 u[y] /. Subscript[N, b] -> {1, 2, 3, 4} /. Subscript[N, t] -> 1 /.
    h -> 1 /. Subscript[G, r] -> 1 /. Subscript[B, r] -> 1 /.
  D[P[x], x] -> 1
  {D + y^2 + y^3/(2 Sqrt[6]) - y^4/(4 Sqrt[6]) -
  1/(24 (8 - 4 Sqrt[6])) (70 + 4 Sqrt[6] - 6 (6 + 4 Sqrt[6]) +
```

```
     3 (12 + 4 Sqrt[6]) - 2 (27 + 4 Sqrt[6])) y^3 Subscript[{-Sqrt[(
     3/2)], 1/12 (3 - 3 Sqrt[17]), 1/16 (6 - 2 Sqrt[57]),
    1/20 (9 - Sqrt[321])}, r],
D + y^2 - 1/72 (3 - 3 Sqrt[17]) y^3 - 1/96 (-3 + 3 Sqrt[17]) y^4 -
 1/(72 (27 - 3 Sqrt[17])) (365 - 6 Sqrt[17] - 6 (6 + 3 Sqrt[17]) +
     3 (12 + 3 Sqrt[17]) +
     2 (56 + 9 Sqrt[17] -
        2 (27 + 3 Sqrt[17]))) y^3 Subscript[{-Sqrt[(3/2)],
    1/12 (3 - 3 Sqrt[17]), 1/16 (6 - 2 Sqrt[57]),
    1/20 (9 - Sqrt[321])}, r],
D + y^2 - 1/96 (6 - 2 Sqrt[57]) y^3 - 1/96 (-6 + 2 Sqrt[57]) y^4 -
 1/(144 (54 - 2 Sqrt[57])) (1446 - 4 Sqrt[57] - 6 (6 + 2 Sqrt[57]) +
     3 (12 + 2 Sqrt[57]) +
     3 (56 + 6 Sqrt[57] -
        2 (27 + 2 Sqrt[57]))) y^3 Subscript[{-Sqrt[(3/2)],
    1/12 (3 - 3 Sqrt[17]), 1/16 (6 - 2 Sqrt[57]),
    1/20 (9 - Sqrt[321])}, r],
D + y^2 - 1/120 (9 - Sqrt[321]) y^3 - 1/96 (-9 + Sqrt[321]) y^4 -
 1/(240 (89 - Sqrt[321])) (3881 - 2 Sqrt[321] - 6 (6 + Sqrt[321]) +
     3 (12 + Sqrt[321]) +
     4 (56 + 3 Sqrt[321] -
        2 (27 + Sqrt[321]))) y^3 Subscript[{-Sqrt[(3/2)],
    1/12 (3 - 3 Sqrt[17]), 1/16 (6 - 2 Sqrt[57]),
    1/20 (9 - Sqrt[321])}, r]}
    QP31[x] =
t[y] /. Z2 -> {1, 2, 3, 4} /. Z1 -> 1 /. h -> 1 /. M1 -> 1 /.
  M2 -> 1 /. S -> 1
```

```
 {-1 - 1/(4 Sqrt[6]) + (70 - 8 Sqrt[6] - 2 (27 + 4 Sqrt[6]))/(
 24 (8 - 4 Sqrt[6])) + y^2 + y^3/(
 2 Sqrt[6]) - ((70 - 8 Sqrt[6] - 2 (27 + 4 Sqrt[6])) y^3)/(
 24 (8 - 4 Sqrt[6])) - y^4/(4 Sqrt[6]), -1 + 1/72 (3 - 3 Sqrt[17]) +
 1/96 (-3 + 3 Sqrt[17]) + (477 + 3 Sqrt[17] - 4 (27 + 3 Sqrt[17]))/(
 72 (27 - 3 Sqrt[17])) + y^2 -
 1/72 (3 - 3 Sqrt[17]) y^3 - ((477 + 3 Sqrt[17] -
    4 (27 + 3 Sqrt[17])) y^3)/(72 (27 - 3 Sqrt[17])) -
 1/96 (-3 + 3 Sqrt[17]) y^4, -1 + 1/96 (6 - 2 Sqrt[57]) +
 1/96 (-6 + 2 Sqrt[57]) + (1614 + 8 Sqrt[57] - 6 (27 + 2 Sqrt[57]))/(
 144 (54 - 2 Sqrt[57])) + y^2 -
 1/96 (6 - 2 Sqrt[57]) y^3 - ((1614 + 8 Sqrt[57] -
    6 (27 + 2 Sqrt[57])) y^3)/(144 (54 - 2 Sqrt[57])) -
 1/96 (-6 + 2 Sqrt[57]) y^4, -1 + 1/120 (9 - Sqrt[321]) +
 1/96 (-9 + Sqrt[321]) + (4105 + 7 Sqrt[321] - 8 (27 + Sqrt[321]))/(
 240 (89 - Sqrt[321])) + y^2 -
 1/120 (9 - Sqrt[321]) y^3 - ((4105 + 7 Sqrt[321] -
    8 (27 + Sqrt[321])) y^3)/(240 (89 - Sqrt[321])) -
 1/96 (-9 + Sqrt[321]) y^4}
 Plot[%, {y, 0, 1}, AxesLabel -> {y, u},
PlotStyle -> {{Black}, {Black, Thick}, {Black, Dashed}, {Green}},
PlotLabel -> {Z2 == {1, 2, 3, 4} , Z1 == 1, h == 1, M1 == 1, M2 == 1,
   S == 1}]
   QP31[x] =
t[y] /. Z1 -> {0.5, 1, 1.5, 2} /. Z2 -> 1 /. h -> 1 /. M1 -> 1 /.
  M2 -> 1 /. S -> 1
  {-0.803366 + y^2 - 0.0365373 y^3 - 0.160097 y^4, -1 - 1/(
```

```
 4 Sqrt[6]) + (70 - 8 Sqrt[6] - 2 (27 + 4 Sqrt[6]))/(
 24 (8 - 4 Sqrt[6])) + y^2 + y^3/(
 2 Sqrt[6]) - ((70 - 8 Sqrt[6] - 2 (27 + 4 Sqrt[6])) y^3)/(
 24 (8 - 4 Sqrt[6])) - y^4/(4 Sqrt[6]), -0.433333 + y^2 -
 0.483333 y^3 - 0.0833333 y^4, -1 + 1/144 (3 - 3 Sqrt[33]) +
 1/192 (-3 + 3 Sqrt[33]) + (
 111 - 9 Sqrt[33] + 4 (-9 - 6 Sqrt[33]) +
  2 (66 + 9 Sqrt[33] - 2 (27 + 3 Sqrt[33])))/(36 (15 - 3 Sqrt[33])) +
  y^2 - 1/144 (3 - 3 Sqrt[33]) y^3 - ((111 - 9 Sqrt[33] +
    4 (-9 - 6 Sqrt[33]) +
    2 (66 + 9 Sqrt[33] - 2 (27 + 3 Sqrt[33]))) y^3)/(
 36 (15 - 3 Sqrt[33])) - 1/192 (-3 + 3 Sqrt[33]) y^4}
 Plot[%, {y, 0, 1}, AxesLabel -> {y, u},
PlotStyle -> {{Black}, {Black, Thick}, {Black, Dashed}, {Green}},
PlotLabel -> {Z1 == {0.5, 1, 1.5, 2} , Z2 == 1, h == 1, M1 == 1,
  M2 == 1, S == 1}]
  {-0.513574 + y^2 +
 0.102062 y^3 - ((70 - 8 Sqrt[6] - 2 (27 + 4 Sqrt[6])) y^3)/(
 24 (8 - 4 Sqrt[6])) - 0.051031 y^4, -1 - 1/(4 Sqrt[6]) + (
 70 - 8 Sqrt[6] - 2 (27 + 4 Sqrt[6]))/(24 (8 - 4 Sqrt[6])) + y^2 +
 y^3/(2 Sqrt[6]) - ((70 - 8 Sqrt[6] - 2 (27 + 4 Sqrt[6])) y^3)/(
 24 (8 - 4 Sqrt[6])) - y^4/(4 Sqrt[6]), -0.615636 + y^2 +
 0.306186 y^3 - ((70 - 8 Sqrt[6] - 2 (27 + 4 Sqrt[6])) y^3)/(
 24 (8 - 4 Sqrt[6])) - 0.153093 y^4, -1 - 1/(2 Sqrt[6]) + (
 70 - 8 Sqrt[6] - 2 (27 + 4 Sqrt[6]))/(24 (8 - 4 Sqrt[6])) + y^2 +
 y^3/Sqrt[6] - ((70 - 8 Sqrt[6] - 2 (27 + 4 Sqrt[6])) y^3)/(
 24 (8 - 4 Sqrt[6])) - y^4/(2 Sqrt[6])}
```

```
{-0.833333 + y^2 - 0.268729 y^3 + y^3/(2 Sqrt[6]) - y^4/(
4 Sqrt[6]), -1 - 1/(4 Sqrt[6]) + (
70 - 8 Sqrt[6] - 2 (27 + 4 Sqrt[6]))/(24 (8 - 4 Sqrt[6])) + y^2 +
y^3/(2 Sqrt[6]) - ((70 - 8 Sqrt[6] - 2 (27 + 4 Sqrt[6])) y^3)/(
24 (8 - 4 Sqrt[6])) - y^4/(4 Sqrt[6]), -0.295876 + y^2 -
0.806186 y^3 + y^3/(2 Sqrt[6]) - y^4/(4 Sqrt[6]), -1 - 1/(
4 Sqrt[6]) + (70 - 8 Sqrt[6] - 2 (27 + 4 Sqrt[6]))/(
12 (8 - 4 Sqrt[6])) + y^2 + y^3/(
2 Sqrt[6]) - ((70 - 8 Sqrt[6] - 2 (27 + 4 Sqrt[6])) y^3)/(
12 (8 - 4 Sqrt[6])) - y^4/(4 Sqrt[6])}
```